IYER, DIVYA SHANKAR, Ph.D. Microbial Interactions with Nanoscale Features (2019)
Directed by Dr. Dennis R. LaJeunesse. 186 pp

Bacteria and other microbes interact with their environment through nanoscale mechanical and chemical processes. Understanding these interactions is critical for controlling bacteria, both in preventing biofilm formation and in using these interactions to control bacterial metabolism and behavior in industrially relevant applications such as fermentation and biomaterial generation. Biofilm formation is a key step in the process of biofouling, a process of great importance in shipping and food processing industries and especially in healthcare where it is of utmost importance to prevent the formation of biofilms on medical equipment which would further prevent infections. In this dissertation, I examine the biological responses of the Gram-negative bacterium, *Escherichia coli* (*E. coli)* to alterations in the surface nanostructure, persistent photoconductivity, and the stiffness of the surface material.

In my characterization of Bacterial interactions with nanostructured surfaces, I examined the behavior of *E. coli* bacteria, when exposed to twenty-one different nanostructured polymeric substrates etched from seven common and industrially relevant polymers. I demonstrated that in the bacteria respond to the surfaces by changing their adhesion, morphology and biofilm formation. Interestingly neither surface energy nor structure appeared to control these behaviors. The predominant effect on bacterial behavior appeared to be directed by the composition of the surface.

To investigate the mechanisms that control the bacterial response to a surface phenomenon known as persistent photoconductivity (PPC), I used *E. coli* strains that were mutant for genes that encoded specific components of adhesion and/or biofilm formation. One goal of microbial bioelectronics is to develop hybrid organic/inorganic interfaces between living cells and electronic devices. Type III semiconductors such as GaN are a good candidate for such interfaces; Gallium nitride and Oxide materials are biocompatible, a growing material system for electronics, and have a property known as persistent photoconductivity (PPC), which is the persistence of a charge after excitation energy such as ultraviolet light is removed. Work in the Ivanisevic and LaJeunesse labs have shown that PPC changes the physiology of the bacterial cells and results in both an increase in intracellular Ca^{2+} and alteration to cell adhesion. To determine which cell surface and adhesive components of *E. coli* are required for the response to PCC, I used a collection of *E. coli* deletion mutants and examined the loss of these cell structures on the bacteria's response to PCC. I found that mutation in the synthetic pathways that generate the LPS, curli, and mutations in flagella significantly alter the response of *E. coli* to PPC.

To determine the bacterial adhesive response to material stiffness, I tested the adhesion of *E. coli* to Polyacrylamide hydrogels of three different stiffnesses (~17kPa, 29kPa and 1547 kPa). Wild type *E. coli* demonstrated the highest adhesion to the soft PA hydrogel and the least on the hard gel. I used single-gene deletion mutants of *E. coli* bacterial surface appendages to determine how the loss of these cellular structures would affect bacterial adhesion to these gels. I compared the adhesion trends of the various knockouts to the WT trend and found that they were vastly different, and with no

particular pattern. Adhesion of bacteria to the soft gels was significantly lower than the adhesion of the WT except for the csgD mutant. All the knockout bacteria adhered more to the hard gels in comparison to the WT adhesion. Identifying the most important deletion remains a challenge, even though all the deletions resulted in a change in bacterial adhesion. This analysis has provided a framework for the further elucidation of genetic pathways involved in the bacterial responses.

MICROBIAL INTERACTIONS WITH NANOSCALE FEATURES

by

Divya Shankar Iyer

A Dissertation Submitted to
the Faculty of The Graduate School at
The University of North Carolina at Greensboro
in Partial Fulfillment
of the Requirements for the Degree
Doctor of Philosophy

Greensboro
2019

Approved by

_____
Committee Chair

DEDICATION

To my family, for their belief in me.

APPROVAL PAGE

This dissertation written by Divya Shankar Iyer has been approved by the following committee of the Faculty of The Graduate School at the University of North Carolina at Greensboro.

Committee Chair _____
Dennis R. LaJeunesse

Committee Members

_____
Eric Josephs

_____
Jianjun Wei

_____
Christopher Kepley

_____
Date of Acceptance by Committee

_____
Date of Final Oral Examination

TABLE OF CONTENTS

Page

LIST OF TABLES

Page

LIST OF FIGURES

Page

LIST OF SUPPLEMENTARY TABLES

Page

LIST OF SUPPLEMENTARY FIGURES

Page

CHAPTER I

INTRODUCTION

I.1. Microbial Biofilms

Biofilms are a complex community of bacteria embedded in an extracellular matrix (EPS) composed of DNA, polysaccharides, proteins, lipids[1,2]. They form on any substrate in proximity to water[3]. The air-water interface is the ideal location for the growth and maturation of biofilms and is found in almost every environment on Earth, from showers and pipes to medical devices[4].

Biofilms are highly problematic for many medical and industrial processes wherein they damage material surfaces, sometimes eating through the material in the process of producing the biofilm[5]. Bacterial biofilms on medical implants, open surgical wounds are a cause of persistent infections[6]. The CDC estimates a ~$33 billion/year worldwide cost in nosocomial infections[7], and approximately 99,000 deaths each year[8,9]. At least 65% of all persistent and chronic bacterial infections are biofilm related[10,11]. The biofilm environment is extremely resistant to antibiotics, most of which have been designed to target freely swimming planktonic cells[11,12]. Antibiotic-resistant bacteria have arisen despite the enormous efforts placed to combat biofilm-related infections. The risk of biofilm-related infections increases every year, posing an urgent need for the development of new methods of biofilm prevention and control.

I.2. The Role of Extracellular Polymeric Substance in Protecting Biofilms

Bacteria exist in the planktonic (single cells in suspension) state as well as in multicellular communities (biofilms). Biofilms are complex communities of cells that are attached to a substrate and themselves by means of an organic glue-like substance known as the Extracellular Polymeric Substance (EPS)[13]. The EPS performs the important structural role of stabilizing the cells and provides a protective bubble-like environment against mechanical damage and shear caused by fluid flow at the interface[14–16]. It is made up of complex polysaccharides, proteins, and extracellular DNA secreted by the members of the biofilm community by processing the nutrients available upon adhesion to the substrate[1,17]. The EPS allows its community members to share nutrients, communicate through chemical signaling molecules (Quorum sensing), pass along genetic information through lateral gene transfer and are even involved in promoting electron transfer[18]. All these functions are enhanced in biofilm communities compared to planktonic cells.

Bacteria monitor, synchronize and adapt to environmental changes through a process known as Quorum Sensing[19]. Quorum sensing allows different parts of the biofilm to communicate, enabling the biofilm to adapt to environmental changes[20]. This effective cell-cell communication is achieved through the release and response of autoinducers, which are quorum-sensing molecules. The release of autoinducers is a function of the number of cells present in the biofilm. The concentration of autoinducers increases due to an increase in cell density[20]. Once a certain threshold is reached, the autoinducers activate genetic pathways in the bacteria to produce the appropriate response[21]. In bacteria, homoserine lactases are the most common form of autoinducers,

although the eukaryotic autoinducer oxylipin has been found to mediate cell-cell communication in *Pseudomonas aeruginosa* [22]. One method of preventing biofilm growth is to prevent the release of autoinducers into the biofilm[23].

Bacterial biofilms provide the bacteria with extensive protection[2,24]. The EPS not only protects the bacteria present in the biofilm from mechanical damage and hydrodynamic stress but also forms a barrier to protect it from antibiotics and antimicrobial treatment[25]. Antimicrobial mechanisms tend to work synergistically, and it has been shown that resistant biofilm cells respond to stress[26,27]. Environmental stressors such as antibiotics[28,29] and nutrient depletion such as nitrogen starvation[30] may lead to the formation of persister cells within the biofilm. These are small populations of bacterial cells that are difficult to destroy due to changes in their phenotype (slow-growing cells)[31]. Persister cells are shielded by the EPS and its components and are found embedded deep within the biofilm, making it very difficult for antimicrobials to reach. When under the influence of environmental stresses, bacteria decrease their ATP levels, forming dormant persister cells[31].

Biofilm associated infections are difficult to treat due to their altered gene expression and growth states[32]. It is difficult to develop treatments and preventative strategies against biofilm-associated infections due to their highly adaptive and protective nature. Global gene expression analyses of biofilms have revealed the involvement of genes related to adhesion (cellular surface structures) (e.g. fimbriae type-1, curli, flagella), auto-aggregation (antigen 43) and stress response (*soxS, hslS*)[33–37]. Niba et al. have used the 'Keio collection'[38] of single deletion mutants of *E. coli* to identify 110

individual genes required for biofilm formation[37]. An alteration to even any one of these genes can cause drastic changes in biofilm formation. *E. coli* biofilms are heavily affected by the motility genes for flagella and fimbriae. Alteration to genes that encode for structural proteins such as *OmpC,* and *slp* (encodes for an outer-membrane lipoprotein) would interrupt the initial adhesion phase of biofilm formation[36].

I.3. Bacterial Biofilm Production

Biofilm formation is a dynamic four-step process involving attachment, colony formation, maturation and finally dispersion[39]. It begins with the initial attachment of a planktonic bacterium to the surface. This initial phase is rapid (occurs within ~1 min) and reversible, involving hydrodynamic and electrostatic interactions[40,3]. The substratum must first be conditioned by its exposure to the fluids, in a process called surface conditioning[41]. Biochemical components such as water, proteins, lipids, ECM molecules, salts, adsorb onto the surface of the substrate to form a conditioning layer [24,42]. Surface conditioning is essential for the formation of a foundation layer which creates a suitable substrate for bacterial adhesion[24]. When the negatively charged bacterial envelope and the substrate interact, the total attractive and repulsive forces of the two surfaces determine the ability of the bacteria to adhere to the substrate. The attachment is influenced by many factors such as the environmental conditions of the medium (pH, temperature) and the inherent properties of the substrate which mediate electrostatic, hydrophobic and van der Waals interactions[3,43,44].

A stable and robust adhesion is the outstanding characteristic of the second phase of bacterial biofilm formation. During this phase, bacteria that have initially adhered undergo changes in gene expression changing them to irreversibly adherent bacteria. Phase II is irreversible due to the involvement of van der Waals interactions[3]. Molecular interactions between bacterial surface structures and the substrate govern this phase of adhesion. These surface structures are a group of filamentous bacterial appendages composed of proteins found on the outer membrane of most bacteria and mediate specific attachment to the substrate[45,46]. These cellular structures include flagella, pili (fimbriae) and curli[46]. These bacterial appendages possess proteins (such as adhesins) upon their terminal end which bind to molecules found on the conditioned substrate and upon contact with the substrate, activate bacterial genetic pathways, such as Rcs and Cpx[47], which initiate the production of EPS[48]. These same genetic pathways also alter the motility of the bacteria, making them adherent by inactivating the flagella [49,50]. The attached bacteria proceed to multiply and form a biofilm matrix that encloses the colonies [51]. Quorum sensing molecules exchanged between bacteria activate different bacterial behavior within the matrix, creating microcolonies within the EPS for various activities[21]. Bacterial cells develop and mature during this stage of biofilm formation, making their community thrive as a consortium of species [39]. Biofilm communities are highly specialized: some produce new EPS[52] and quorum sensing molecules[20], others are responsible for nutrient recycling[53,54], protection and persistence[29,31]. Several genes are switched on during this transition from planktonic to sessile biofilm, chiefly the ones

associated with the appendage control such as *motA, motB,* and *fimA*[27]. In *E. coli,* ~4000 genes have been identified as being involved in biofilm production[34,36].

During stage III of biofilm formation, planktonic cells detach from the mature biofilm and proceed to colonize at other locations[39]. When the biofilm reaches a critical mass, fragments of biofilm and planktonic cells from deep within the mass disperse due to external forces such as shear, enzymes, and stresses.

I.4. Sensing the Environment

The sense of touch is very important, even to bacteria. It enables the bacteria to sense the environment, avoid hazards and detect surfaces. Bacteria have the ability to sense chemical signals (chemosensation) as well as respond to mechanical stimuli (mechanosensation).

I.4.i. Chemosensation

Bacterial cells use chemical gradients to identify and respond to environmental signals such as nutrition depletion[30]. These chemical gradients are sensed through outer membrane (OM) lipoproteins such as porins. OmpF is one such porin in which acidic pH triggers the reversible closing of the channel[55]. These OM proteins further activate signal transduction pathways to yield a response to this chemical stimulus[56]. During biofilm formation, chemical gradient sensing impacts bacterial function and cell-cell communication[57].

A local microenvironment is created around cells trapping ions and molecules close to the surface, which induces a change in the intracellular pH and ATP levels[58] and extracellular osmolarity[59]. These processes are controlled by the Cpx two-component system, which is activated by envelope stress[60,61]. Some surfaces release chemical molecules known as chemoattractants which draw bacteria closer to the surface and promote bacterial adhesion. The interspecies quorum-sensing signal autoinducer-2 (Al-2) doubles as a chemoattractant in *E. coli*. The self-activation of highly motile bacterial cells by Al-2 enables cellular aggregation and the ability to form surface-enabled structures[62]. As cells draw closer to the surface and closer together, this chemosensitive process inhibits the mechanosensitive flagellar function, ceasing bacterial motility and activating biofilm formation. This is promising for the future of antibacterial surfaces; using chemoattractants to lure bacteria onto contact killing surfaces[63], for instance.

I.4.ii. Mechanosensation

Mechanosensation is the biochemical response to physical stimuli[64]. An increase in turgor pressure at the lipid bilayer of the cytoplasmic membrane activates mechanosensitive ion channels that further activate signal transduction pathways[65,66]. Mechanosensitive channels (MS channels) are proteins found in cell membranes that open nanoscale pores in response to force-induced perturbations[66]. There are two major classes of MS channels: mechanosensitive channel of large conductance (MscL) and mechanosensitive channel of small conductance (MscS)[64]. MscL is thought to play an important role in regulating the bacterial turgor pressure[67]. During osmotic shock,

bacteria rapidly eliminate some of its components to compensate for the osmolarity, thereby maintaining homeostasis[68,69]. Understanding the gating mechanism and controlling the forces that activate these channels could help in the production of antimicrobials. MS channels modulate biochemical signals in response to mechanical forces. Bacteria are frequently equipped with mechanotransmitters to aid in this process.

Mechanotransmitters are structures that propagate mechanical force and induce downstream genetic responses to the physical stimuli. These mechanotransmitters are in the form of extracellular surface organelles, flagella, pili, and curli, that mediate specific adhesion interactions with extracellular materials and other cells[52]. The roles of these structures in biofilm formation have been described below.

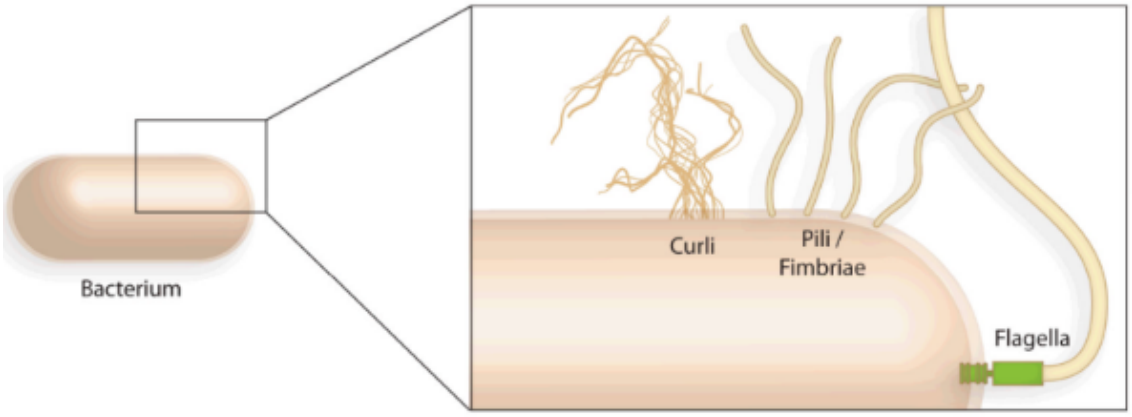

Figure 1.1 Bacterial Surface Appendages as Depicted in "Bacteria-Surface Interactions"[278]

I.4.ii.A. Flagella

The flagella are an external appendage of the bacteria that can rotate, providing the bacteria with locomotory ability and directionality[70]. The bacterial flagellum plays an important role in recognizing when to stop as the bacteria encounters the substrate [71]. During initial surface contact, bacteria sense surfaces through the obstruction of the rotation of its flagella[46,72]. This activates the DegS/DegU two-component system[73] where the DegS senses the inhibition of the flagellar rotation and in combination with DegU upregulates genes for biofilm formation[73]. The flagellar motor is deactivated, and initial biofilm processes begin. Flagella respond to environmental cues by altering its speed, torque, and direction[58]. The highly conserved flagellar motor[74] structurally adapts to the environmental cues. This explains how bacteria sense changes in fluid properties like viscosity. Flagella work simultaneously with another mechanotransmitter, pili to control bacterial movement[72] and biofilm formation. An effective strategy to prevent bacterial adhesion is to inactivate or target the removal of flagella using compounds such as c-di-GMP, thereby inhibiting motility and the chance to propagate.

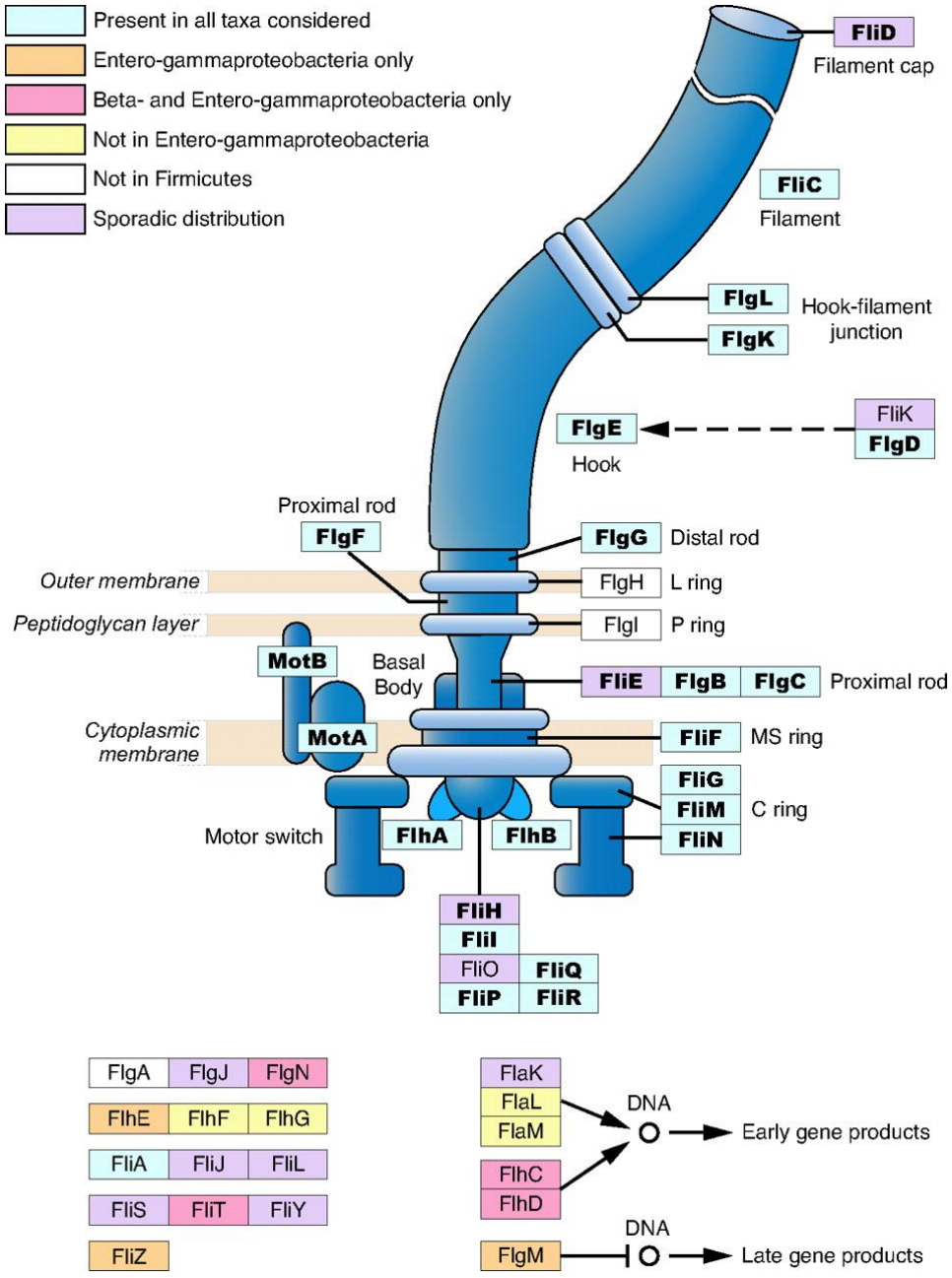

Figure 1.2 Distribution of Flagellar Proteins as Depicted in "Stepwise Formation of the Bacterial Flagellar System"

I.4.ii.B. Pilus

Pili, also known as fimbriae, are the many hair-like appendages composed of the protein pilin that are found on the cell membrane of bacteria[75]. Pili are mechanically actuated organelles that alternatively extend and retract pulling the bacterium forward[76]. When pili attached to a surface, its movement is controlled by the force generated by pilus retraction.

They possess highly adaptive responses and are known for their adhesive, motility and horizontal gene functions as well as their involvement in virulence and host colonization[77]**.** The different types of pili are classified according to their architecture and assembly: chaperone/Usher (CU) pili, type1 pili, type IV pili, and conjugative F-pili. Pili are regulated by the *fim* and *pap* gene clusters. The two major subtypes are type 1 pilus (T1P) and Type 4 pilus (T4P). The T4P extends and retracts from the cell poles and controls its motility using physicochemical forces. Type 1 pili (mannose-specific adhesin fimH) is necessary for the initial surface attachment of the bacterium[78]. When not bound to mannose, it promotes stable adhesion. Mechanical surface contact induces an increase in the production of cAMP[79]. Modulation of cAMP levels controls bacterial twitching and virulence [80,81].

The most ubiquitous pili biogenesis pathway in *E. coli* is the chaperone/usher (CU) pathway[82]. A chaperone binds the pilus subunits together and they are further polymerized at the outer membrane by a protein called the usher[83]. Pili activity begins immediately upon initial adhesion. Adhesion using pili leads to altered outer membrane

composition[84]. Other systems that control its formation and function are the two-component rcsB[85] and two-component chemosensory Chp[80,81] systems.

Bacteria use T4P to crawl, walk and slingshot on surfaces [86,87]. Biofilm formation on surfaces requires the cooperation of flagella and pili. Flagella are responsible for the detection of substrates and their transition from planktonic to sessile state. As soon as the flagellar machinery switches off, the pilus is activated. Adhesin molecules present at the tip of the pili enable adhesion during biofilm formation. As bacterial flagella are also responsible for their swarming activity, the density of bacteria on the surface increases through this switch [88,89]. Targeting this switch, i.e. the initial adhesion mechanism of biofilm formation is a strategy that is being employed to remove biofilms. Another strategy is using chemicals to remove the adhesin molecules from the tips of the pili to reduce adhesion.

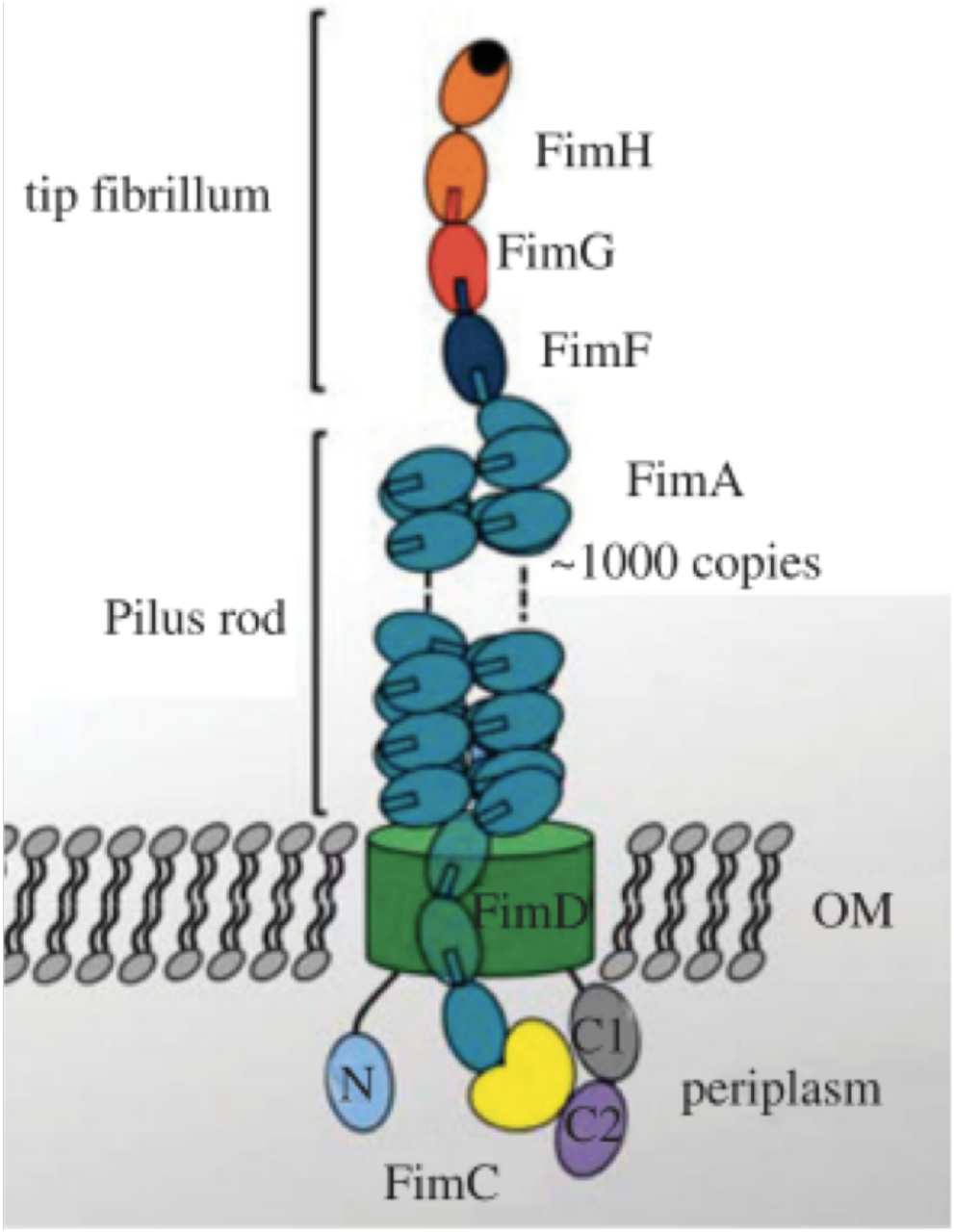

Figure 1.3 Type-1 Pili Assembly as Depicted in "Chaperone-Usher Pathways: Diversity and Pilus Assembly Mechanism"[82]

I.4.ii.C. Curli

Curli are extracellular bacterial structures and belong to a class of fibers known as amyloids. They function during the initial attachment phase of biofilm formation and heavily contribute to adhesion, cell-cell aggregation, and biofilm production[90]. Curli are a major component of the EPS. Curli production is influenced by environmental factors such as temperature, nutrient limitations. The 2-component regulatory systems OmpR/EnvZ[91] and CpxA/R[92] and the Rcs pathway[93] moderate curli production, although new evidence has surfaced that the CpxA/R system may not be activated in surface sensing and biofilm formation[94]. Its production is turned off when the Cpx and Rcs pathways are activated. The csgBA and csgDEFG operons control curli biogenesis and function[95]. The csgD gene controls the transcription of both these operons[95]. Curli are secreted by the interaction of the OM proteins csgG, csgE and csgF. csgG is in the form of a pore and is found dispersed on the OM. csgA is the major curli subunit; it interacts with csgB to assemble into an amyloid fiber[96]. CsgE interacts with csgG to secrete csgA to the OM for assembly while csgF assists in the assembly of csgA and csgB[96,97].

The expression of csgD is stimulated by C-di-GMP, a secondary messenger responsible for reducing flagellar activity [90,98]. The production of ECM requires csgD as it regulates curli expression and indirectly regulates cellulose production, which is an integral component of biofilms. csgD activates AdrA which in turn synthesizes cyclic-di-GMP, which is required for the production of the cellulose component of the EPS[99,100].

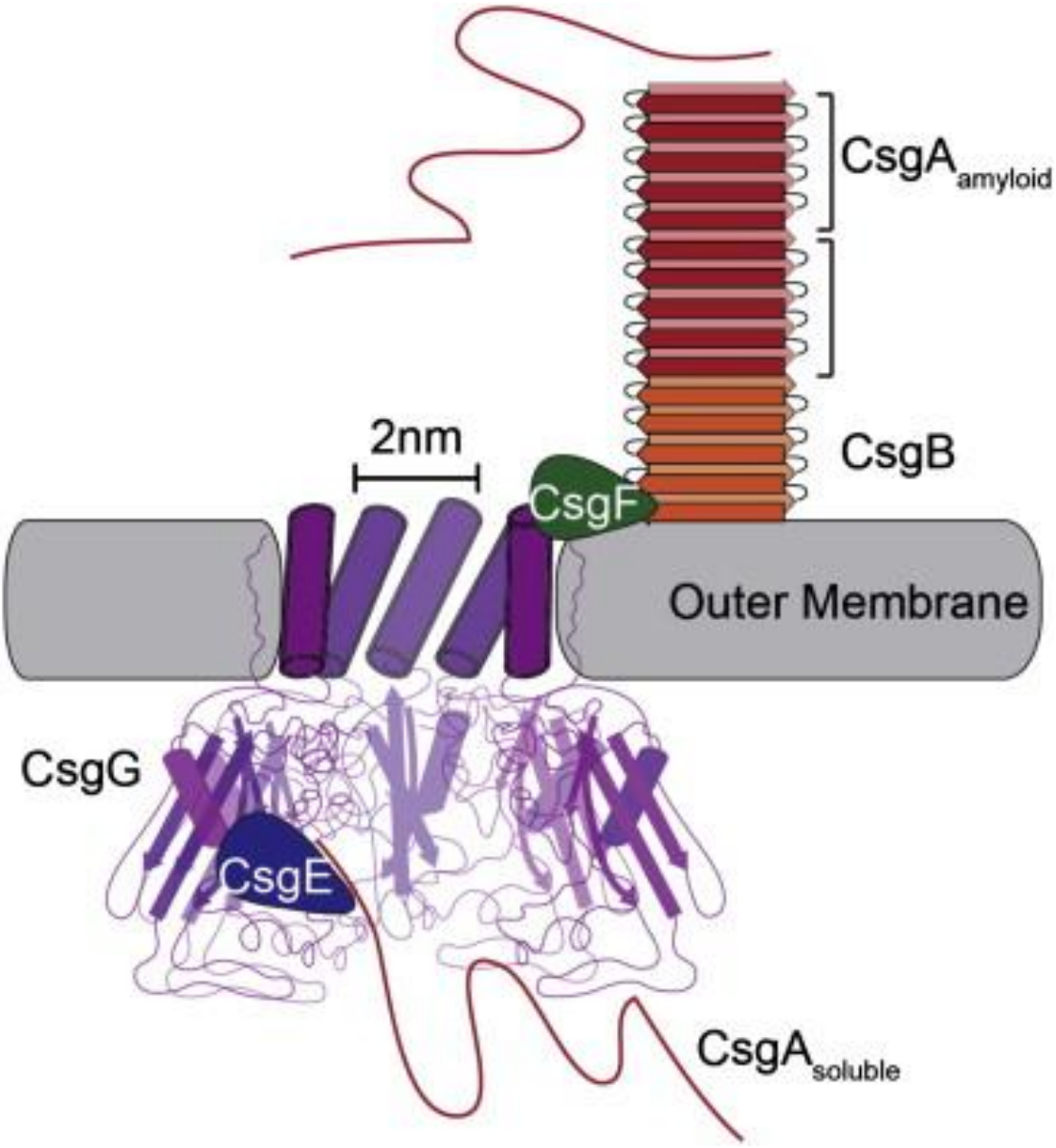

Figure 1.4 Curli Structure as Depicted in "Curli Biogenesis: Out of Disorder"[97]

I.4.ii.D. LPS

The distinguishing feature of Gram-negative bacteria is the presence of lipopolysaccharide (LPS) on its outer membrane. LPS serves as a permeable barrier that allows only low molecular weight, hydrophilic compounds through passages known as porins. Its primary function is the protection of the cell, but it also aids in adhesion when the cells do not have surface appendages. The OM layer of bacteria is elastic; when confronted by a large mechanical load, it bears the mechanical stresses, thereby stabilizing the OM.

LPS structure can vary amongst bacteria, but the core structural components remain the same: hydrophobic lipid A region anchored on the bacterial OM, core oligosaccharide linked to the lipid A region and O-antigen (O-specific polysaccharide)[101]. The O-antigen of the LPS layer promotes virulence and stimulates immunogenic responses. Bacterial surface attachment induces virulence in hosts due to the endotoxic nature of the Lipid A layer. Chemo-sensitive channels such as Toll-like receptors (TLR) and transient receptor potential ion channels (TRP) are activated by LPS and trigger inflammatory responses in the host[102–104].

When exposed to stresses (mechanical, osmotic, etc.), the LPS biosynthesis is disturbed, activating envelope signal transduction pathways RpoE sigma factor and RcsB[105]. Defects in the OM caused by asymmetrical LPS production can cause local stresses upon the OM. Biofilm associated lipid-A palmitoylation (incorporation of lipid-A) i.e. remodeling the OM and peptidoglycan layer can rescue cells from lysis[59,106,107].

The adaptable nature of LPS and its resultant anti-virulent nature provide biofilms with robust protection against external forces.

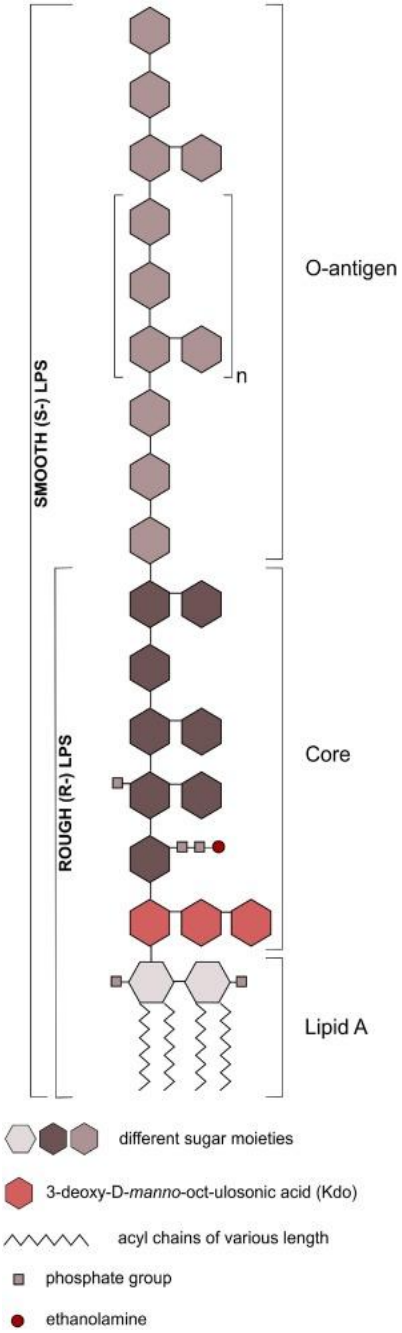

Figure 1.5 Lipopolysaccharide Structure from "Structure and Function: Lipid A Modifications in Commensals and Pathogens"[101]

I.5. Bacteria/Extracellular Substrate Interactions

Bacterial biofilms form on bacteria-surface interactions, making the study of the properties of the substrate critical in biofilm control[15,108]. This is especially true when attempting to prevent the initial adhesion of the bacteria. Increased attention notwithstanding, it remains difficult to attribute specific effects upon bacteria to the various material properties. Contradictory results regarding the importance of individual material surface properties on bacterial adherence have been reported. For instance, some scientists found that roughness promotes bacterial adhesion[109–111], others found that it reduces adhesion[112–116] while some scientists have found no correlation whatsoever[115,117]. Taking into account some other influential surface properties such as surface energy, chemical modification and stiffness, a direct relationship between the properties and bacterial adhesion behavior has yet to be found. Is surface energy more important than surface roughness? What is the correlation between bacterial adhesion and the stiffness of the substrate? The resolution of this debate will require a mechanistic understanding of the biochemical components that govern these processes.

Thus far certain properties to play critical roles in bacteria/substrate interactions have been identified: hydrophobicity, material composition, roughness, chemical modification, topography. These properties change the near-surface interaction dynamics. Their roles are not necessarily unrelated. For example, Hydrophobicity, chemical modifications and change in roughness can result from change in topography. Understanding the roles of these properties can lend to our understanding of biofilms and the microcolonies formed within.

I.5.i. Surface Roughness

The relationship between bacterial adhesion and roughness has long been studied[110,111,118,119]. In general, smooth surfaces are found to be more hydrophobic and supposedly colonize fewer bacteria. An increase in roughness promotes bacterial adhesion due to increased surface contact[108,120]. Adhesion events are directly related to maximizing the cell-surface contact points and further control the location of bacterial deposition[73]. Rough substrates allow for an increased rate of initial deposition and conditioning.

The presence of nanoscale properties reduces the surface potential barrier for the bacteria coming in contact with a surface[119]. Roughness may affect other substrate properties which in turn influence bacterial adhesion. For instance, the roughening of polypropylene discs showed a higher rate of bacterial adhesion than the smooth surfaces[121]. While many different substrates of varying roughness have been tested, it was found that bacteria preferentially adhere to surfaces of comparable size[122].

I.5.ii. Surface Energy/Wettability

Bacterial adhesion is commonly thought to be affected by the wetting properties of the substrate[123–125]. Wettability studies typically measure the contact angle of a liquid on a substrate[126–128]. Wetting properties on the macroscale are a result of the nanoscale composition of the material[129]. A contact angle less than 90° indicates hydrophilic surfaces, while above 90° indicates hydrophobicity or low wettability[126]. In the extreme case, surfaces with contact angles above 150° are known as superhydrophobic, while

those with contact angles below 10 are superhydrophilic[111,126]. Both superhydrophobic and superhydrophilic substrates prevent bacterial adhesion[129]. Some naturally occurring superhydrophobic surfaces are the lotus leaf[130] and gecko's feet[131]; their hierarchical structures have made way for products that have both anti-wetting, antifogging and antiadhesive properties[127,131–133]. Naturally occurring superhydrophilic surfaces such as elephant's ears and red blood cells' plasma membranes have inspired its utilization in commerce such as the self-cleaning windows and ultrafiltration membranes[134]. Both hydrophobicity and hydrophilicity have been utilized to develop anti-bacterial technologies. A significant reduction of microbial adhesion was seen on chemically functionalized hydrophobic hydroxyapatite surfaces[135] as well as superhydrophilic co-polymer coatings on dentures[136].

Recent evidence supports the theory that water contact angle measurements are not a good way of assessing biological responses to materials[137]. For most studies in the past, biological materials were considered akin to solid inert particles. However, due to the immense complexity of biological materials, they do not adhere to the same set of rules as inert particles[138]. The general assumption until now has been that hydrophobic surfaces prevent bacterial adhesion and vice versa with hydrophilic surfaces[139,140,141]. Recent advances have shown that this is not necessarily true. Several studies have shown that hydrophobicity promotes bacterial adhesion[142,143], and in one case even shows that a contact angle of 90° produces the highest amount of bacterial retention[144]. This shows that there is no exact relationship between the hydrophobicity of the material and the adhesion of bacteria. Hydrophobicity can be considered to be a product of topography

and chemistry. The hydrophobicity of bacteria, however, can play an important role in adhesion. Hydrophobic bacteria prefer hydrophobic surfaces and vice-versa[145]. When wetting properties are considered along with surface charges, it is seen that bacterial adhesion is greatest on hydrophilic surfaces with a positive charge, followed by hydrophobic surfaces with negative charge [142].

I.5.iii. Surface Charge (Electrostatic Attraction and Repulsion) and Surface Chemistry

Bacteria, in general, possess negatively charged outer membranes due to the presence of numerous carboxyl and phosphate groups. Both Gram-positive and negative bacteria possess a peptidoglycan layer, which is a polysaccharide made of two alternated glucose derivatives: N-acetylglucosamine (NAG) and N-acetylmuramic acid (NAM), that are cross-linked. The teichoic acid (a glycopolymer) found embedded only in the peptidoglycan layer of Gram-positive cell wall lends it a net negative charge, which is essential for developing proton motive force (pmf) within the bacteria. The structure of Gram-negative bacteria is more complex than Gram-positive bacteria, with fewer peptidoglycan layers but possess an outer membrane (OM). The LPS layer, which is anchored to the OM possesses carboxyl and phosphate groups, lending the OM a net negative charge.

Generally, a negatively charged surface reduces bacterial adhesion due to greater repulsion between the negatively charged substrate and bacterial surface[146]. To study this property, Terada et al modified polyethylene sheets by adding a negative charge. He

found that *E. coli* adhere preferentially to the positively charged surfaces (23x higher than the negatively charged surfaces)[147] but leads to the disruption of their cellular membranes[142]. These properties can be used to prevent biofilm formation. There have been some conflicting reports regarding the influence of surface chemistry upon bacteria, but this is to be expected due to the varied characteristics of the substrates in use and the different strains of bacteria in play.

The charge of the substrates can be inherent or introduced during processes such as plasma etching and UV radiation[148]. The surfaces can be functionalized using different types of plasma etching[149]. Due to the material removal effect of etching, exposed functional groups such as aldehyde and hydroxyl have an influence on the net substrate surface charge [150,151].

Substrate functional groups can influence the adhesion, viability, and morphology of bacteria [152]. Negatively charged species on the substrates and those on the surface of bacteria interact via Ca^{2+} bonds. These electrostatic interactions, or surface charge, are commonly referred to as zeta potential. Quaternary ammonium salts, which have bactericidal properties, are amongst the most common cationic groups used for functionalizing antimicrobial surfaces[15]. Zwitterionic surfaces are amongst the most effective anti-biofilm strategies. They contain positive quaternary ammonium salts and negative functional groups such as carboxylate, phosphate and sulfate[153]. A cellulose-based coating with pH-sensitive charges[154] is amongst the latest in Zwitterionic surface design.

The surface charge of both the bacteria and the substrate can change upon varying external conditions such as protein adsorption, ionic strength, and pH[14,155]. This has been shown to be the case during surface conditioning of materials[156]: materials that originally resist bacterial adhesion now have a conditioning layer rich in nutrients and perfect for attachment.

An interesting case of the effect of surface chemistry upon bacteria is the prevention of bacterial adhesion on superhydrophobic surfaces due to the entrapment of air[119]. This occurs commonly in small micro pocket topologies. The local environments so created experience short-range forces known as Lewis acid-base interactions, which are governed by hydrogen bonding. The long-range forces are mainly electrostatic and *van der Waals* interactions [157,158]. The adhesion of bacteria to substrates can be modeled using the Derjaguin–Landau–Verwey-Overbeek (DLVO) theory[159]. The classical DLVO theory considers microbes as inert particles leading to inaccurate predictions. Due to its inability to account for divalent cations, an extended DLVO theory was created [138,159] which is valid only if surface charge of the substrate and hydrophobicity of bacterial surface are significantly different[146]. The Lifshitz van der Waals theory was later developed taking into account all the electrostatic forces from neighboring molecules and interactional forces[160]. These forces are generally attractive and operative over a relatively long-distance range. Electrostatic forces can either be attractive or repulsive depending on their magnitude or distance range, as determined by ionic strength and pH of the solution. The Lewis acid-base theory is used to measure the short-range forces.

These are acid-base interactions between hydrogen-donating and hydrogen-accepting groups that can also be attractive or repulsive.

I.6. Biofilm Control

I.6.i. Antibiotics

The conventional method of controlling bacterial infections is to use antibiotics. Their general mechanism of action is to target specific and unique bacterial targets such as enzymes or specific lipid components of a bacterial cell that human cells lack[161]. For example, beta lactam antibiotics, such as penicillin and vancomycin, target the bacterial cell wall biosynthesis [39,162], Fluoroquinolones inhibit DNA synthesis by unwinding bacterial DNA[29] and tetracyclines inhibit protein synthesis[29]. The major issue with using antibiotics to control biofilm formation is the evolution of antibiotic resistance bacteria at rates faster than the ability of doctors to treat infections [32,161]. Microbes also develop resistance if exposed to more than optimal dosage (greater than the minimum inhibitory concentration)[163]. More concerningly, the heredity of antibiotic resistance has been confirmed[29].

I.6.ii. Matrix Degrading Enzymes

High throughput screens of small molecule chemical compounds that inhibit certain gene expressions required for biofilm formation are being investigated [164,165]. A potent broad-spectrum anti-biofilm peptide 1018 with a marked increase in adaptive resistance to conventional antibiotics has recently been developed[11]. It works by blocking

the expression of (p)ppGpp[11], an important marker of biofilm development[166]. Other chemical molecules, such as GH12 have been shown to target the EPS matrix of *S. mutans* that have infected rats[167]. The list of such molecules to interfere with biofilm formation is increasing at a rapid rate. The mechanisms of action of these molecules are still largely unclear and beget further investigation.

I.6.iii. Nanoparticles

Nanoparticles (NP) have the distinct advantage of being small in size (10^{-9} m). This allows them to travel into regions that would normally prohibit entry to antibacterials. Nanoparticles attach to the surface of the biofilm with ease, penetrate and migrate within it. They can be made with any number of materials with different functionalities and different shapes and sizes within the nanoscale. Material properties tend to work differently at this scale and this has been used as an advantage in anti-biofilm processes. Silver and gold NP are the most commonly used in this field, although they can be made of almost any material. Silver possesses naturally antibacterial properties, while gold is inert, has unique optical properties and can be traced *in vivo* if necessary. Silver is an ancient and powerful bactericidal agent and has popularly been used as an antibacterial coating [168–170]. The discovery that the antibacterial effects of silver are primarily due to the presence of the silver ion changed the ways silver is used[169]. However, coating medical devices with metallic silver has surprisingly been ineffective and limited in application, largely due to the inactivation of silver ions upon contact with blood [171,172]. A study recently conducted upon metallic cadmium, copper and

silver materials, has shown that these metallic surfaces are antibacterial through a phenomenon known as contact killing, whereby bacteria are killed within minutes to hours upon contact[168]. This study also introduces the novel concept of oxide formation and metal ion dissolution being key factors for a metal to be antibacterial[168]. Silver nanoparticles have found to prevent biofilm formation by many pathogens such as *E.coli, S. aureus* [170]. A study by Graves et al regarding the exponential increase of silver NPs to bacteria has shown that bacteria can develop tolerance to the silver nanoparticles upon repeated exposure[173]. This clearly indicates that resistance can be conferred from repeated exposure to even nanoparticles, and thus care should be taken in its usage. Surfaces have also been modified by coating with metallic films to induce antimicrobial activity. In a research study conducted upon copper and silver nanofilms on nosocomial infections, it was found that copper surfaces showed better activity than silver surfaces[174].

Since polymers are used so abundantly in medical studies, the use of polymeric nanoparticles is useful. In 2018, Sanchez et al prepared polymeric PolymP-n Active nanoparticles to study their antimicrobial properties against a subgingival (dental) biofilm[175]. Tan et al loaded chitosan NP with drugs (oxacillin and Deoxyribonuclease I) to treat biofilm-related infections[175]. The results of both these experiments are promising and *in vivo* studies should be considered for their application.

I.6.iv. Anti-biofouling Coatings

Since biofilms are generated by bacteria residing on a solid surface rather than as floating planktonic collection of cells, an approach that has been employed is to coat surfaces with bactericidal substances [176,177]. Antimicrobial materials focus upon the modification of surfaces to prevent biofilm formation. Initial modifications involved the covalent linkage of antibiotics (such as Vancomycin) to Titanium surfaces[178]. Although this approach was innovative, it still relied on antibiotics and its eventual lead to antibiotic resistance.

Another strategy is to prevent biofilm formation and block or slow the initial adherence of the bacteria to the surface. Anti-biofouling agents are biomaterial coatings that prevent microbial adhesion that are different from antimicrobial coatings, which kill microbes when they come in proximity to the coating[179]. There has been recent concern regarding the development of antimicrobial resistance from anti-biofouling agents. One such case examined whether an anti-biofouling paint containing heavy metals that could potentially select for antimicrobial resistant genes[179]. Although the paint did not contribute to resistance, a close look must be taken at all products entering the market.

Understanding the mechanisms of attachment could possibly help in designing strategies to prevent early adhesion, thereby controlling biofilm formation. Recently, a team of biophysicists has discovered that the contact area between the bacterium and the surface does not have to be large in order to result in a strong adhesive force[180]. Different appendages are involved in the process of bacterial adhesion. Bacterial appendages include fimbriae, pili, curli and flagella. In *E. coli*, curli have been identified as the

appendages responsible for early development of biofilm architecture and their irreversible attachment[46]. Thus, many antiadhesive coatings target curli in their attempt to curb bacterial adhesion.

I.6.v. Nanoscale Topographies for Biofilm Control

Biofilms growing in all environments have developed increasing resistance to antibiotics, biocides and other chemical anti-biofouling methods. This has created a need for other non-toxic methods of biofilm prevention and removal. Researchers have spent considerable effort in developing anti-adhesive coatings to deter initial biofilm attachment and diminish the adhesion strength of bacteria to the substrates. This development can be accelerated through nanotechnology.

An area of interest has been the use of mechanical forces to impact biofilm formation. Most innovative technological fields take their inspiration from nature. Nanotechnology too has taken inspiration from naturally existing biomechanical interactions. One of the most popular and well-studied examples of nanotechnology in nature is the ability of the gecko to walk on walls. It was not altogether surprising when they were also found to possess biocidal properties as well. Biotemplate replicas of the nanotipped hairs of gecko skin were shown to kill pathogenic bacteria with high efficiency[131]. Researchers branched out further to gain inspiration from nature. Watson *et al.* have spent many years examining the cuticular micro- and nanostructures on insects. Not only do these structures exhibit incredible anti-wetting, anti-drag, and various photonic properties, the varied nanotopographical structures on the insect cuticles have

also been shown to be antibacterial[181]. Cicadas, in particular, have been shown to naturally exhibit an antimicrobial wing topology [182,183,184].

An important question that has arisen is whether the antimicrobial effects of surfaces are due to their topographies or due to some other behavior such as their wetting nature. For instance, the superhydrophobic nature of cicada wings could be attributed to their killing[185], however other groups have also shown that the antimicrobial nature of the cicada wings is due to the physio-mechanical interactions that occur and not its ability to repel the microbes [182,183].

Nowadays, bioinspired nanoarchitecture is not uncommon. Researchers have attempted using several different materials, from Titanium to Carbon Nanotubes, and various polymers to make these nanostructures. These have provided varying degrees of success, from the complete elimination of bacteria to control over adhesion on the surfaces.

It is important to consider the effects of these nanostructures upon the bacteria they encounter. The low effectiveness and safety of traditional disinfectants such as UV, chlorine, and heat, have spurred researchers to develop innovative methods of controlling microbial biofilms. In this regard, many antimicrobial surfaces coated with a range of antibiotics, nanoparticles, and anti-adhesives have been developed, focusing on the initial adhesion phase of biofilm development. Since these coatings do not last for long periods of time, a more effective solution is needed. By developing materials that inherently possess antibacterial or anti-adhesive qualities, scientists aim to curb biofouling.

Nanostructured surfaces occur abundantly in nature, from the superhydrophobic surfaces of lotus leaf which provide anti-adhesive quality to the various cuticular structures of different insects with anti-wetting, anti-drag and even optical properties [181]. The cones and needles (of different aspect ratios depending on the variety) present on the surface of cicada wings provide a topological barrier against microbes. They have been shown to cause the cell-wall rupturing of *S. cerevisiae* [181] and are also lethal to *P. aeruginosa* [186].

Naturally occurring bactericidal surfaces are useful in providing a starting point in the design of antimicrobial structures. Ivanova et al have had success in fabricating various bactericidal nanostructures (nanograss, pillars, and cones) on black silicon[187]. Biomedically implantable materials such as Titanium, have been nano patterned to resemble the surface of dragonfly wings and shown to possess selective bactericidal activity[188]. The use of polymeric surfaces has offered a much greater deal of control in terms of methods of fabrication and the ability to synthesize composite materials[189,190]. The infusion of antibacterial substances such as nanoantibiotics and nanoparticles with polymeric materials provides a broad range of substrates to choose from while developing antibacterial surfaces[191].

The current approach, however, is largely trial and error based. This is evidenced in the numerous research papers in this area, each of which has used different materials (each with different properties such as stiffness and tensile strength) which would affect bacterial adhesion and biofilm formation in their own way[120]. While they have had a modicum of success, there has not been clear-cut reasoning behind their approach besides

availability or ease of manufacturing. There has recently been a shift in this trend to a more informed method of engineering surfaces[192]. Researchers are now attempting to tease apart the factors that guide bacterial adhesion to purposefully design surfaces.

I.6.vi. Bioelectronic Interfaces

Bioelectronic interfaces are the bridges between advanced electronics and biological materials. Nowadays they are commonly found in everyday life. From glucose monitors for diabetes management to ingestible electronics to detect intestinal bleeds[193], the bioelectronics field has advanced at an unprecedented rate. As the world develops more nanotechnology, its association with biology is becoming indistinguishable. Living things have developed strategies to overcome nature's biggest challenges. Bioelectronics interfaces pre-existing biological reactions with electronic equipment for human use.

Bacteria are ideal candidates for this purpose. They are miniature living bioreactors capable of sensing a variety of biomolecules, chemical, and mechanical signals. They have relatively short generation cycles and are compatible with almost any environment in the world. We are now using their evolutionary adaptations as biosensors. They offer the potential uses of their various biosensing strategies: optical, mechanical, electro sensing. Bacteria are also used due to their inherent electrochemical activities. They can perform similar oxidation/reduction reactions as on electrodes. Since their environment is basically an ionic solution, it lends itself to the conductance of electricity.

Bacteria can also naturally produce electricity. These electrogenic bacteria are even more amenable to being used in electrochemical systems. They allow the transfer of electrons to and from their membrane using a process known as extracellular electron transfer (EET)[194]. EET process connects intracellular pathways of bacteria to external environmental electrodes and other bacteria using the EPS[18]. One such electrogenic bacteria that has been studied extensively is *Lactobacillus*[195,196].

Bacterial regulation of gene expression and the consequent production of molecules for intra biofilm communication is known as quorum sensing. Bacteria use this as a method of microbe-microbe interaction communication. Once the quorum sensing molecules reach a certain threshold, genetic mechanisms are activated thereby enabling cross-talk within biofilms. Single swimming bacteria can sense electrical signaling to join surface colonies[197]. Intra and interspecies communication can take place through the regulation of quorum sensing molecules. Another method of bacterial communication is via electromagnetic fields. Sound and light waves are thought to generate these electromagnetic fields around bacteria[198].

By combining this natural mode of communication with semiconductor materials, scientists have developed bioelectronic devices. In the nano world, nanostructured electroconductive materials such as metal/semiconductor have been extensively studied to aid in electrocatalysis[199]. An excellent review of such advancements has been written by Kato et al[200].

GaN is one such semiconductor material. It is a group III/IV wide bandgap semiconductor material that possesses a phenomenon known as persistent photoconductivity (PPC). Photoconductivity is when photons get converted to electrons. It is a common feature of group III/IV semiconductors. However, the electrons remain on the surface longer during persistent photoconductivity[201].

We assumed that bacterial adhesion could be affected by the application of an electric field. Gall et al. hypothesized that the electric field would impact the electrostatic energy barrier between the bacterial cell and the charged substrate[202]. They noticed that a negative potential increased the rate of bacterial adhesion and vice versa. Other scientists noticed that the bacteria were alive after passing cathodic current, while they became inactive with the application of anodic current. Cathodic currents seemed to create a significant change in the extent of the detachment of the bacteria[203]. When physiologically relevant levels of current (5 and 20 mA) were applied to cultures of *P. aeruginosa, S. aureus* and *E. coli*, no change in growth was reported although there was a reduced rate of growth in Pseudomonas[204]. More recently, Berthelot and Neethirajan applied low voltage currents (0, 0.07 and 0.125 mA) to cultures of *P. aeruginosa, E. coli* and methicillin-resistant *Staphylococcus aureus* (MRSA) and noticed that the current induced an increase in cellular directionality and a drop in velocity[205]. None of the studies mentioned that there was any change to the size of the individual bacteria upon electrical stimulation. When scientists exposed bacteria to persistent photocurrent produced by UV light on ZnO powder, as in the research by Ann et al, they noticed that there was a potential bactericidal effect[203].

Examining the mode of attachment under different physiological conditions provides an insight into what is happening at the biointerface. Snyder et al. examined such interactions at the interface of the persistent photoconductive semiconductor GaN with PC12 cells[206]. They noticed a significant change in the adhesion of the PC12 cells to the charged substrate due to the charge accumulated on the surface. The same group branched out to see the effect persistent photoconductivity had on other microbes. There noticed a change in membrane voltage of the yeast, *S. cerevisiae* [207] and have proven that there are internal physiological responses within bacteria such as *Pseudomonas aeruginosa* when exposed to photocurrent[208]. Changing the surface chemistry by UV radiation can influence biofilm properties. This information is helpful to know while designing interfaces. GaN has proven to be an invaluable substrate for biocomputational purposes due to its photoconductive properties, biocompatibility, and ease of chemical functionality leading to different surface properties.

I.6.vii. Tuning Substrate Stiffness for Bacterial Control

Another method of biofilm control is through the alteration of substrate stiffness. Changing the stiffness of substrates that stem cells grow on has shown to influence their differentiation and lineage [209–212]. Substrate stiffness increases the organization of the cystoskeleton[213]. For the most part, if the stiffness of the substrate is similar to the biological equivalent in the human body (e.g., tissue, muscle), the stem cell differentiates into that lineage[210]. Normal (non-stem cells) tissues also respond to changes in the substrate stiffness [214,215,216]. Their individual responses depend on cell type [217]. Altering

such a basic property can influence the choice of materials for biointerface applications. The stiffness property is not exclusive of the other material properties such as surface chemistry, material chemistry or topography[218]. A proper evaluation would involve the combined consideration of all these properties and not their individual effects.

Stiffness or elasticity is the ability of a material to return to its original conformation in response to an applied force[219]. There is a difference between stiffness and strength: a material can be strong and elastic or strong and stiff. The mechanical property that denotes this relationship is called Young's modulus. It is the measure of the ability of a material to withstand changes in length while undergoing tension.

Young's Modulus:

$$Y = \frac{\sigma}{\epsilon}$$

Where Stress σ: force on an object on an area perpendicular to force

$$\sigma = \frac{F}{A}$$

and strain ϵ: length change relative to absolute length.

$$\epsilon = \frac{YA}{l}\Delta l$$

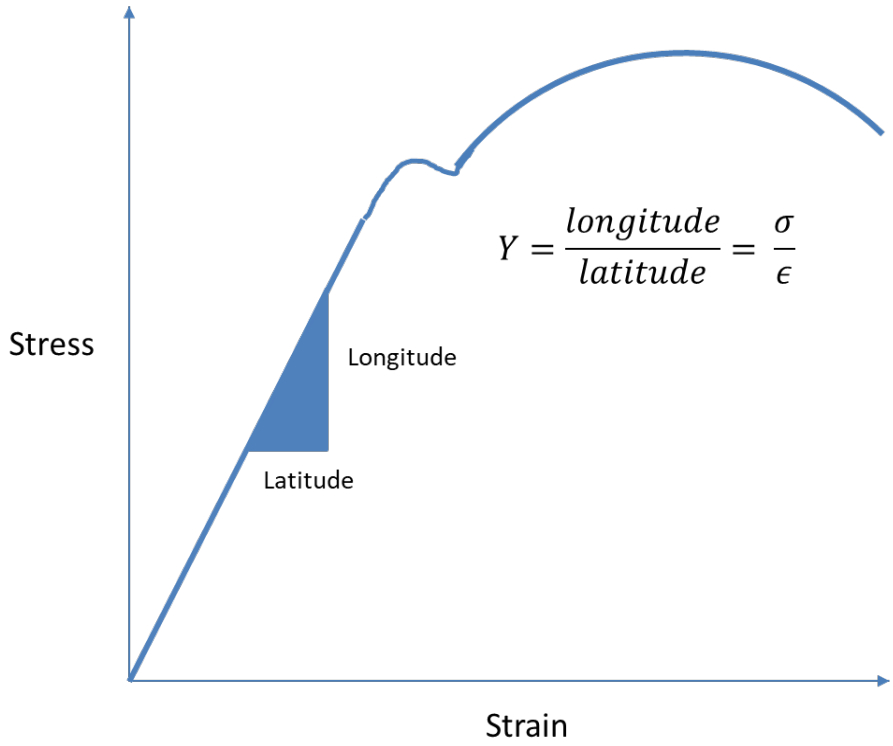

Figure 1.6 A Standard Stress-Strain Curve used to Measure the Modulus of Elasticity.

Altering the stiffness of substrates has been shown to influence bacterial adhesion [220,221]; fewer bacterial cells adhere to softer surfaces. Song *et al*. have gone further and shown that bacteria adhering to the harder surfaces are more susceptible to antibiotic activity [222]. This result has resulted in a shift in the paradigm of creating antibacterial surfaces. The discovery by Kolawi et al that bacteria adhere more to thinner hydrogels[223] also has implications in possible wound healing. This area is still new, and few papers exist that evaluate the mechanisms affecting bacterial adhesion. The most noteworthy amongst these is by Song et al, having discovered that motility of the bacteria is greater on stiff surfaces during early biofilm formation[224]. They further investigated whether motility

was in any way responsible for the bacterial response to changes in stiffness. The *motB* (isogenic flagellar mutant) is affected during this response.[224]

I.7. Bacterial Stress Responses

Bacteria have evolved strategies to survive a vast number of unfavorable conditions. Their stress responses allow them to acclimate to changes in their environment. External sensors trigger transmembrane cascades that induce morphological plasticity in cells[225]. Some bacteria change their shape to account for environmental stresses, while others go into sporulation mode and wait until conditions are more favorable to grow[225]. *Pseudomonas putida* develops vesicles on its OM to alter its hydrophobicity as an adaptive response[226]. In yeast, external stressors encourage the hyphal state to change into the normal state to assist in host colonization[227]. Different mechanisms are involved in detecting the various types of stresses: temperature shock, osmotic, shear, antibiotic and even biofilm induced stresses. These stress responses are actually useful for the bacteria. For example, Staphylococci increase their mutability in response to oxidative stress[228]. Repeated exposure to stressors can even lead to antibiotic tolerance[229].

These stressors direct spatial coordination within biofilms. Different layers within the biofilm are assigned specific functions depending on their location and proximity to stressors[230]. They help determine which phase of growth to adapt, either stationary or proliferative[225]. It can be concluded that stress responses guide biofilm architecture, bacterial morphologies, and microcolony functions[230].

Bacteria initiate the cell envelope stress response (CESR) following exposure to mechanical perturbations[225]. These responses have evolved to help the bacteria adapt to their environment. A common regulatory mechanism involves sigma factors (σ). These are a group of small proteins that bind to RNA polymerase which targets genes to induce specific stress responses[166]. Stress proteins maintain physiology and homeostasis of the bacteria. They are also essential for viability[231].

During conditions of duress, *E. coli* accumulate a specialized sigma factor, RpoS (sigma factor σ^s). They function only when there is a high enough number of cells in the stationary phase to warrant a response. Measuring the activity of catalase, an important enzyme that protects cells from reactive oxygen species (ROS) damage, is an indirect indicator of RpoS activity[166]. Stress proteins also affect mitochondrial activity, increasing the accumulation of ROS species (H_2O_2, NO, H_2S, etc.). Sigma factors function as cell-induced cellular messengers and activate proteins OxyR, SoxR[231]. The intensity of stress controls whether the cells survive.

In response to mechanical stresses, several envelope stress pathways become activated: Cpx, Psp, EnvZ/OmpR, Bae, and Rcs[232]. The Cpx/ Rcs pathways are the most important amongst these. Both the Cpx and Rcs pathways are switched on by outer membrane proteins known as porins. Porins act to convert mechanical stimulation into intracellular signals. The Cpx pathway is activated as a response to misfolded proteins on the outer membrane of the bacteria[225]. The Cpx pathway regulates both curli operons: csgDEFG and csgBA and controls pili function[225,233]. Rcs also responds to outer membrane stress. It negatively regulates csgD, which is responsible for the regulation of

csgBA[166]. In this way, the Cpx and Rcs pathways act as on/off switches for biofilm formation.

These genetic changes within the bacteria in response to mechanical stresses induce physical changes to the cell envelope protein development. Some cells lose their cell wall (L-forms) in response to osmotic stresses or antibiotic-induced membrane perturbations. The elongation of cells (filamentation) is a common response to DNA damage as is the shape change from rod-shaped to coccoid morphology[225]. When bacteria are starved, they become spores until more favorable conditions appear. Other morphological changes include the addition of external adhesion-related appendages[84]. For example, contact with solid surfaces induces the production of swarmer cells, i.e. cells with more flagella[225].

The next few chapters deal with bacterial responses to change of the substrate topography, photoconductive stimulation, and stiffness. This work lays the foundation for the creation of better bio interfaces.

I.8. Conclusion

The control of biofilm formation is an ongoing problem. A potential strategy to combat its growth and prevent its initial adhesion is to modify substrate properties. Such properties include surface chemistry, topography, chemical composition, wettability, mechanical load, etc. In this thesis, we examine the physiological effects of three specific material properties on the bacteria *E. coli*. We hypothesize that changing the substrate's material properties will alter the microbial biological response.

CHAPTER II

BACTERIAL ADHESION AND BIOFILM FORMATION ON POLYMERIC NANOSTRUCTURED SURFACE

II.1. Introduction

Biofilms are three dimensional microbial thin films that are composed of living cells and an array of secreted biomolecules that includes cell wall and adhesion proteins, polysaccharides, lipids, and DNA[234]. Interfaces whether between air/liquid or liquid-solid, serve as the ideal locations for biofilm development and hence, these complex living communities are found on virtually every surface on earth[15]. Although biofilm composition varies from microbial species to species, they serve similar functions providing protective barriers from mechanical, chemical and physical damage; controlling microbial physiology to drive drug resistance and structurally organized diverse microbial communities that enable adaptation and evolution[235].

Many antibiotic-resistant microbes demonstrate enhanced biofilm production and adhesion[161]. Furthermore, the communal aspect of biofilm compounds the risk of antibiotic resistance by creating an environment that promotes the spread of antibiotic resistant genes through processes like conjugation and transformation[32].

At least 65% of all persistent and chronic bacterial infections are biofilm related[8,236,237]. Subsequently, biofilm formation in the context of medicine has caused billions of dollars of losses in industry and are responsible for numerous deaths[8,236,238]. Due to the growing tolerance to antimicrobials, which are generally designed to treat freely swimming planktonic cells, it has become increasingly difficult to treat biofilm-related infections[239].

Microbial biofilms form in a multi-step process [235,240,122] that begins with the initial and perhaps most crucial step the immediate and reversible attachment of planktonic bacteria to a surface. This step is controlled by surface topology, composition, and local interfacial physicochemistry[24,241]. Under favorable conditions, these adsorbed microbes will develop stronger and irreversible adhesive interactions that are followed by proliferation of the attached microbes, the secretion of extracellular materials, and the formation of a biofilm matrix that encloses the colony [15,1].

Surface topology has been demonstrated to control the adsorption/adhesion of a broad range of cell types including microbial cells. It was discovered that bacteria possess preferential adhesion, i.e. the ability to select adhesion sites [242–244]. Roughening the surfaces has the dual capability of promoting and preventing bacterial adhesion. For instance, it is utilized widely to improve the adhesion of biofilms in bioreactors[245]. When the roughness was reduced to the nanoscale bacterial adhesion was seen to increase although different bacteria had different attachment patterns [246,247]. Surface roughening is more commonly known for its ability to prevent bacterial adhesion. Roughened surfaces can act in both bactericidal and anti-adhesive capacities. Naturally occurring rough

surfaces such as the lotus leaf possess nanostructures that provide a superhydrophobic surface property[130], which enables liquids to simply roll off. Ivanova et al. were the first to report that naturally occurring nanostructures present on cicada wings rupture microbial cells upon contact[183]. Biomimetic surfaces have been influenced by such patterns and have improved the development of antibacterial surfaces. Black silicon [187,248–250], titanium oxide[188,251,252] and various organic polymers [243,253–256] are some materials that have been used for anti-biofilm patterning of surfaces. Depending on the technique used for surface modification, the material used and chemical modifications[168], a plethora of patterned structures can be produced. Direct penetration of nanostructures kills bacteria by piercing through their cell membranes [257]. Other antibacterial surfaces work by stretching the cellular membrane over carefully spaced pillars[114]. Determining the range of parameters required for developing antibacterial nanostructures is ongoing.

However, little work has been shown to demonstrate whether there is a relationship between the immediate response of bacteria to different nanostructured surfaces and the physical properties that are a product of these surfaces. To address this, I have examined the acute interactions of *E. coli* when in contact with twenty-one different polymeric nanostructured surfaces. I test the hypothesis that nanostructured polymeric surfaces will control bacterial deposition (the initial phase of biofilm formation) and will alter cell viability and adhesive potential. I show that changes to nanoscale modification of polymeric surface often change the acute response of *E. coli*, these changes are not predicted by changes to the formation of specific surface morphologies or changes to surface energy. I conclude that the observed changes in bacterial behavior is controlled

foremost by the surface composition, perhaps by its mechanical properties or subtle changes to interfacial chemistry. Many of the observed changes in bacterial behaviors that are exhibited by the *E. coli* bacteria on these surfaces are reduced or eliminated which suggests that these bacteria are able to adapt to surface features, even those that appear to be initial deleterious.

II.2. Materials and Methods

II.2.i. Fabrication of Polymeric Nanostructured Surfaces via Reactive Ion Etching

The following polymers substrates were used: Polycarbonate (PC), polyimide (PI), Perfluoro alkoxy alkane (PFA), Polyethylene (PE), Acrylonitrile Butadiene Styrene (ABS), Acetal polyoxymethylene (POM), Polyethylene Terephthalate Glycol-modified (PETG; McMaster and Carr). The polymer substrates were thin films and had a uniform thickness of 0.005" (127 μm) except for PETG at 0.0625" (1587.5 μm). Polymer thin films were cleaned by ultrasonication for 10 min in isopropyl alcohol (IPA) to remove surface contamination. The samples were etched via oxygen plasma cleaning using a South Bay Technology Model PC-2000 plasma cleaner. Control over directionality (i.e. anisotropic versus isotropic etching) was achieved as described by Nowlin and LaJeunesse (2017). The instrument specifications are as follows: RF discharge at frequency 13.56 MHz capacitively coupled plasma (CCP) operated at forward power 100W with a chamber pressure 180-200mT. The exposure times of 10 min for the isotropic etch and 1 min for the anisotropic etch were used. Each polymer sample was cut

into 1 cm^2 squares before use and then placed at the bottom of the PEGylated well for assays.

II.2.ii. Scanning Electron Microscopy

I characterized all Polymeric NSS using a Zeiss Auriga Scanning Electron Microscope (SEM) located in the electron microscopy facility at the Joint School of Nanoscience and Nanoengineering. Images were collected using an accelerating voltage of 5kV after the deposition of 5nm of gold/palladium using a Lieca EM ACE2000 sputter coater. I characterized the surface morphology of the polymeric substrate fabricated for these experiments before and after exposure to the bacteria using). The polymeric samples containing microbes were prepared as follows: 1cm2 pieces of each polymeric substrate with bacteria were prepared as described above, fixed in Karnovsky's solution (2.5% glutaraldehyde / 2% formaldehyde solution in 1 M cacodylate buffer (pH 7.4)) overnight at 4℃ and dehydrated with an ethanol dehydration series (35%, 50%, 75%, 90%, 95%, 100%). The dehydrated samples were mounted on SEM stubs and sputter-coated with 5 nm Au using a Leica EM ACE2000 before SEM analysis at EHT = 3kV.

II.2.iii. Contact Angle Measurements of NSS Polymeric Surfaces

Static contact angle (CA) measurements were made using the Ramé-Hart 260-F4 contact angle goniometer and analyzed using the DROPimage Advanced software. 2 µl of deionized water drops were placed on the surfaces. The contact angles were made on

at least 3 different locations on each surface and ten measurements were taken. Data were analyzed using student t-test function in MS Excel.

II.2.iv. Bacterial Strains and Culture

I used an *E. coli DH5α* GFP expressing plasmid that also carried an Amp^r selection gene. For each experiment, a colony was selected from a freshly streaked LB plate that contained Ampicillin; cultures were grown overnight in a 5 ml LB liquid culture containing ampicillin. All the liquid cultures were grown at 37℃ in a shaking incubator. At this point, a solution of 20% L-arabinose was added to the growing culture at a ratio of 1:100 (arabinose: total culture volume). The overnight culture was used to start/spike fresh cultures the next day and adjusted to an OD_{600} of 0.05. This was allowed to grow to an OD_{600} of 0.1 measured on the Thermo Scientific NANODROP 2000C. All the assays were performed in PEGylated 24-well plates in a shaking incubator at 37℃.

II.2.v. Cell Adhesion, Membrane Integrity, Cellular Proliferation/Colony Unit Forming Assays

The preparation of the microbes for all cellular assay is as follows: 1 ml of an 0.1 OD_{600} *E. coli* culture was added to a well in a 24-well Polyethylene Glycol (PEG treated plate which contained a polymeric sample at the bottom – PEG pretreatment of the well limited the binding of cell to the well bottom and walls, PEG treated was also used as a negative control; the bacteria cells/sample were incubated with the surface for 1h at 37 ℃ in a shaking incubator; after incubation, the well/sample was manually washed twice with

1x PBS; then used to perform one of the standard assays: adhesion, membrane integrity/viability, colony unit forming (CFU).

For cell adhesion, bacteria that have been labeled with GFP were mounted onto a slide and the number of cells/fields of view were manually counted using Zeiss Axio Vision spinning disc confocal microscope. At least 3 images were obtained from each sample at 100x. The total number of cells was counted per field of view and averaged. For the membrane integrity assay, cells were labeled with 0.5 µl/ml acridine orange/ethidium bromide in 1x PBS for 1 min followed by another wash with 1x PBS. The fluorescence was assayed using the Zeiss Axio Vision spinning disc confocal microscope with ex488/em 518 for acridine orange (intact cells) and ex535/em617 ethidium bromide (permeabilized cells). At least 3 images were obtained from each sample at 100x. The total number of cells in each channel was counted manually and by a Gen5 plate reader and the ratio of red to total cells (red and green-labeled cells) was determined and averaged. An additional membrane permeability study was performed using Propidium iodide (PI) to support EtBr observations.

To perform a standard CFU/ml assay to determine the density of living cells on the polymeric nanostructured surfaces [183,258]. Serial dilutions were performed, and plating was done on LB agar plates with Amp. Colonies were counted after 24 h of incubation at 37˚C. Plate colonies are representative of the viable cellular concentration in CFU/ml which were then extrapolated according to the dilution factor to obtain actual concentrations. All experiments were performed in triplicate with at least 3 biological and 3 technical replicates.

II.2.vi. Statistical Analysis

A standard t-test and a one-way ANOVA were performed on all values to determine the statistical difference ($p<0.05$) in Microsoft Excel.

II.3. Results

II.3.i. Fabrication/Characterization of Polymeric NSS Materials

To generate the twenty-one different surfaces to examine early *E. coli* interactions with nanostructured topologies, I modified seven different polymeric thin film substrates using two different oxygen plasma etching parameters: an isotropic etch and a directional anisotropic etch Figure 7A.

Polymers are a common component of many biomedical devices and allow a great deal of control in terms of methods of fabrication and the ability to synthesize composite materials [259,260]. Oxygen plasma etching is a relatively well-understood technique to allow surface modification of polymers to increase surface energy, hydrophobicity and reduce bacterial adhesion to surfaces[261]. Plasma etching has been shown to etch nanotopographies onto various materials while also having the advantage of allowing the polymer to retain its bulk properties [150,262–265]

A

List of Polymers	Bulk CA	Isotropic CA	Anisotropic CA
Polycarbonate (PC)	98.64 ± 0.08	29.74 ± 0.09	49.59 ± 0.16
Polyimide (PI)	73.05 ± 0.08	17.94 ± 0.48	37.65 ± 0.10
Perfluoroalkoxy alkane (PFA)	111.34 ± 0.19	132.09 ± 0.04	121.22 ± 0.07
Ultra High Molecular Weight Poly Ethylene (UHMW PE)	79.02 ± 0.06	8.6 ± 0.74	80.46 ± 0.25
Acrylonitrile Butadiene Styrene (ABS)	112.36 ± 0.09	12.1 ± 4.27	60.76 ± 0.16
Acetal Polyoxymethylene (POM)	74.62 ± 0.07	75.075 ± 0.05	67.25 ± 0.30
Poly Ethylene Terephthalate Glycol-modified (PETG)	85.06 ± 0.06	22.125 ± 0.05	18.28 ± 0.05

B

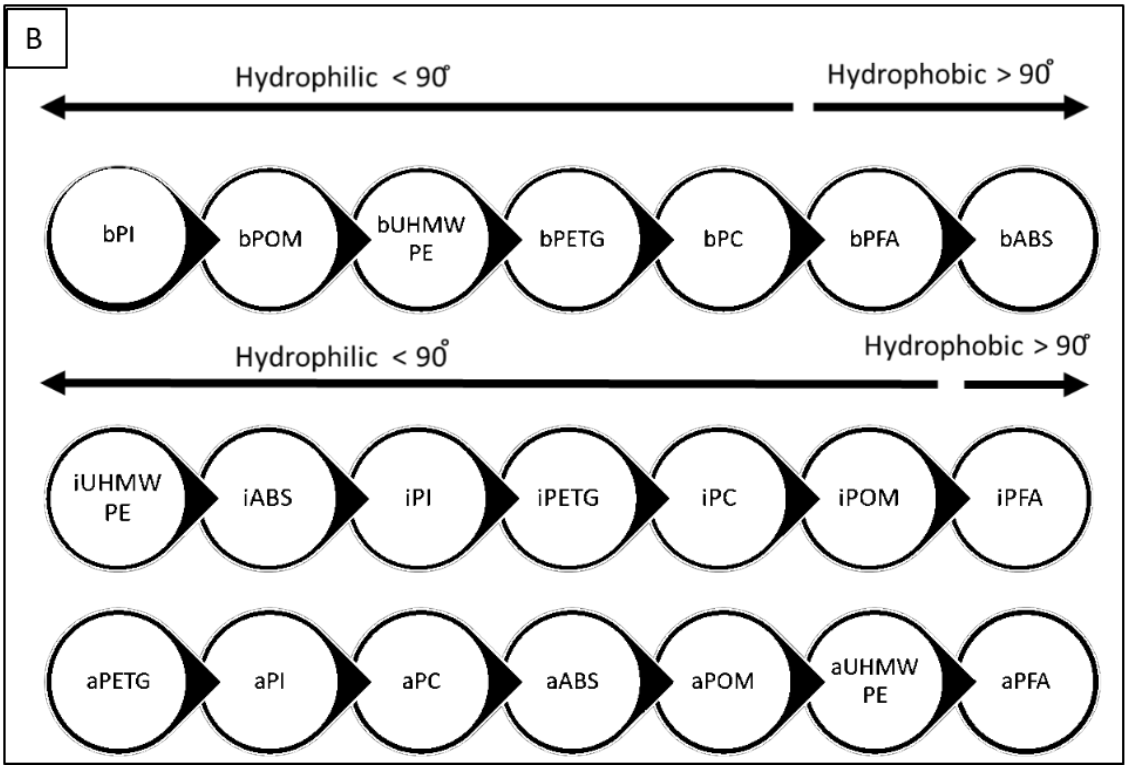

Figure 2.1 List of Polymers and Contact Angles. A)The list of polymers used in this study and their corresponding contact angles measured using a Rame Hart Goniometer. B) The contact angles of the 7 different plastics and their etched counterparts listed in order of their wettability.

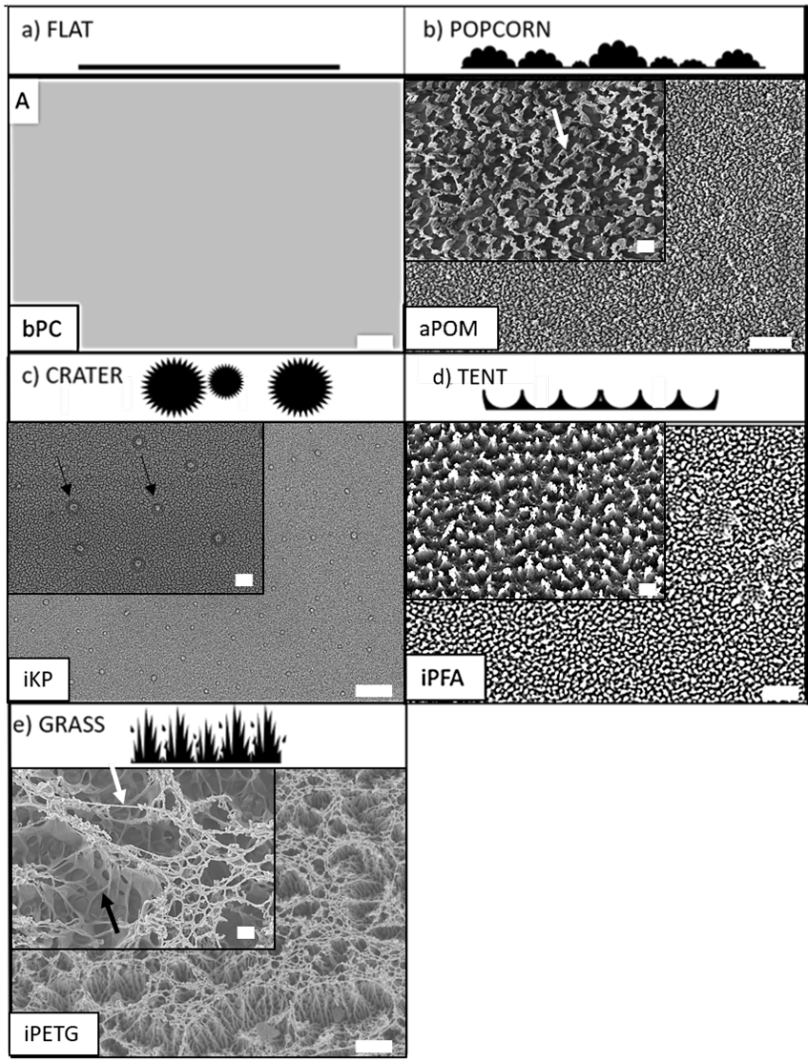

Figure 2.2 Topographies Obtained Through Oxygen-Plasma Etching .Figure indicates the different topographies obtained after oxygen plasma etching treatment of the bulk polymers. A)a Flat B) Popcorn; white arrow indicates the irregularly etched polymeric material with canyon-like features C) Crater: Similar to the popcorn surfaces in roughness but has circular rings etched as well. D) Tent; Conical projection formed through the etching procedure E) Grass; found only on the iPETG, the plasma has eaten away at the material leaving behind a stringy network and porous base. White arrow points to the stringy connections and black arrow indicates the pores. The scale bars of the insets are 200 nm, and all the rest are 1μm in length.

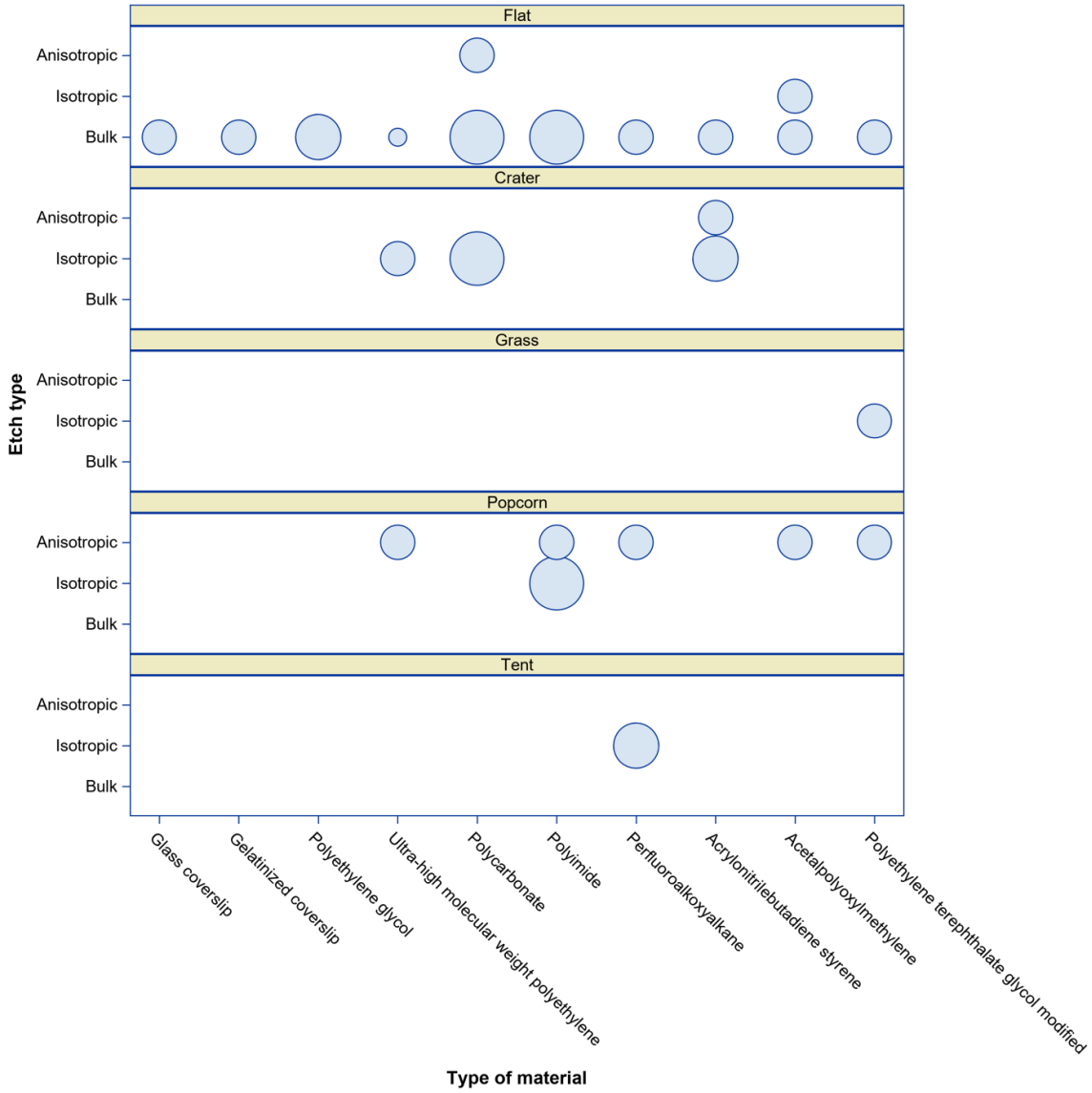

Figure 2.3 Pattern Distribution by Etch Type and Material. The distribution of patterns obtained through oxygen plasma etching of the 7 polymers. †Graph developed by Dr. Cary Cotton, UNC.

Plasma etched polymeric surfaces exhibited four distinct nanoscale topographic configurations: “flat”, “popcorn”, “crater”, “tent”, or “grass” (Fig. 8, Supplemental figure 8). All the bulk samples were flat, with no protrusions or defects (Fig 8). The only etched sample that was flat was the anisotropically-etched polycarbonate (aPC), with small features (440 nm) that lended angular sharpness to the surface but was otherwise flat (Supplemental Image 1). The distribution of the patterns obtained through plasma etching of the polymers is displayed in Figure 9.

The most common nanoscale morphological feature produced by our etching processing was the “popcorn” feature (Figure 9). Four polymeric surfaces, isotropically etched PolyImide (iPI), anisotropically etched Polyimide (aPI), anisotropically etch perfluoroalkoxy alkane (aPFA), and anisotropically etched Polyethylene terephthalate glycol-modified (aPETG) displayed a “popcorn” morphology (Fig. 8b: arrow). The “popcorn” structures are nanoscale waffle-edged structures with sizes that range between 22 and 70 nm and are distributed on the surface with densities of (minimum 10 features/ 1 μm^2 to maximum 100 of features/1 μm^2). The anisotropically etched acetal polyoxymethylene (aPOM) has a popcorn feel due to the increased distance (~100 nm) between the popcorn structures. Anisotropically etched Ultra High Molecular Weight Polyethylene (aUHMWPE) has preferential directional etching with popcorn texture.

Four surfaces, isotropically etched polycarbonate (iPC), acrylonitrile butadiene styrene iABS, aABS, and Ultra-high molecular weight polyethylene (iUHMW PE) exhibited a “crater” surface topology; a crater topology was defined as irregular circles created as a result of the etching process. The craters on the surface of iPC (5-10 per 10

μm^2; i.e. 144 μm^2) were between 100-400 nm in diameter. The craters on the iABS were between 300-500 nm in diameter, but they were sparsely distributed, with only 2-3 per 10 μm^2 (144 μm^2 at 10,000x magnification (Table 1, figure 8c). In sharp contrast, the craters on the aABS surface were dense and interconnected.

The tent configuration (figure 8d), which was present only on the iPFA, exhibited small pyramidal formations (between 200-400 nm) capped with 3-8 spherical structures that ranged in size between 25-50 nm in diameter.

I only observed the "grass" morphology on a single etched surface, iPOM. The "grass" surface (figure 8e) was composed of an interconnecting web of nanoscale thin tubes (~25 nm in diameter) on ridged mounds (Supplementary Image 6).

Like many nature-inspired nanostructured surfaces [127,131,132,266], several of the fabricated surfaces also displayed hierarchical structures in the micron-scale range. For instance, on iPFA, the surface appears to be popcorn at the micron level. The surface of the iUHMWPE has parallel striations, while aUHMWPE exhibited preferential directional etching, with deep micron-scale grooves (approximate size) that was composed of popcorn texture.

II.3.ii. Contact Angle

To characterize changes to the surface energy of these polymeric surfaces I performed a static contact angle analysis [267,268]. While contact angle is a macroscopic effect the data reflect a detail of nanoscale physicochemsitry of the surface as a function of free energy and therefore is a powerful surface characterization tool [128,269]. Surfaces

that demonstrate contact angles below 30° are considered hydrophilic, with contact angles below 10° being superhydrophilic, while those with contact angle greater than 120° are considered superhydrophobic [267,268,126]. High contact angles denote low surface energy with reduced free bonding opportunities, while low contact angle materials have higher free energy [126]. Surface modification via plasma etching of all polymeric materials used in this study resulted in changes to the contact angle when compared to the initial bulk materials (see figure 7). I observed contact angle measurements in our fabricated nanostructured surface ranging between 8.6° for the cratered surface, iUHMW PE (8.6° ± 0.74°) (Figure 7A) to the highest angle was for "tent' surfaced, iPFA, 132.09° ± 0.04°. PFA surfaces, bulk, isotropic and anisotropically etched, were uniformly hydrophobic, with above 110°. The material that showed the greatest degree of variability compared to its etched counterpart is ABS (bABS = 112.36° ± 0.09°; iABS = 12.1° ± 4.27°

II.3.iii. Bacterial Adhesion to Polymeric NSS Materials

In these experiments, I used *E. coli* transfected expressing a GFP reporter gene (REF for the GFP plasmid). I examined bacteria adsorption on untreated glass coverslips as a control to establish a baseline of bacterial adhesion[270]. I used polyethylene glycol (PEG) treated glass slides as a negative control – PEG treatment reduces cellular adhesive interactions with surface substrates[270]. I also used gelatin (50% w/v) treated glass slides as another positive control; gelatin treatment has been demonstrated to enhance the adhesion of several different cell types to surface substrates including

bacterial cells [271,272]. As expected, I observed virtually no bacteria per field of view (10 μm^2) on PEG-treated surfaces (2 ± 0.3 cells /10 μm^2; Figure 14); while glass surfaces treated with gelatin exhibited higher numbers of bacterial cells per 10 μm^2 than untreated glass (175 ± 0.5 cells vs 40 ± 0.3 cells; Figure 14).

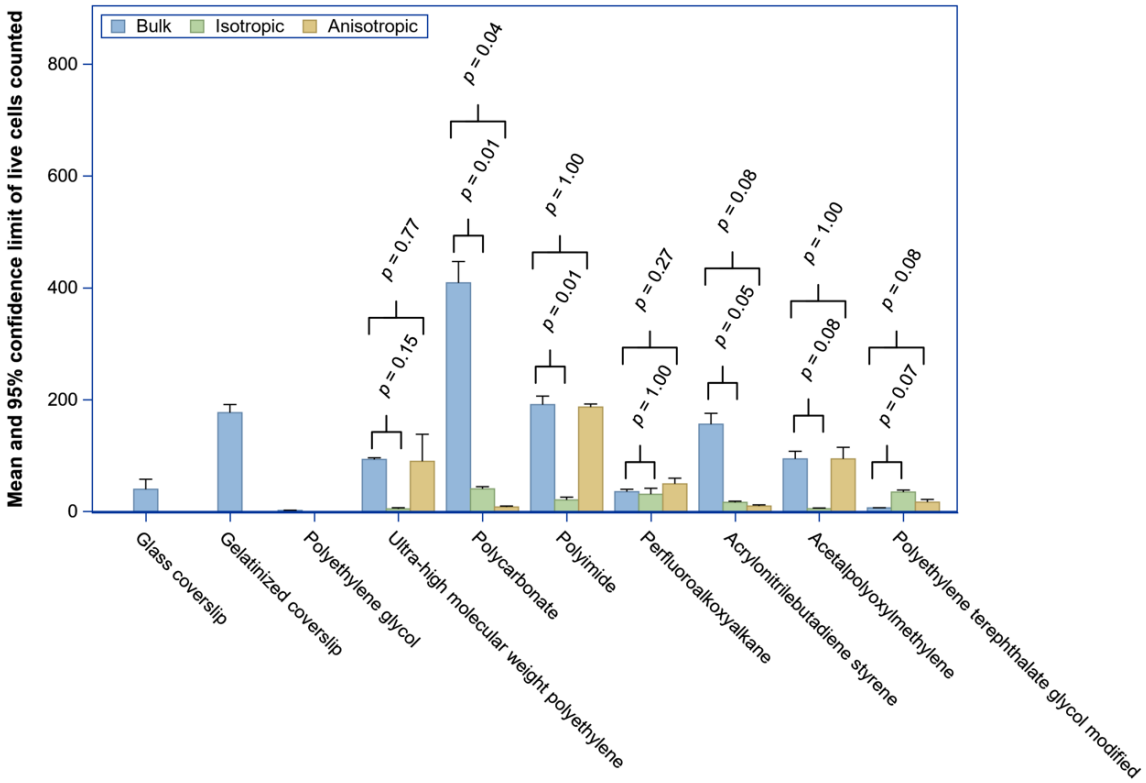

Figure 2.4 Statistical Analysis of Live Adhered Cells by Material and Etch Status. Mean Count of Live Adherent Cells Counted by Material and Etch Status, with the Upper 95% Wald Confidence Limit and Two-sided p Values for the Exact Savage Multi sample Test Comparing Etch Status Within Materials. †Graph developed by Dr. Cary Cotton, UNC.

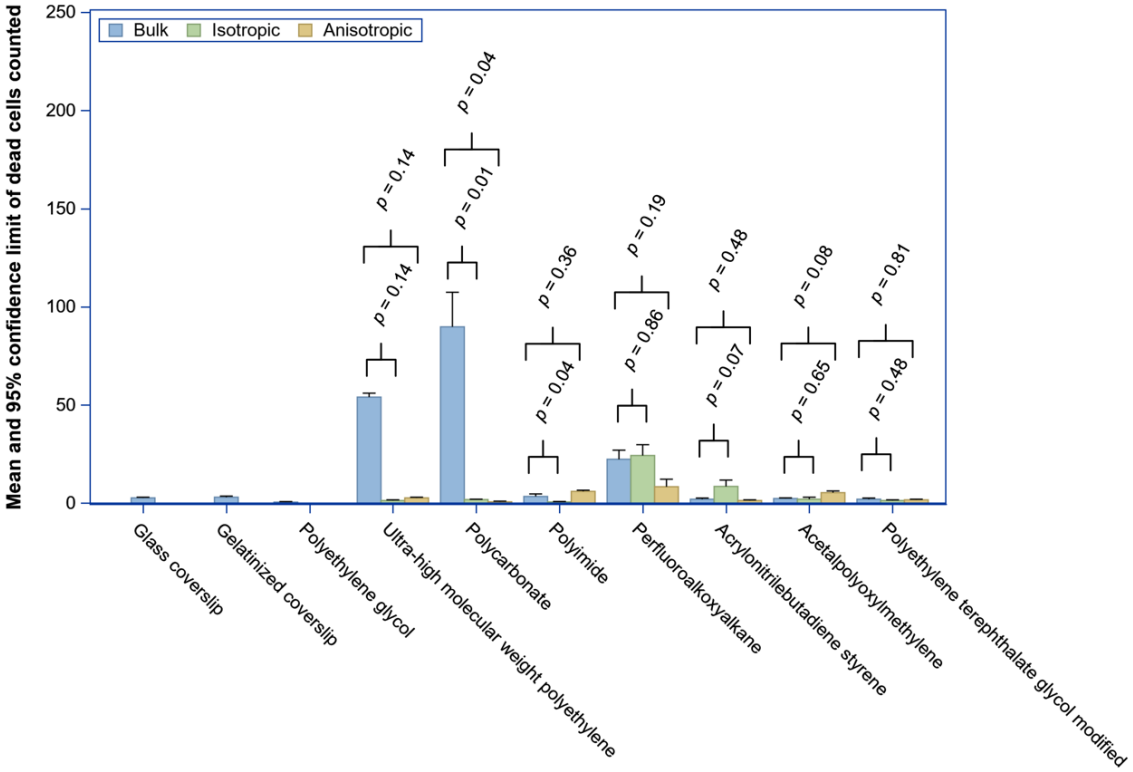

Figure 2.5 Statistical Analysis of Dead Adherent Cells by Material and Etch Status. Mean Count of Dead Adherent Cells Counted by Material and Etch Status, with the Upper 95% Wald Confidence Limit and Two-sided p Values for the Exact Savage Multi sample Test Comparing Etch Status Within Materials. †Graph developed by Dr. Cary Cotton, UNC.

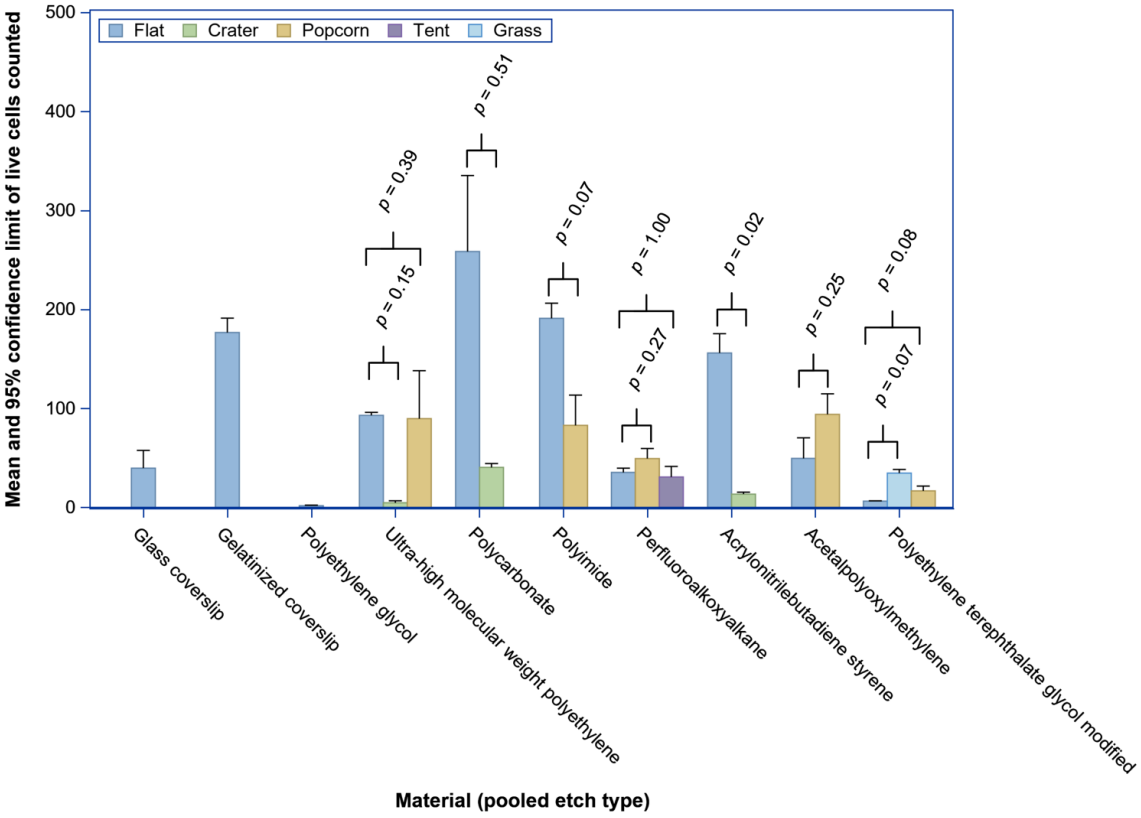

Figure 2.6 Statistical Analysis of Live Adherent Cells by Material and Pattern. Mean Count of Live Adherent Cells Counted by Material and Pattern, with Pooled Etch Status, with the Upper 95% Wald Confidence Limit and Two-sided p Values for the Exact Savage Multi sample Test Comparing Pattern Within Materials. †Graph developed by Dr. Cary Cotton, UNC.

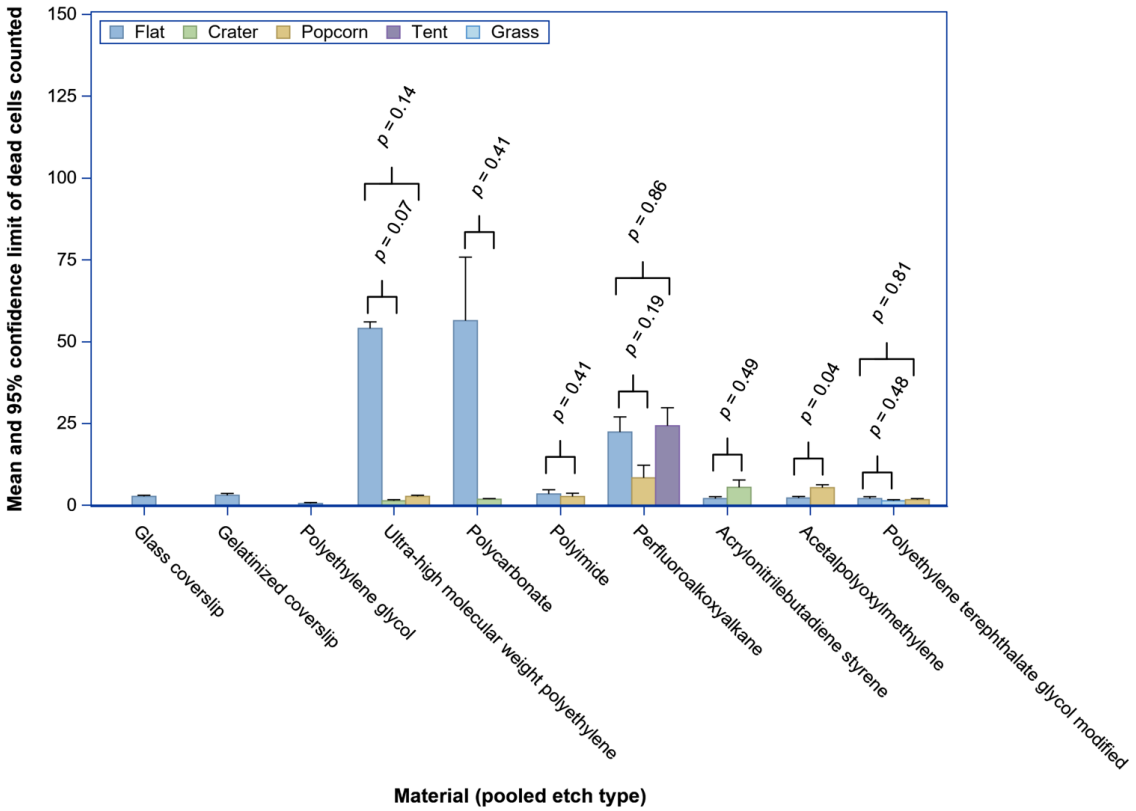

Figure 2.7 Statistical Analysis of Dead Adherent Cells by Material and Pattern. Mean Count of Dead Adherent Cells Counted by Material and Pattern, with Pooled Isotropic Status, with the Upper 95% Wald Confidence Limit and Two-sided p Values for the Exact Savage Multi sample Test Comparing Pattern Within Materials. bUHMWPE, bPC, bPFA, aPFA showed in decreasing order the number of dead cells per surface. †Graph developed by Dr. Cary Cotton, UNC.

I observed a range of bacterial adhesion on the nanostructured polymeric surfaces that I had generated for these experiments. I predicted that changing the surface texture at the nanoscale of a polymeric material would impact bacterial adhesion. However, this hypothesis was not uniformly supported in all materials. Some surfaces like PFA and PETG did not exhibit any differences in adhesion of the bacteria between the bulk and etched counterparts (Supplementary Figure 3, 7). PC, PI, UHMW PE, ABS and POM materials exhibited significant differences in the number of bacteria/10 μm^2 when

comparing the bulk processed substrates and etched versions (Supplementary Figures 2, 4, 5, 6). In some cases, the binding of cells to our polymeric surfaces exhibited enhanced binding when compared to untreated and gelatin treated controls. For instance, the highest level of bacterial cell adhesion was on the flat unprocessed bPC (408 ± 40 cells/0.1 mm^2; Fig. 3, Supplementary Figure 1). However, bacterial adhesion of plasma etched PC surfaces was significantly reduced, including an isotropic plasma etched (iPC; Supplementary Figure C) or an anisotropic etched PC (aPC; Supplementary Figure E).

Several polymeric substrates demonstrated reduced affinity to bacteria cells when compared to the glass coverslip control, although none were similar to the PEG-glass negative control. These surfaces included, the only surfaces to have a fewer number of cells were: iPC, iPI, iUHMW PE, iABS, aABS, iPOM, bPETG and aPETG (Supplementary Images 1, 2, 4, 5, 6, 7). The common trend of each of these surfaces is that the surfaces that didn't bind bacteria tended to be hydrophilic.

I also examined bacterial adhesion after 24-hour incubation on these surfaces. In most cases, I observed an increased number of cells when compared to a 1-hour incubation and that all surfaces regardless of their treatment exhibited statistically similar numbers of cells/0.1mm^2, which suggests that bacteria have the capacity to overcome surfaces with properties that were not initially optimal for colonization. In four cases (bPFA, iPFA, aPI and UHMWPE; Supplementary Figures 3 B, D, 2 F, 7 F) I observed fewer cells/0.1 mm^2 at 24 hours than at 1 hour, which suggests that the processing of these materials may inhibit the growth of bacterial biofilms.

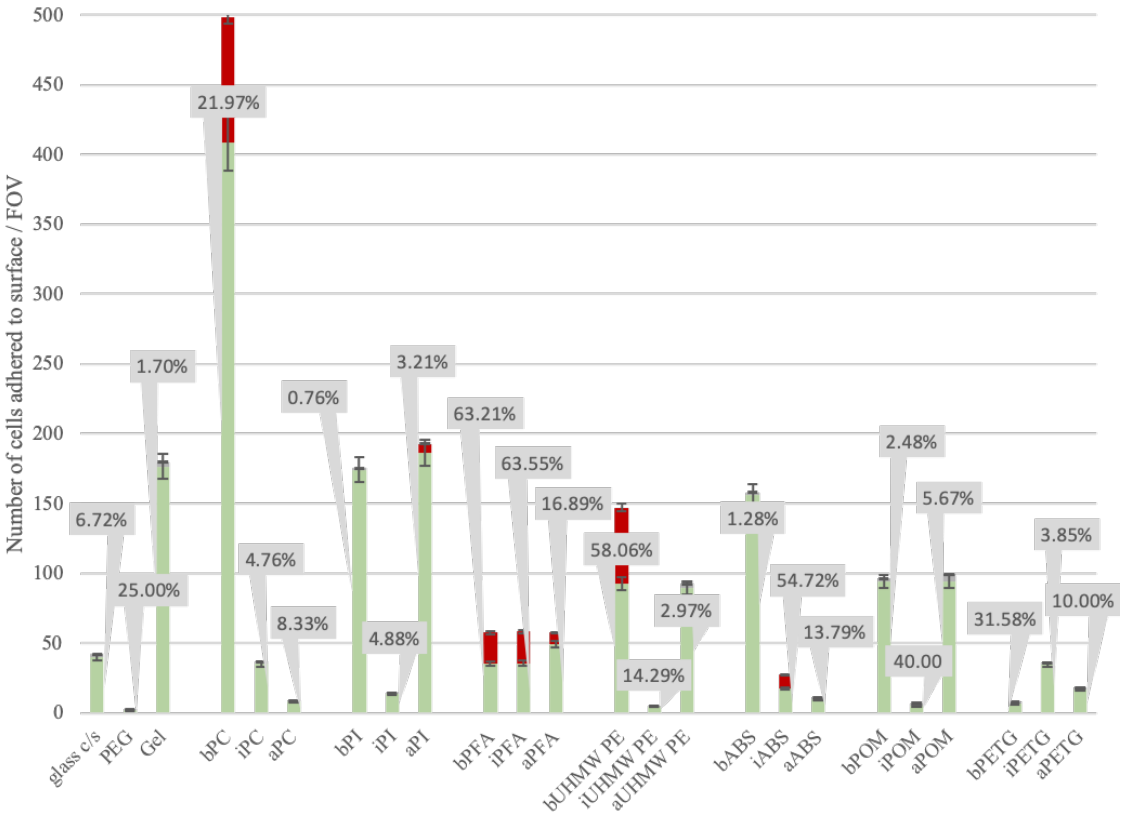

Figure 2.8 Membrane Permeability Assay. Percentage of dead cells per sample displayed as a fraction of the total number of cells for that sample. The graph represents the cumulative adhesion data recorded upon 1 hour of incubation of the E.coli on the bulk, isotropic and anisotropic surfaces. Gelatin was used as a positive control and PEG as a negative control. There is no consistent trend, but a similar pattern of adhesion exists on the PI, UHMW and POM surfaces. The callout boxes indicate the percentage of cells with membrane damage on each surface. While in some cases the percentage of permeability is high, eg. bPFA, it should be considered relative to the total number of bacterial cells adhered per polymeric topographical surface.

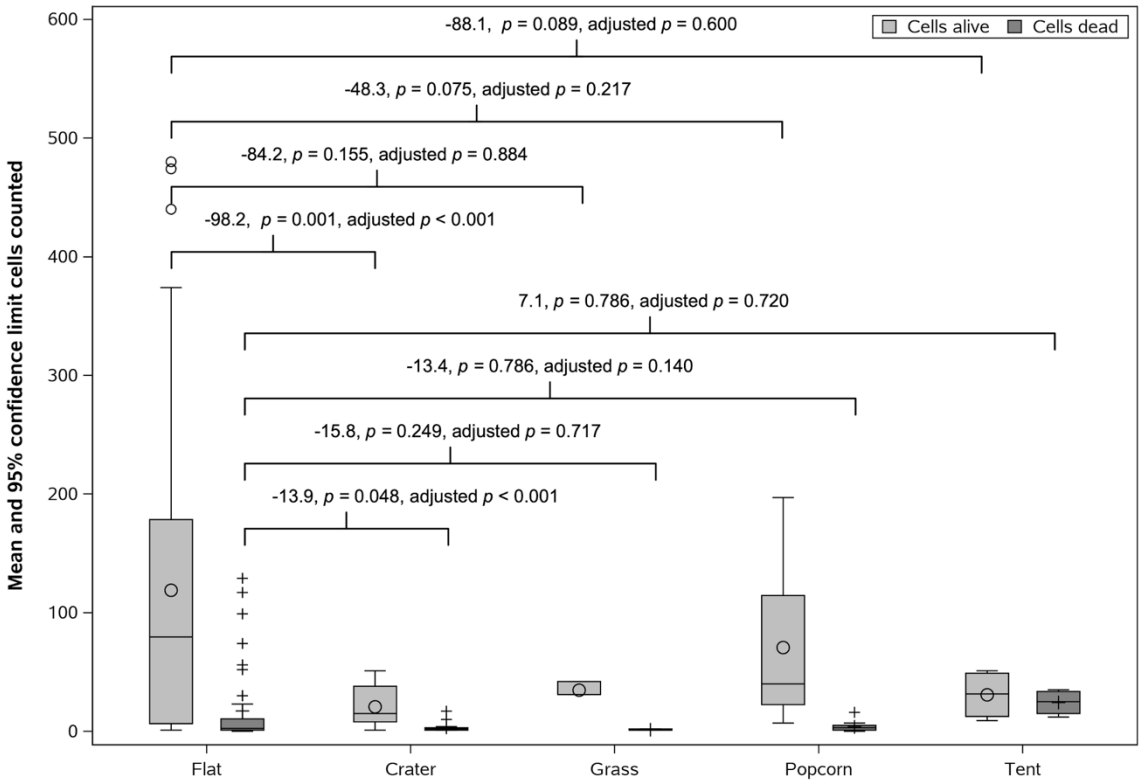

Figure 2.9 Pooled Analysis of Live and Dead Adherent Cells by Pattern. Mean Count of Live and Dead Adherent Cells Counted by Pattern, with Pooled Material and Etch Status, with the Upper 95% Wald Confidence Limit and Mean Difference in Cells Counted with p for unadjusted Comparison and Comparison Adjusted for Material, Estimated by General Linear Model with Exact Estimator of Variance.
†Graph developed by Dr. Cary Cotton, UNC.

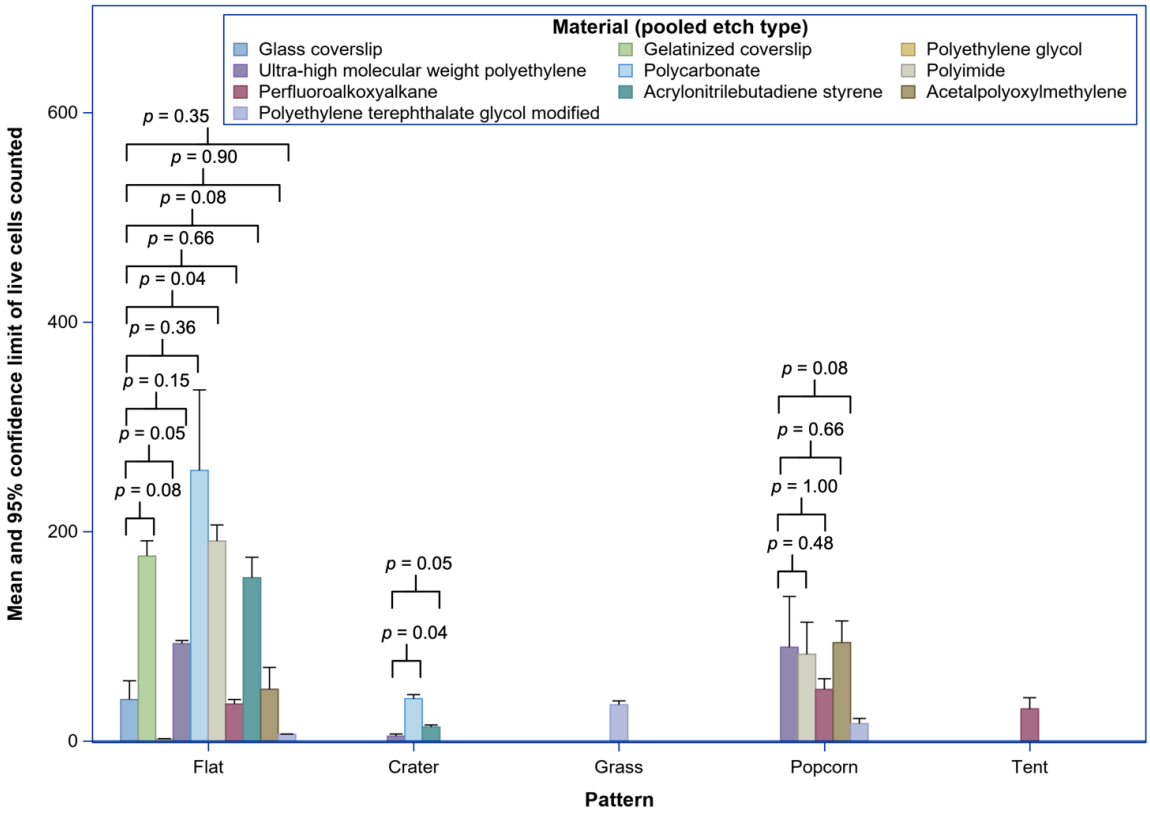

Figure 2.10 Statistical Analysis of Live Adherent Cells by Pooled Pattern Type. Mean Count of Live Adherent Cells Counted by Material and Pattern, with the Upper 95% Wald Confidence Limit and Two-sided p Values for the Exact Savage Multi sample Test Comparing Etch Status Within Patterns. †Graph developed by Dr. Cary Cotton, UNC.

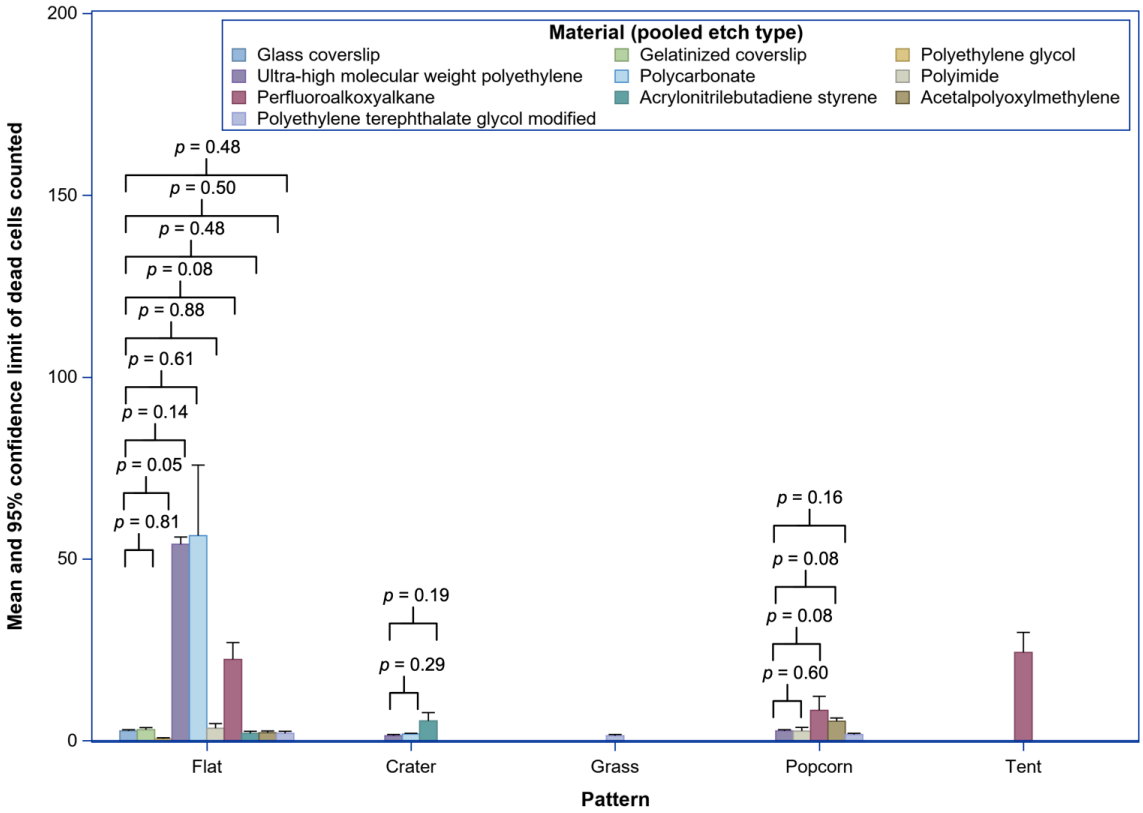

Figure 2.11 Statistical Analysis of Dead Adherent Cells by Pooled Pattern Type. Mean Count of Dead Adherent Cells Counted by Material and Pattern, with the Upper 95% Wald Confidence Limit and Two-sided p Values for the Exact Savage Multi sample Test Comparing Etch Status Within Patterns. †Graph developed by Dr. Cary Cotton, UNC.

II.3.iv. Contact Angle does not Affect Adhesion at the Nanoscale

None of the differences observed in bacterial adhesion correlated with the topological features or with the observed changes in contact angle (Figures 18 and 19) For a given material, the pattern influenced the number of adherent cells. Among the flat materials, the number of adhered cells was directly proportional to the contact angle (Figures 18 and 19). The contact angle did not have a major effect on popcorn or crater patterns.

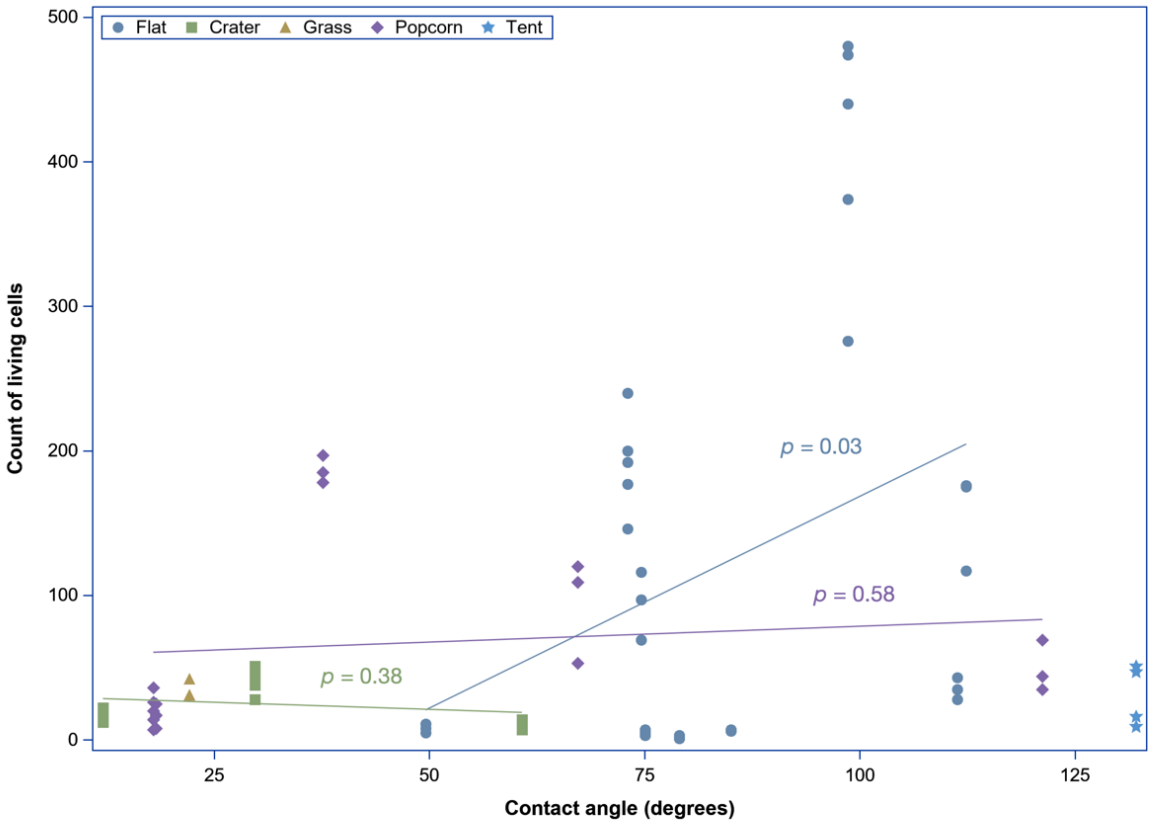

Figure 2.12 Statistical Analysis of Live Adherent Cells by Contact Angle. Mean Count of Live Adherent Cells Counted by Contact Angle and Pattern, with the Upper 95% Wald Confidence Limit and Two-sided p Values for the Exact Savage Multi sample Test Comparing Etch Status Within Patterns. †Graph developed by Dr. Cary Cotton, UNC.

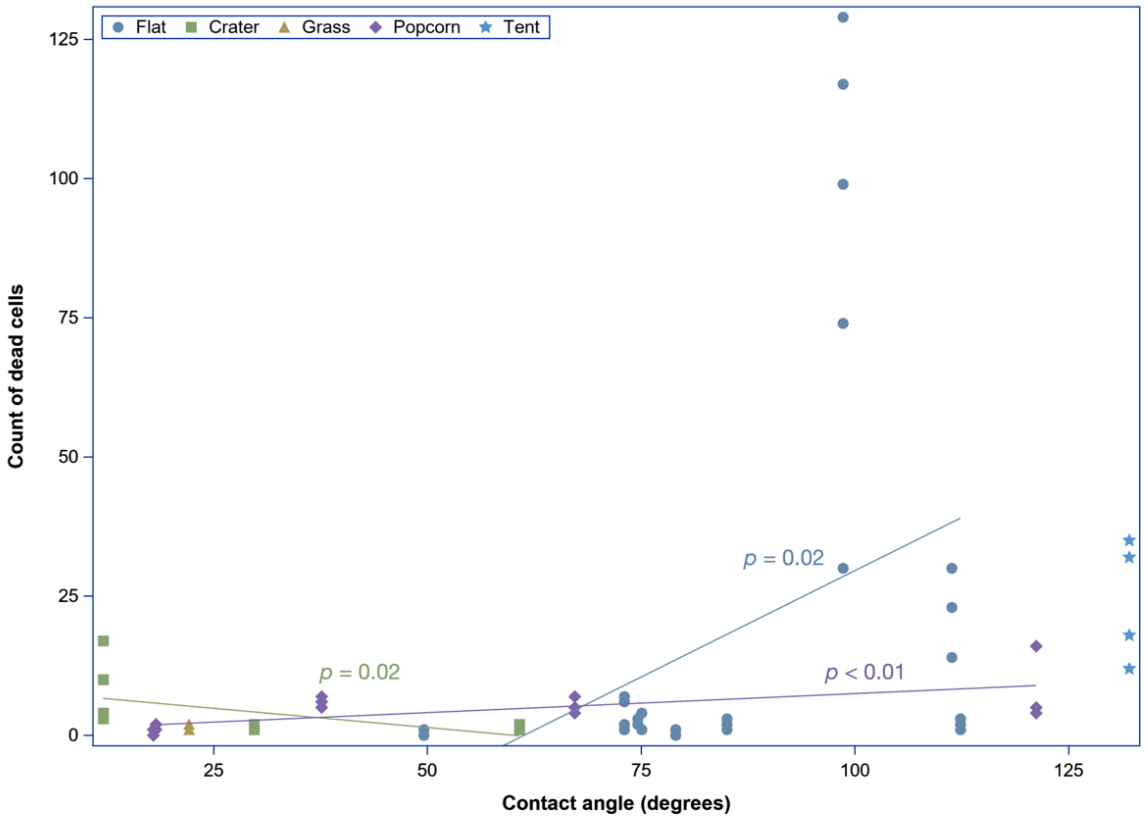

Figure 2.13 Statistical Analysis of Dead Adherent Cells by Contact Angle. Mean Count of Dead Adherent Cells Counted by Contact Angle and Pattern, with the Upper 95% Wald Confidence Limit and Two-sided p Values for the Exact Savage Multi sample Test Comparing Etch Status Within Patterns. †Graph developed by Dr. Cary Cotton, UNC.

II.3.v. Alteration of Bacterial Membrane Integrity and Viability to Polymeric NSS

Microbial interactions with many chemicals and materials, including many nanoscale materials, disrupts the plasma members, which often results in a reduction in viability [273–276]. To determine whether interactions of the *E. coli* with our nanostructured polymeric surfaces, I examined the changes to the permeability of the bacterial plasma membrane, using the vital dye propidium iodide (PI). PI is a nucleic acid dye that is plasma membrane-impermeable and will only label cells that have a disrupted plasma

membrane [275]. Bacterial cells exposed to untreated glass substrates exhibited a background level of 6.72 ± 0.27 % of PI labeled cells. In the positive control experiment of sodium hypochlorite treated bacterial cells, we observed 100% of the cells labeling with PI. On our experimental surfaces, I observed a range of cells exhibiting plasma membrane perturbation. Some surfaces resulted in an elevated level of plasma membrane disruption as demonstrated by PI labeling: bPFA, 63.21 ± 3.78%, iPFA 63.55 ± 4.77%, bUHMW PE 58.06 ± 1.41% and iABS 54.72 ± 2.80% all exhibited high percentage of *E.coli* cells that labeled with PI after one hour of contact, suggesting that these surfaces may damage or stress the integrity of the plasma membrane (Figure 14). However, other surfaces, even those with the same composition as the plasma membrane disrupting surfaces, showed no significant PI labeling when compared to the controls (Fig 14). For example, the percentage of permeable cells on the following surfaces: iPC, aPC, all the PI substrates, aUHMW PE, bABS, bPOM, aPOM, iPETG, and aPETG, was within the range I had accounted for using the glass coverslip control substrate. In many cases, there were significant differences in the percentage of PI labeled cells on substrates that are composed of the same material but have different surface topography due to the etching process, suggesting that plasma membrane stress may be the result of bacterial interaction with specific features of these surfaces. However, as with the adhesion, there was no correlation between the general classification of surface feature or surface composition that predicts plasma membrane perturbation. The only material to exhibit a significant difference in PI labeled *E. coli* when compared to the substrate control (~10%) after 24-hour exposure was the popcorn surfaced aPETG, in which I observed a higher number of

membrane perturbed cells (Supplementary Figure 7L; aPETG at a percentage of 19.67 ± 0.27%).

In many cases, PI labeled cells are unviable or dying[277]; however, there has been some evidence that microbes may tolerate higher levels of membrane permeability and thus label with PI but not be dead or dying[273]. To determine whether the observed PI labeling correlates with reduced viability I conducted a standard colony forming unit assay[258] (CFU) on the substrates at 1 hour (figure 20) and 24 hours of culture (supplementary figure 12).

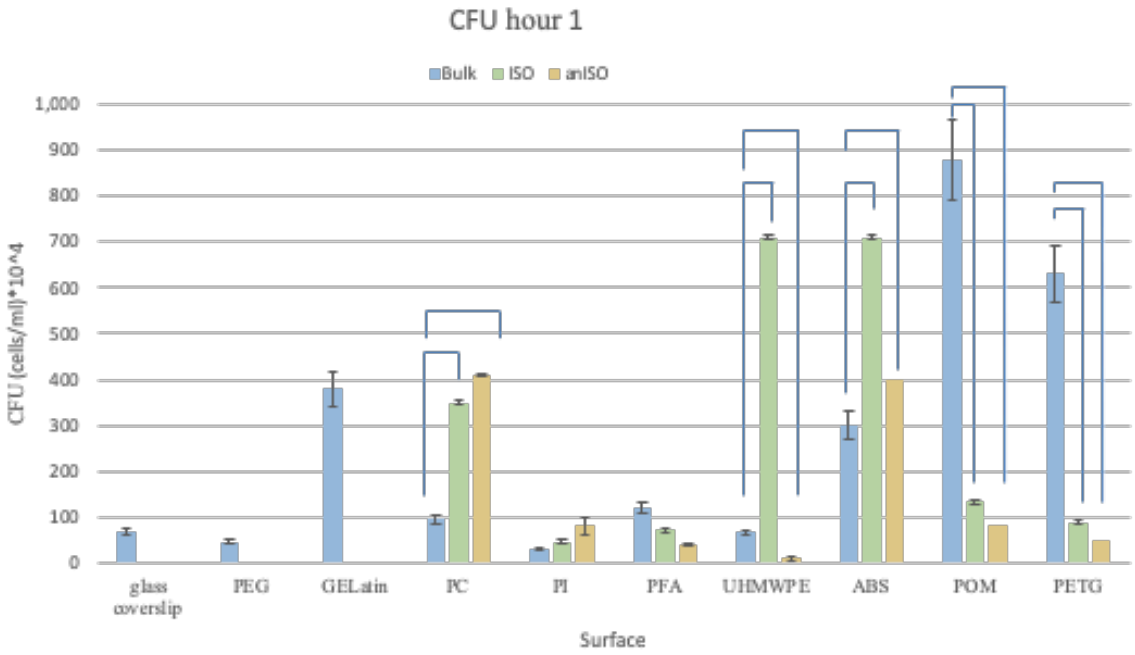

Figure 2.14 CFU Assay after 1h Incubation. Graph indicates the results of a colony forming unit (CFU) assay performed after 1 hour of incubation of the E. coli on each polymeric nanostructured surface. Several of the bacteria were damaged but viable after 1 hour of contact with the samples (see tall bars). Polyimide, PFA and aUHMWPE retained bacterial cells that were the least viable amongst all the surfaces tested. $p<0.05$.

II.3.vi. Change in Bacterial Morphology upon Contact with the NSS

The interaction of bacteria with different surface substrates have been shown to alter overall bacterial morphology as a result of stress[225]. I also observed changes to bacterial cell morphology on these polymeric nanostructured surfaces including changes in length and the presence of cellular appendages. On untreated glass surfaces, *E.coli* bacteria have a cylindrical shape that is 3-5μm long (Fig 17). However, shorter bacteria, i.e.≤ 3μm, were seen on several surfaces, including iPC, bPFA, bPETG and aPETG (supplementary figures 1I, 3G, 7G and 7K), while on several other surfaces I observed longer bacterial cells (≥ 10 μm), aPC, bABS, and aABS (Supplementary Figures 2L, 5H and 5L). On some surfaces (aPI and iPFA: Supplementary figures 2L and 3J) I observed a range of sizes. I also observed qualitative differences in the presence of different cellular projections in cells associated with different surfaces (Fig 18). On most surfaces, the bacteria exhibit the same morphology (Figure 18e) which includes the presence of bacterial surface adhesion appendages. However, *E. coli* associated with aUHMW PE and iUHMW PE exhibited a higher level of biofilm secretion at the end of the bacterial cells (Figure 18 b, 18f). *E. coli* on aPFA and aPC appear to secrete materials that bridge contact points on the surface (Fig 18 c, 18 d) reaching out for adhesion points on the surfaces. The bacteria on iPOM demonstrate an increased surface area to maximize contact points (Supplementary image 6J).

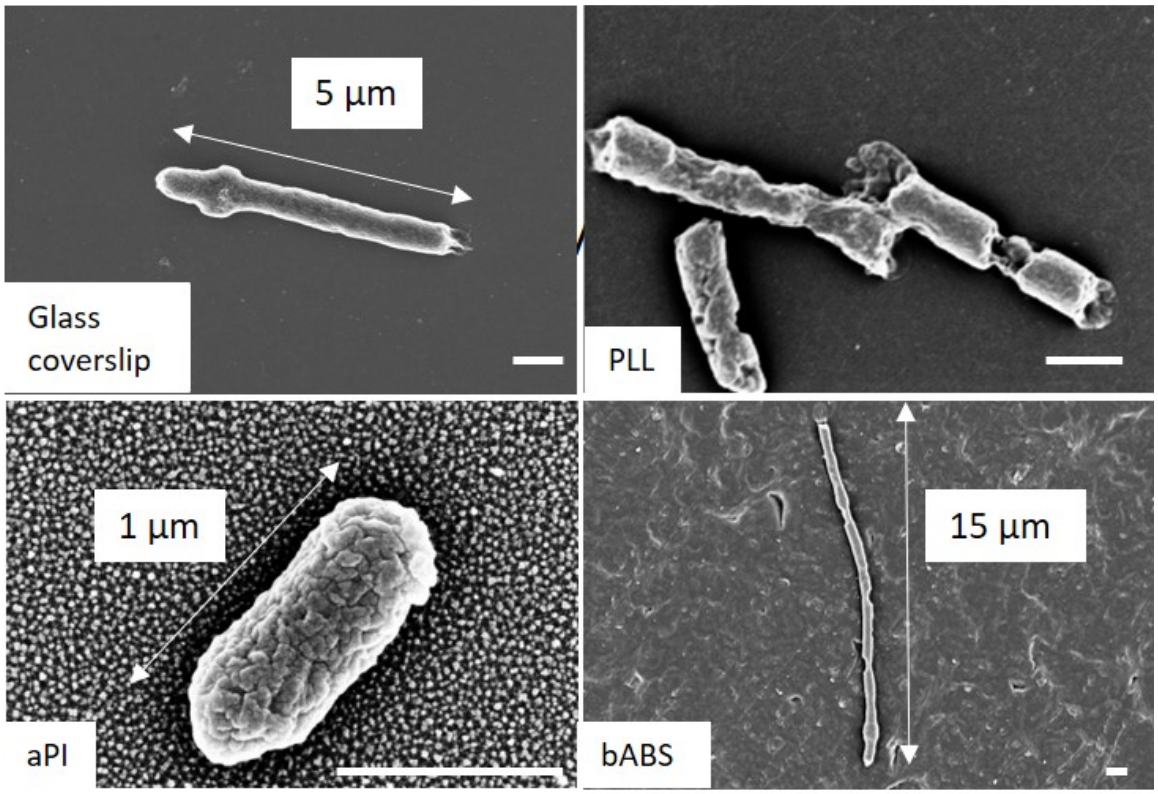

Figure 2.15 Morphological Changes the E. coli Undergo Upon Contact with the Polymeric Nanotopographies. The glass coverslip and Poly-L-lysine were used as negative and positive controls respectively. The E. coli on the glass coverslip depicts an unaltered, unmodified, unstressed bacterium of average length. Poly-L-lysine is known to be lethal to bacteria; this is represented in the picture above indicating extreme morphological strain. The bottom two figures represent examples of bacterial size variations; on the aPI, E. coli were small, with an average length of 1µm; the bacterium on the bABS shows E. coli that have undergone filamentation. The polymeric nanotopographies are seen to induce different responses related to cell division and growth.

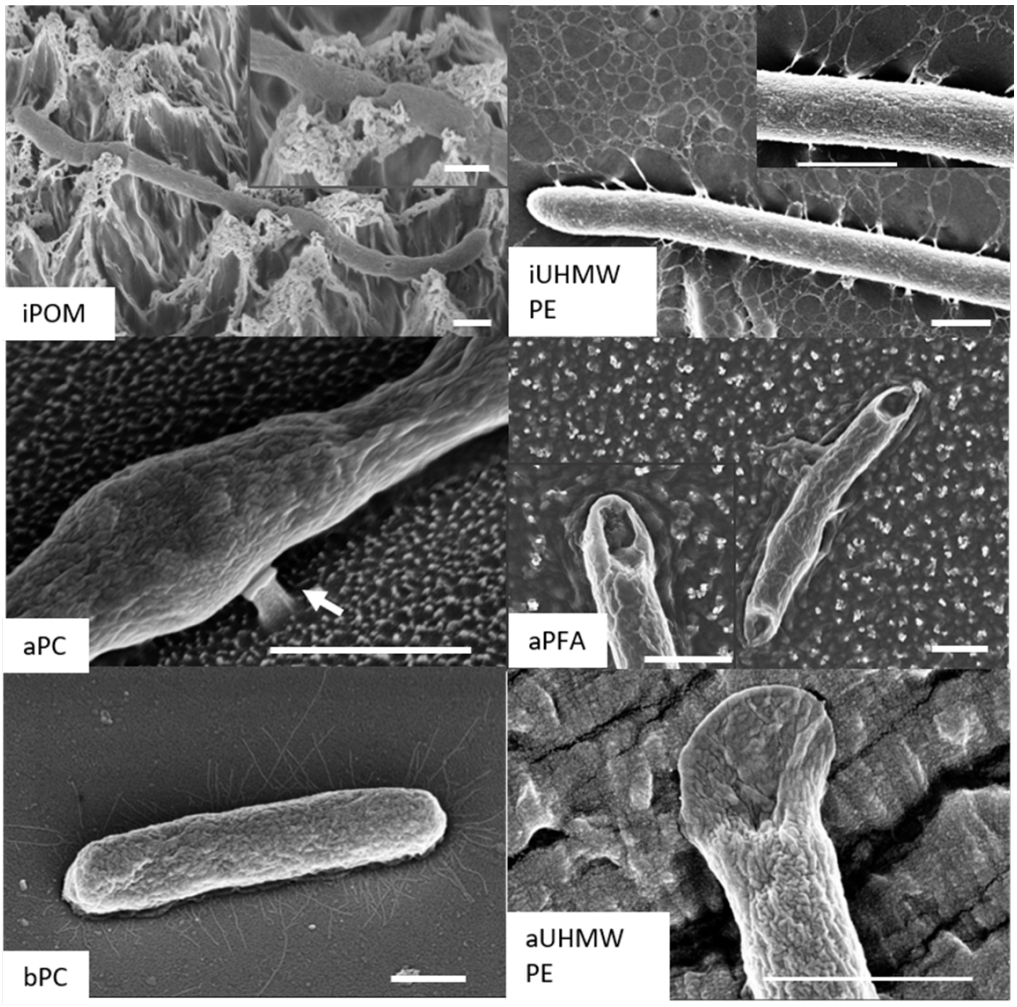

Figure 2.16 Modes of Adhesion to the Polymeric Nanotopographies. iPOM shows a pockmarked, isolated E. coli bacterium on the isotropically etched POM surface clinging to the stringy substrate. iUHMW PE shows a web-like biofilm secreted by the bacterium to assist in adhesion. Strings from the web are clearly seen to be interacting with the bacterium. The bacterium on aPC shows that bacteria can produce a bridge-like connection between the cell and surface. The cell in the aPFA image is seen clinging to nanoscale adhesion points on the etched PFA surface. bPC shows the typical adhesion response of bacteria; surface appendages (short and long pili and flagella) are seen on the extremities of the bacterium aiding in adhesion. The end of the bacterium depicted in the UHMW PE image shows that bacteria can secrete biofilm at the poles to aid in adhesive behavior.

II.4. Discussion

I have shown that nanoscale surface modification alters *E. coli* absorption to polymeric substrates. Although I generated a range of morphologies and surface chemistries none of these features or properties had a major deterministic role in controlling adhesion; instead, I found that the overarching factor that determines *E. coli* binding to a surface is surface composition and how this aspect determines is unclear and may involve mechanical or other interfacial chemistry. Preventing the initial adhesion of bacteria is a key step in controlling biofilm formation. Numerous material properties have been reported to influence the initial adhesion including hydrophobicity, roughness, topography, surface chemistry and charge [278]. Studies have shown that many bacterial strains prefer to attach and grow on smooth surfaces, and hydrophobic surfaces while texturing surfaces tend to reduce microbial adhesion [139,279]. The high aspect ratio nanoscale cones and needles (of different aspect ratios depending on the variety) present on the surface of cicada wings provide a topographic barrier against microbes. They have been shown to cause the cell-wall rupturing of *S. cerevisiae* [183] and are also lethal to *P. aeruginosa*[186]. Nanostructures fabricated (nanograss, pillars, and cones) on metals and polymers are also bactericidal.

The current approach in developing these surfaces, however, is largely trial and error based. This is evidenced in the numerous research papers in this area, each of which has used dissimilar materials (each with different material properties such as stiffness and tensile strength) which would affect bacterial adhesion and biofilm formation in their own way. While they have had a modicum of success, there has not been clear-cut

reasoning behind their approach besides availability or ease of manufacturing. There has recently been a shift in this trend to a more informed method of engineering surfaces. Researchers are now attempting to tease apart the factors that guide bacterial adhesion to purposefully design surfaces. Hsu et al. have altered silica surfaces to produce shapes with different dimensions (circular and rectangular wells of assorted sizes and spacings) and have found that feature size and shaping have an effect on bacterial attachment and even the orientation of their attachment [280]. Dickson et al have observed that small, more closely spaced nanopillars made of PMMA showed fewer adherent cells[127]. The studies conducted by Ren et al have validated the use of 10μm hexagonal patterns on PDMS to control the orientation of bacterial attachment and adhesion[281]. These studies are a starting point for the purposeful design of surfaces. They suggest that nanoscale topographical features and their geometries affect bacterial adhesion. No specific set of rules has been established yet.

II.4.i. Fabrication of NSS on Polymers with Varying Topographies and Wettabilities

In this study, I chose polymers that mimicked the mechanical properties of biological samples, following the "biological triangle" , wherein biological materials exhibit low Young's modulus at moderate extensibility[282]. The use of polymeric surfaces has offered a great deal of control in terms of methods of fabrication, the ability to synthesize composite materials and the tunability of moduli of the materials [259,260]. Oxygen plasma etching is a relatively well-understood technique to allow surface modification of [150,151,265]. Oxygen etching offers greater biocompatibility to the polymeric

substrate[283]. Plasma is defined as an ionized gas containing equal proportions of negatively and positively charged particles[261]. Plasma etching has been shown to etch nanotopographies onto various materials while also having the advantage of allowing the polymer to retain its bulk properties [262,263150,264,265]. I used an oxygen plasma to etch the surfaces of 7 commonly available polymers isotropically (10 min, 200 W) and anisotropically (1 min, 200W). In our study, five different nanopatterns were produced through plasma etching. The differences in material composition i.e. the number and arrangement polymeric chain repeats, can influence the etch rate[284]. More energy is required to break some bonds than others, leading to this disparity.

Generating plasma also introduces a great number of unstable oxygen species, thereby functionalizing the surfaces and leading to differences in hydrophobicity[263]. Nanoscopic roughness and hydrophobicity of nanostructured surfaces go hand in hand. Depending on the intrinsic hydrophobicity of the material, nanoscopic roughness increases or decreases hydrophobicity[285]. While the introduction of nanoscale topography promotes hydrophilicity, nanoscale surface modification can also limit adhesion by discouraging the hydrophobic interaction by creating the substrata-bacteria repulsion. My results clearly indicate that even within the same material, the topography and wettability can be altered by plasma etching. Results from previous studies indicate that a contact angle 90° represents a moderate level of hydrophobicity, while extreme hydrophobicity and hydrophilicity reduce adhesion[144]. Our observations concur (for the most part) with this result. Combining the results from the adhesion experiment, structural and hydrophobicity analysis, I concluded that all the surfaces that showed less adhesion than

the glass coverslip were hydrophobic in nature (<90°), with most of them tending to be on the lower end (between 8°-30°). A more global multi-variable analysis revealed that contact angles influenced the adhesion of cells only on the flat surfaces. The contact angle did not alter the adhesion of bacteria onto the nanoscale modified substrates.

In a study by Yoshida et al, the polymers used in the study showed an increase in hydrophobicity[283] instead of the wide range we observed. Our results further indicate that there is a fine line between adhesive to non-adhesive. An interesting observation made during this time was the change in contact angle after a certain period. Contact with liquids also changed the nature of these surfaces. Incubation in liquid, such as media, convert the contact angle to a hydrophilic state. This is referred to as the conditioning of surfaces[126]. Proteins present in solution interact with the surface thereby altering the surface chemistry regardless of the original surface properties[263,286].

II.4.ii. FTIR

Fourier Transform Infrared Spectroscopy (FTIR) was used to identify changes in surface composition after etching. Polymers were etched for as long as possible to see whether the etch rate would affect surface bond formation. Isotropic and anisotropic samples were etched for 15 min and 2 min respectively. Only slight differences were seen in the IR readings even though the samples were etched for longer periods of time. All the etched samples showed a decrease in bond intensities when compared to the bulk unmodified material. The FTIR graphs have been added to the supplementary figures.

II.4.iii. Bacterial Responses to NSS

Understanding the bacterial response to a specific structure brings us a step closer to developing substrates that can tune the behavior of bacteria. Bacteria are found in every environment and have developed resistances over millennia. When the environment is not suitable for the bacteria, they tend to exhibit stress responses[287]. These could be due to osmotic or thermal changes, for instance. These stress responses help the bacteria understand its environment and transmit this information to its cohorts, thereby altering the biofilm production for its specific needs[288]. Such responses can be seen when bacteria encounter surfaces with different topographies[287]. One such common response is death. Most bacterial death attributed to high aspect ratio nanostructures is due to their ability to pierce through bacterial cell membranes[289]. Researchers have utilized this fact to produce antibacterial surfaces capable of popping microbes. Others have developed surfaces that prevent bacterial adhesion, thereby preventing any initial bacterial adhesion for biofilm formation on the surface. These surfaces do not necessarily have a high kill rate but are still effective. The polymeric nanostructured surfaces were used to demonstrate (a combination of) these responses.

In our experiments, I noticed that *E. coli* bacteria exposed to surface substrates composed of PFA, UHMW PE and ABS all exhibited significant differences in PI labeling when comparing the bulk unmodified versions of the plastics to their isotropic and anisotropic etched versions (Figure 3). However, with other polymers, I noticed that only one type of processing resulted in changes to PI permeability. For instance, both the

POM and the PETG exhibited differences between the "bulk" unmodified substrate and their isotropic counterparts (Figure 14).

Despite the surfaces showing high percentages of membrane disrupted cells (PI values), these percentages are in relation to the total number of cells adhered/surface. So, while bPFA and iPFA may show the highest percentages of membrane disruption, they have only an average of 35 cells/0.1 mm^2 on their surfaces.

We have come away with the knowledge that not every material can recreate a specific topography or induce an identical response from bacteria. However, predetermined patterns can be used to gain an understanding of bacterial growth[290]. Microscopic structures etched onto substrates in a specific pattern can direct the bacteria[118]. Note that most research done in this field deals with microscopic structures; structures comparable in size to the bacteria. Nanoscopic responses are hardly examined. Our research includes this form of structure. Several nanoscopic structures in nature have inspired the production of biomimetic nanostructures[291] and hierarchical microstructures[247]. The most notable ones are the patterning of substrates to mimic the surface topography of the cicada wing. There is a varying degree of responses to these structures; some bacteria are killed immediately upon contact [187,248,250] while others show a delayed response to these surfaces which may suggest some sort of conditioning to the surface or adaptation by the cells. Future work will be needed to determine the reasons why some cells rupture relatively easily while others do not. When other microbes such as yeast are exposed to the NSS of cicada wings, the adhesion dynamics have been shown to change. These results have given researchers a place to start. However, with the many

materials available, there is an incredible number of choices of material and the nanostructures that could be made with them. The same material/topography can produce different responses within strains. Individually adhering bacteria can increase the local surface heterogeneities to yield different adhesion responses that trigger the emergence of several microenvironments within the biofilm[292]. Others say that decreasing the topography can increase the adhesion of bacteria. This disparity results from a lack of procedural uniformity and the use of different strains and species of microbe. There is, however, some consensus in the fact that a minimum aspect ratio is required to pierce through the bacterial cell membrane [293,294,295,289]. Surface roughness is a property commonly associated with topographical features. The contradictory results could be a product of procedural non-uniformity. Surface roughness can be measured using 14 different parameters[129]. Results can vary depending on the type of roughness measured, and hence the disparity. I have avoided examining surface roughness as a parameter due to these reasons.

Another common property associated with topography is its wettability, measured through contact angles. Contact angles allow us to differentiate a surface as hydrophilic (<<90 degrees) or hydrophobic (>>90 degrees). Hydrophilic surfaces tend to allow more particles to cling to their surfaces, thereby increasing the likelihood of bacterial adhesion, while the opposite is true for hydrophilic surfaces[296]. Our analyses broadly concur with this.

While experimenting with the polymers, I noticed that the surface contact angle varied over the course of a month[137]. This can be attributed to the inversion of bonds. It led me to the possibility that perhaps water (or the liquid) used could also influence contact angle. These changes reflect the differences in chemical bonds present on the various substrates, indicating that physicochemical properties need to be considered as well [147,296]. Our results reflect this need for such a dual analysis. Our use of different polymers accounts for the change of material (different material properties could be a factor even within the kingdom of polymers[297]), and the etching I performed generated the different topographies. The oxygen plasma generated during the etching process was not only responsible for the removal of material from the surface but also uncovering chemical bonds[150]. Thus, I was able to do an analysis between polymer materials, and the physicochemical properties that could have arisen due to the etching.

The surface area: volume ratio is also a major player in maintaining cell homeostasis[298]. Increased exposure to the surface area would allow more area for adhesion [299,298]. This is possibly why more bacteria adhered to the bulk substrates. Bacteria maximize the adhesion sites creating preferential adhesion to certain areas [242,243]. This can be seen in photo (Supplementary Image 9 A). Bacterial morphology was seen to change drastically upon contact with the different topographies. Stress responses were evident in bacteria grown on certain surfaces (dips, holes, shortening). The size of the bacteria was the most striking difference in morphology. This morphological plasticity indicates that certain topographical features can stimulate specific bacterial responses[300]. Bacteria have been known to adapt in size according to environmental cues. The genomic

processes are sufficiently interrupted to enhance cell division (short cells) or delay septation (longer cells) Fig. 5.

Different aspects of the NSS could be a stimulus for the bacteria to express emergent properties. Upon initial adhesion, bacteria release a substance known as EPS (extracellular polymeric substances) into the environment[285]. The production of EPS is not very well understood but it functions to help condition the surface and surroundings for the bacteria. This initial response is very important for the formation of biofilms[17]. I noticed several different biofilm release strategies. Some cells were found embedded within the EPS (supplementary figure 9D) while others secreted it at specific locations (such as the ends) to aid in possibly different modes of adhesion (figure 6 F). Bacterial mechanisms of adhesion vary upon contact with different topographies [114,122,287]. This is evidenced by the nanostructures I show in fig 6. Bacteria use several modes of adhesion bacteria and each is tightly regulated by the environment [301,280,302]. In contrast to other studies that have dealt with identifying the mechanisms of adhesion[287], I noticed that different topographical features elicit different surface appendages to make a play. This could be the result of the activation of different mechanosensitive pathways. Only the substratum properties have been analyzed in this paper. Properties of the medium itself (pH, ionic strength, viscosity, etc.) and the bacterium of choice (Gram-negative or positive, the presence or absence of surface sensing appendages) also play a big role in determining cell-surface adhesion as well as cell-cell interactions.

II.5. Conclusion

I hypothesized that by changing the material properties (in this case, topographical features) over a range, I should see a change in the biological response of the bacteria. Seven different polymers with variations in material properties, etched with oxygen plasma were chosen to see if slight changes in material composition and nanoscale topography play roles in prompting uniform bacterial responses. While I had predicted that I would see a trend in the biological responses of the bacteria, what was seen was that bacteria behaved differently on all the surfaces tested, regardless of the topology, material composition or hydrophobicity. It is possible that several of these properties are related to one another. For instance, the wettability of a substrate is a product of its topography.

The bacteria displayed variations in morphology, biofilm formation and adhesive behavior upon all the polymers and their etched counterparts. I have conclusively verified that bacteria respond to differences in material properties, but not necessarily in a predictable fashion. This could be due to several reasons, ranging from the altered surface chemistry to the stiffness of the polymeric substrate. Bacterial behavior could depend on more than one material character not just solely composition or wettability for example. I have been unable to isolate one single property due to the sheer amount of data.

While I may not have tested the exact material property that would have shown us the trends I was expecting, I hypothesize that there is a yet-to-be-determined material property that will make the bacteria react consistently upon changing specific parameters that have thus far prevented the development of a generalized model. The lack of

understanding stems from rudimentary approaches, oversimplification of microorganisms and a lack of understanding of the biological events involved in the process. An understanding of the process of pre-conditioning i.e. protein deposition on the substrates, should provide some insight into the initial adhesion of bacteria during early biofilm formation. This is part of our ongoing work.

II.6. Supplemental Figures

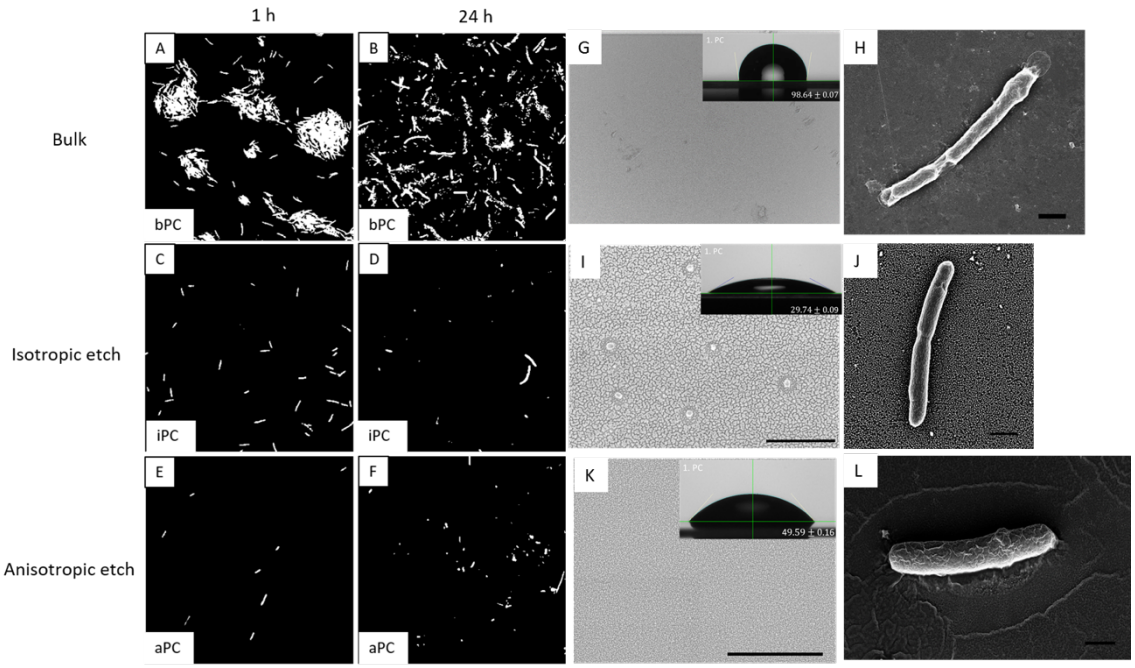

Supplementary Figure 2.1 Confocal Microscopy Images of E. coli Grown on Bulk, Isotropically Etched and Anisotropically Etched Polycarbonate after 1 and 24 Hours of Incubation.

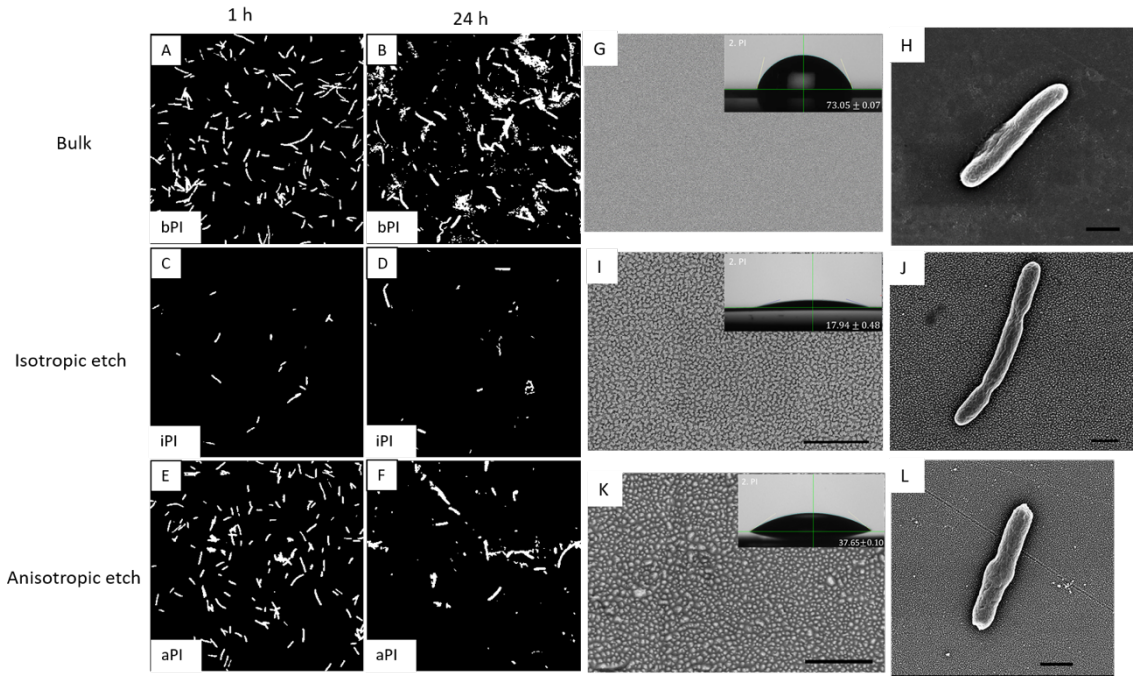

Supplementary Figure 2.2 Confocal Microscopy Images of E. coli Grown on Bulk, Isotropically Etched and Anisotropically Etched Polyimide after 1 and 24 Hours of Incubation.

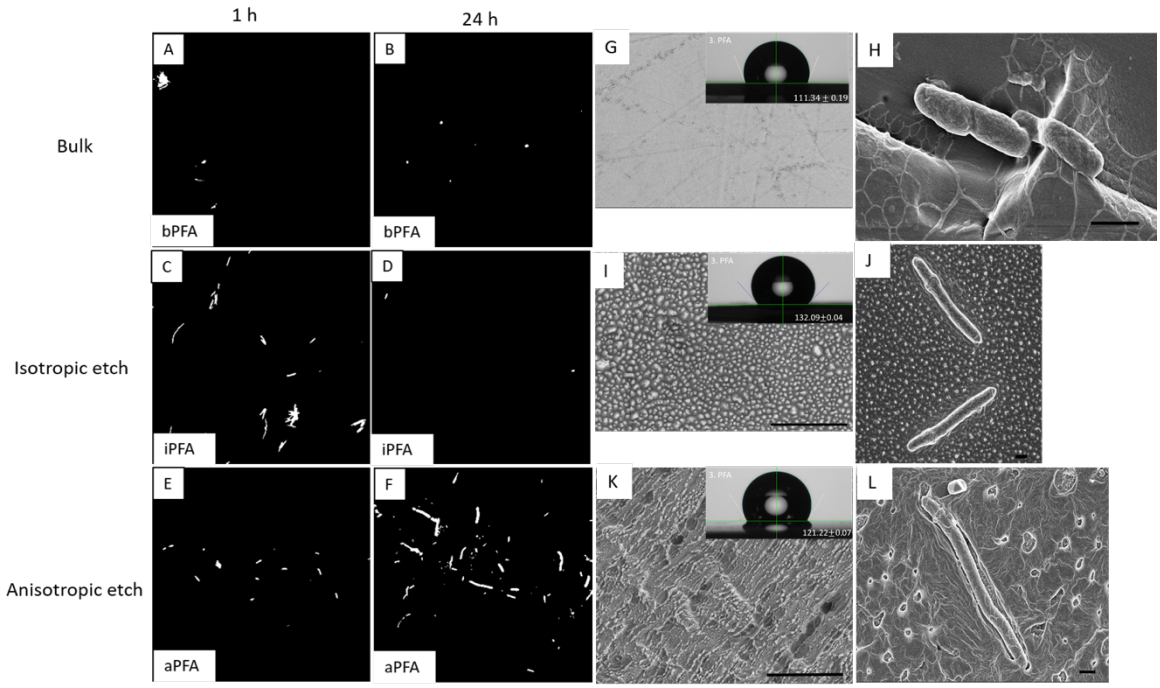

Supplementary Figure 2.3 Confocal Microscopy Images of E. coli Grown on Bulk, Isotropically Etched and Anisotropically Etched Perfluoroalkoxyalkane after 1 and 24 Hours of Incubation.

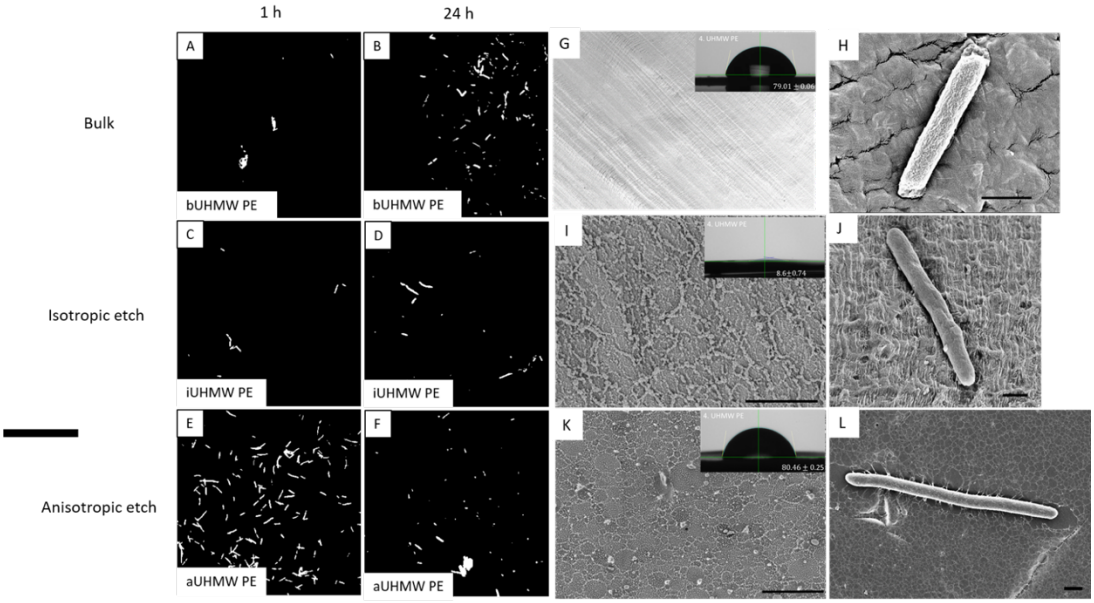

Supplementary Figure 2.4 Confocal Microscopy Images of E. coli Grown on Bulk, Isotropically Etched and Anisotropically Etched Ultra-High Molecular Weight Polyethylene after 1 and 24 Hours of Incubation.

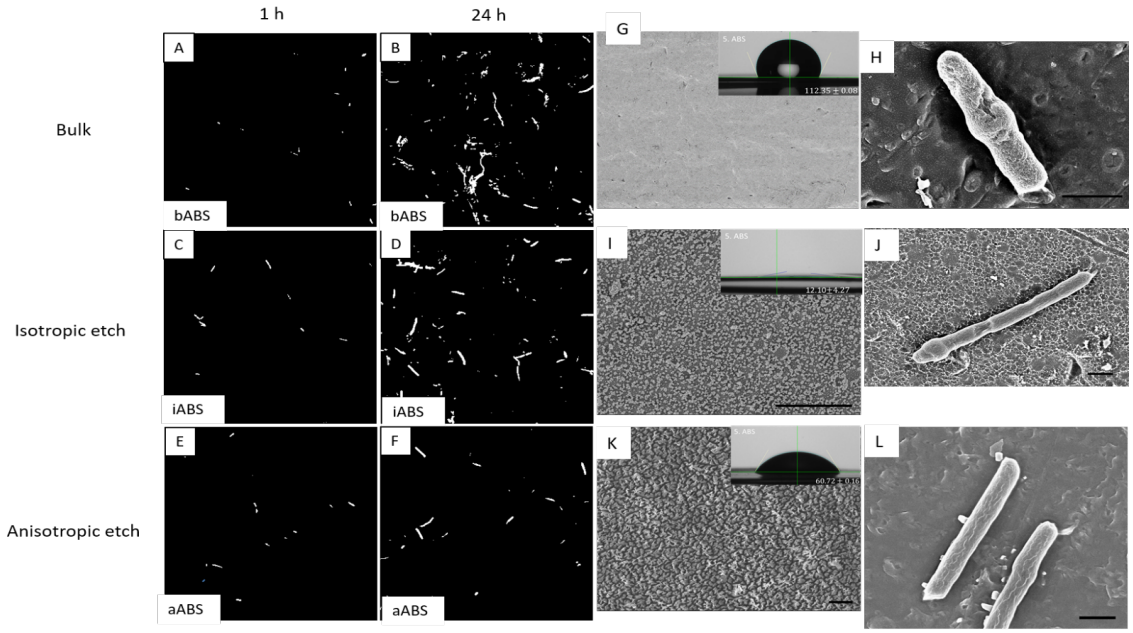

Supplementary Figure 2.5 Confocal Microscopy Images of E. coli Grown on Bulk, Isotropically Etched and Anisotropically Etched Acrylonitrile Butadiene Styrene after 1 and 24 Hours of Incubation.

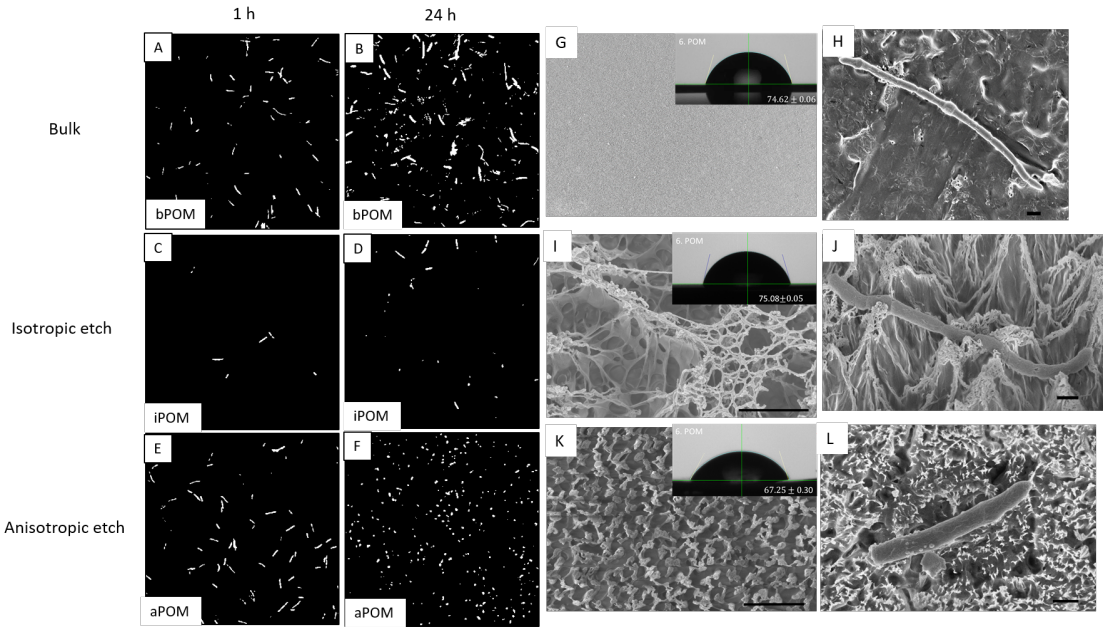

Supplementary Figure 2.6 Confocal Microscopy Images of E. coli Grown on Bulk, Isotropically Etched and Anisotropically Etched Acetal Polyoxymethylene after 1 and 24 Hours of Incubation.

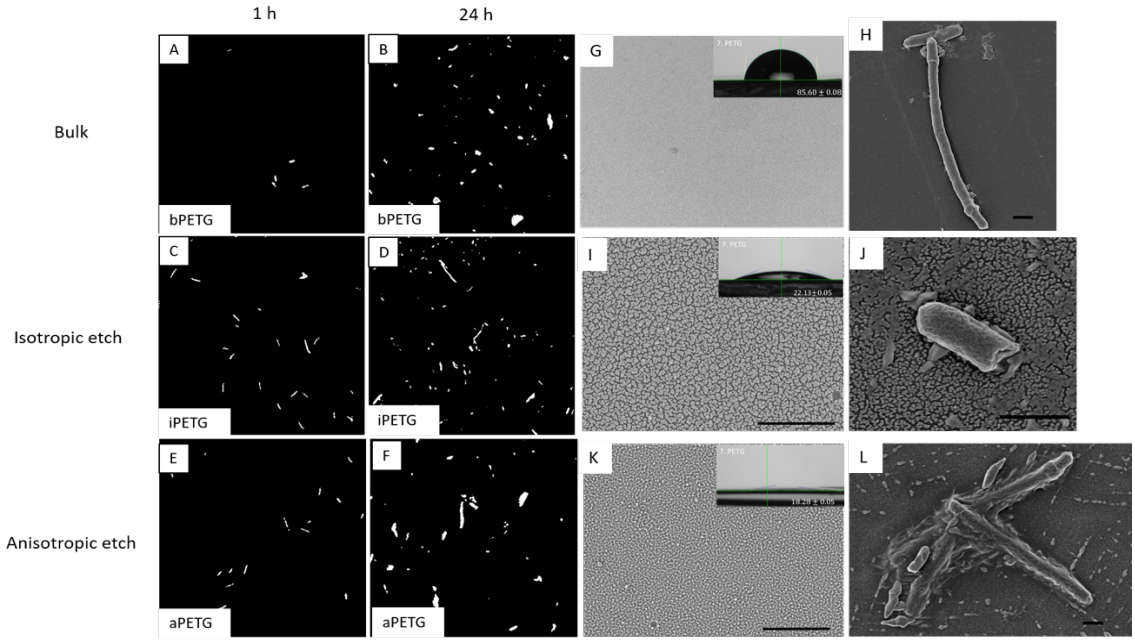

Supplementary Figure 2.7 Confocal Microscopy Images of E. coli Grown on Bulk, Isotropically Etched and Anisotropically Etched Polyethylene Terephthalate Glycol-Modified after 1 And 24 Hours of Incubation.

Supplementary Table 1.1 Categorization of the Different Polymers Based on Pattern Obtained after Etch. The table shows the various polymers and their etched counterparts broadly categorized under the different topographies.

Flat	**Popcorn**	**Crater**	**Tent**	**Grass**
All bulk polymers	iPI, aPI	iPC	iPFA	iPETG
	aPFA	iABS, aABS		
	aPOM			
	aPETG			
	aUHMW PE	iUHMW PE		

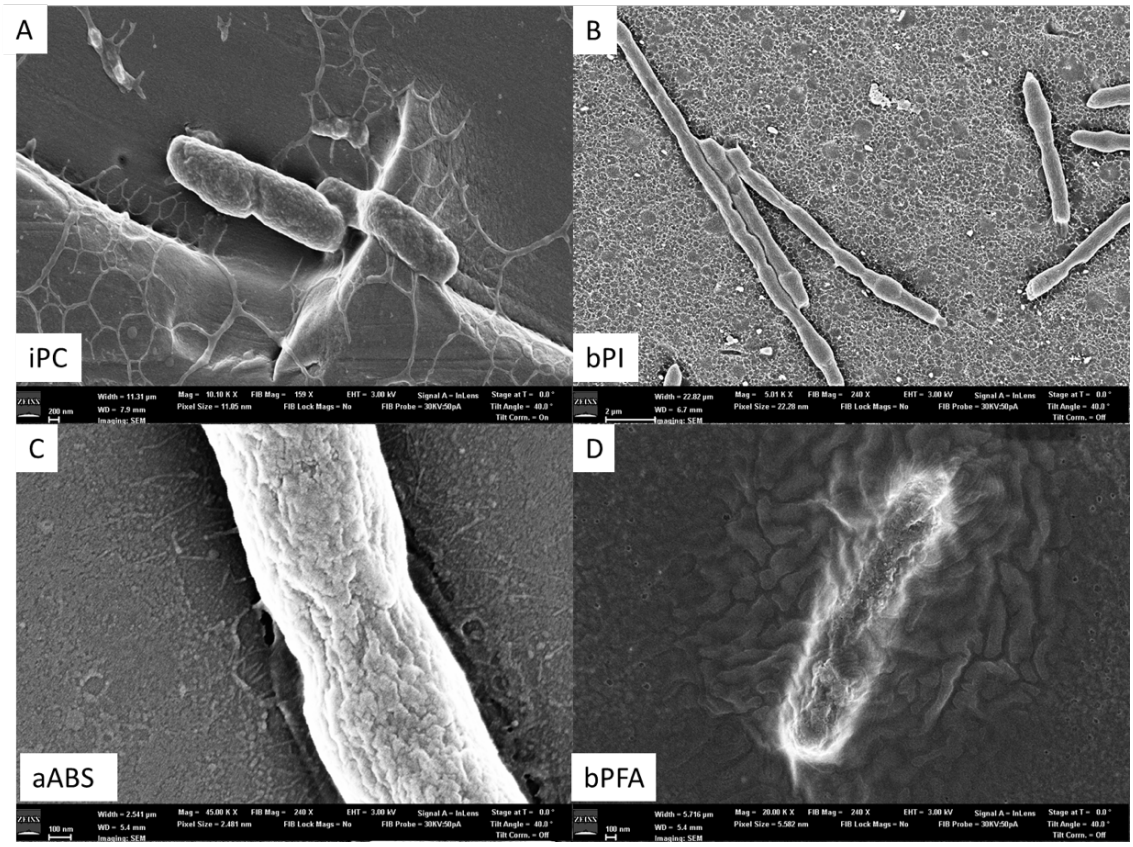

Supplementary Figure 2.8 Bacterial Attachment. A) bacteria cling to the corners of iPC to increase the surface area for adhesion B) examples of filamentous bacteria. Here, they are seen growing on bPI. C) Bacteria on aABS show signs of adhesion appendages D) Bacteria firmly entrenched in EPS on bPF.

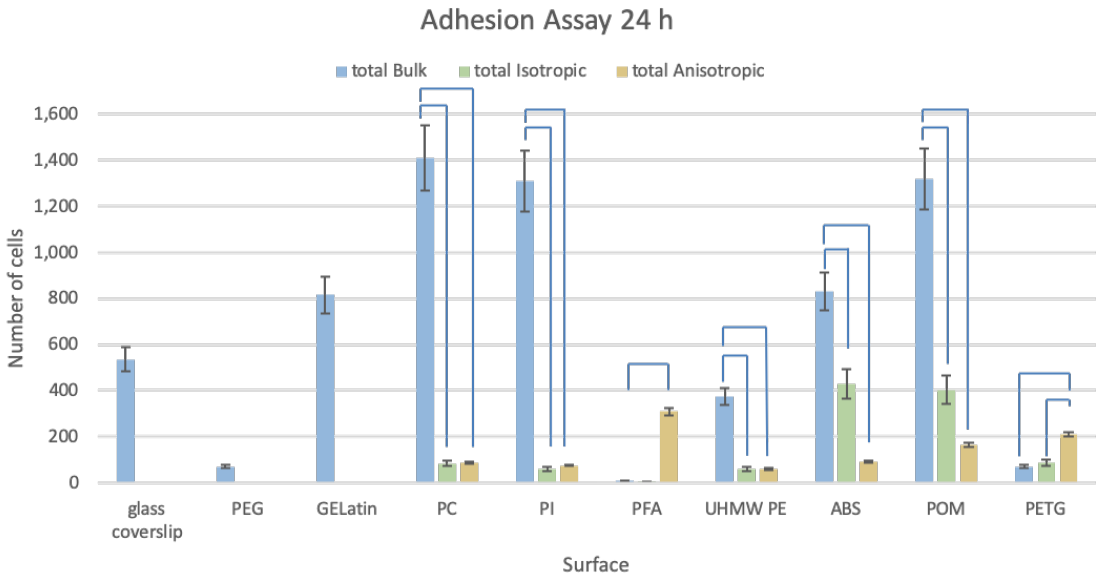

Supplementary Figure 2.9 Adhesion Assay Performed after 24h of Incubation.

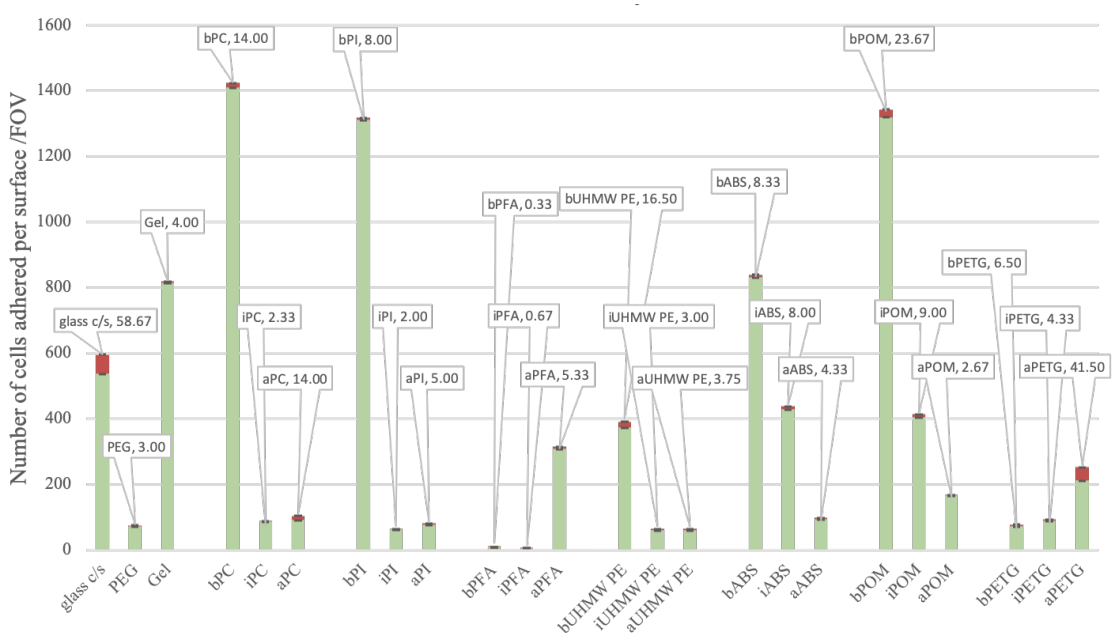

Supplementary Figure 2.10 Membrane Permeability Assay after 24h. Percentage of dead cells per sample displayed as a fraction of the total number of cells for that sample. The graph represents the cumulative adhesion data recorded upon 1 hour of incubation of the E. coli on the bulk, isotropic and anisotropic surfaces. Gelatin was used as a positive control and PEG as a negative control.

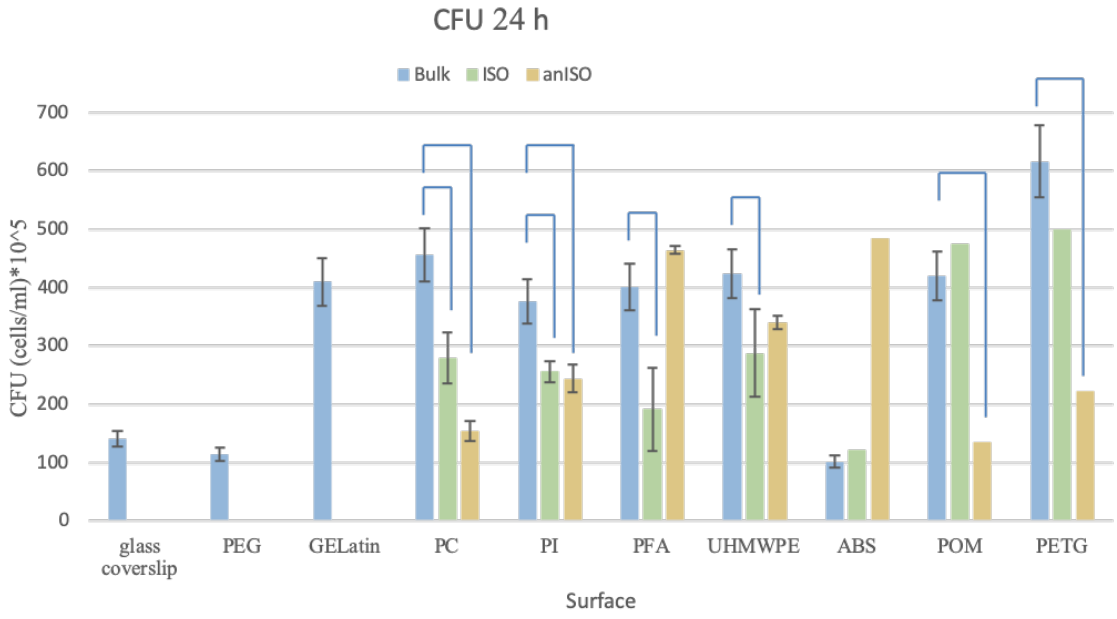

Supplementary Figure 2.11 CFU Assay after 24h Incubation. Graph indicates the results of a colony forming unit (CFU) assay performed after 24 hour of incubation of the E. coli on each polymeric nanostructured surface. Several of the bacteria were damaged but viable after 1 hour of contact with the samples (see tall bars). Polyimide, PFA and aUHMWPE retained bacterial cells that were the least viable amongst all the surfaces tested. $p<0.05$

CHAPTER III

E. COLI SURFACE MORPHOLOGY CONTROLS THE CELLULAR RESPONSE TO GaN PPC

III.1. Introduction

Group III-V wide bandgap semiconductor materials, including those composed of Ga, possess a property known as Persistent Photoconductivity (PPC), which is the build-up of transient photo-induced current on the surface the material after photoactivation [303,304]. Recent work has demonstrated that these materials serve as an excellent interface between cells and electronic devices [196,207,305]. In the experiments, photoactivated GaN materials alter the cell adhesion, plasma membrane potential, cell physiology, biofilm formation, and mitochondrial activity [206,207306]. Recent work has shown the photoactivated GaN substrate generates locally high levels of ROS species, which may explain some of these changes to cell behavior and physiology.

Bacteria, like *E. coli*, use a variety of surface appendages to engage their extracellular environment both mechanically and chemically. [66,102] *E. coli* has several important surface structures that have been involved in these types of signaling include flagella, pili, curli, and LPS [46,278,288]. Each of the other appendages performs a different function during biofilm formation: pili (adhesion)[75,85], curli (adhesion, aggregation and biofilm formation)[90,97] and LPS (permeability barrier and virulence)[105].

Understanding their involvement in the process of adhesion to photoconductive surfaces will provide a new perspective and inform the development of new bioelectronic platforms. However, the structural or surface aspects of the cell that control and enable these responses to PPC are unclear.

In this chapter I systematically analyze specific morphological components of the *Escherichia coli* (*E. coli*) required for bacterial adhesion to PPC GaN. To determine the manner in which *E. coli* bacteria associate with GaN substrates and how these interactions control bacterial behavior, I examined the behavior of *E. coli* bacteria that contained deletions for genes that are associated with these surface structures. I hypothesized that the presence of a surface charge will have a direct effect on the adhesion of secreted ECM molecules and therefore the ability of bacterial cells to adhere. To test this hypothesis, I tested the effect of PPC on adhesion in knockout cells to determine the contribution of structural elements vs ECM deposition, if the dominant factor is due to ECM deposition, I hypothesized that structural mutants should not affect adhesion to charged surfaces.

III.2. Experimental Section

III.2.i. Bacterial Strains and Growth Conditions

Table 3.1 E. coli Strains and Genotypes used in this Paper

Name	Keio Library Strain #	genotype
WT	BW 25113	F-, *Δ(araD-araB)567, ΔlacZ4787*(::rrnB-3*), λ-, rph-1, Δ(rhaD-rhaB)568, hsdR514*
ΔfimA	JW4277-1	F-, *Δ(araD-araB)567, ΔlacZ4787*(::rrnB-3), *λ-, rph-1, Δ(rhaD-rhaB)568, ΔfimA782::kan, hsdR514*
ΔfimB	JW4275-1	F-, *Δ(araD-araB)567, ΔlacZ4787*(::rrnB-3*), λ-, rph-1, Δ(rhaD-rhaB)568, ΔfimB780::kan, hsdR514*
ΔfimH	JW4283-3	F-, *Δ(araD-araB)567, ΔlacZ4787*(::rrnB-3*), λ-, rph-1, Δ(rhaD-rhaB)568, ΔfimH788::kan, hsdR514*
ΔcsgD	JW1023-1	F-, *Δ(araD-araB)567, ΔlacZ4787*(::rrnB-3*), λ-, ΔcsgD781::kan, rph-1, Δ(rhaD-rhaB)568, hsdR514*
ΔcsgG	JW1020-1	F-, *Δ(araD-araB)567, ΔlacZ4787*(::rrnB-3*), λ-, ΔcsgG778::kan, rph-1, Δ(rhaD-rhaB)568, hsdR514*
ΔFliC	JW1908-1	F-, *Δ(araD-araB)567, ΔlacZ4787*(::rrnB-3*), λ-, ΔfliC769::kan, rph-1, Δ(rhaD-rhaB)568, hsdR514*
ΔFlgE	JW1063-1	F-, *Δ(araD-araB)567, ΔlacZ4787*(::rrnB-3*), λ-, ΔflgE745::kan, rph-1, Δ(rhaD-rhaB)568, hsdR514*
ΔgmhB	JW0196-2	F-, *Δ(araD-araB)567, ΔgmhB725::kan, ΔlacZ4787*(::rrnB-*3), λ-, rph-1, Δ(rhaD-rhaB)568, hsdR514*
ΔrfaH	JW3818-1	F-, *Δ(araD-araB)567, ΔlacZ4787*(::rrnB-3*), λ-, rph-1, ΔrfaH783::kan, Δ(rhaD-rhaB)568, hsdR514"*

The bacteria used for this paper were obtained from the Keio library[38] of single deletion mutants with the parent strain *E. coli* BW25113. Prior to experimental use, a fresh bacterial colony was seeded from a mother plate and cultured overnight in Luria Broth medium in a shaker incubator at 37°C.

III.2.ii. Bacterial Surface Characterization

To characterize the changes to the physical surface properties of mutant bacterial cells for determining whether these changes could help determine the mechanism or properties that are critical for interaction with GaN materials, I performed two assays: a Material Adhesion To Hydrocarbons (MATH) assay and a Zeta potential analysis. To prepare cells for these assays , I cultured cells of the appropriate strain overnight and then diluted the culture to an OD_{600} ~0.1. 750 µl of the culture was added to a cuvette followed by the dip cell electrode (Product Number ZEN2002). Zeta potential measurements were obtained using a Malvern Zetasizer Nano ZS.

I performed a MATH assay (Material Adhesion To Hydrocarbons) [309] to determine relative hydrophilicity. The description of this procedure in brief, 5 ml of overnight cultures of the bacterial cells were pelleted, resuspended in 1xPBS and diluted to an OD_{600} of ~0.1. The OD_{600} values of the preprocessed samples were recorded. 1 ml of octane was added to 4 ml of each of the bacterial cultures. These samples were vortexed vigorously for 2 minutes and allowed to stand for 20 minutes. The OD_{600} value of the aqueous part of the cultures was noted. The following formula was used to determine the relative hydrophobicity of each bacterial knockout strain:

$$\% \text{ hydrophobicity} = \left(1 - \frac{OD600\ before}{OD600\ after}\right) \times 100$$

III.2.iii. Adhesion Assay

A bacterial adhesion assay was performed using the direct microscopic count (DMC) method on a Zeiss inverted spinning disc confocal microscope. Cells were grown overnight at 37°C in a shaker incubator and adjusted to an OD_{600} of ~0.1 the following day. 100 µl of OD_{600} adjusted bacterial cells were incubated with SYTO9 in the dark at room temperature (~23°C) for 20 minutes. The cell-dye combination was pelleted and resuspended in 1 ml 1x PBS. 100 µl of labeled bacteria were incubated on charged and uncharged GaN substrates for 5 minutes at room temperature. They were then washed gently with 1x PBS and immediately imaged. The number of bacteria per field of view (100 m^2) at 100x magnification were counted. At least 15 images were taken per sample. The experiment was repeated three times.

III.2.iv. Membrane Potential Assay

A Baclight Bacterial Membrane Potential Kit (Thermo Scientific; catalog number B34590) was utilized to monitor the membrane potential of cells interacting with charged and uncharged GaN. A working solution of the stock membrane potential monitoring dye [3mM $DiOC_2(3)$] was prepared by diluting 1 µl of the stock solution in 1 ml of sterilized PBS. 10 µl of this working solution was then added to the cells. CCCP was similarly diluted. Cells were grown overnight at 37°C in a shaker incubator, adjusted to an OD_{600} of 0.05 the next day and allowed to grow to OD_{600} = 0.6. 100 µl of this cell culture was pelleted and resuspended in 1 ml PBS. A control tube containing cells, but no dye was kept aside. 10 µl of the $DiOC_2(3)$ working solution was then added to the 1ml of

cells in PBS. 100µl of this cell-dye solution was added to each substrate in a 96-well plate and allowed to incubate at room temperature for 30 minutes. The CCCP working solution was added to the cell culture tube and this was used as a positive control. Plain PBS with the dye solution and plain PBS were used as negative controls along with a well containing cells but no dye. The working CCCP solution was added to the working dye solution as a control for dissipating membrane potential. After the 30-minute incubation period, the GaN substrates were carefully removed using forceps and placed upside down on a cover glass and imaged using a Zeiss inverted spinning disc confocal microscope. At least 15 images were taken per sample. The experiment was repeated three times with at least two different overnight bacterial cultures.

III.2.v. Catalase Activity

The catalase colorimetric activity kit from Thermo Fisher (Catalog Number: EIACATC) was used to measure ROS. The catalase standard provided was used to generate a standard curve. The *E. coli* cultures were grown overnight, diluted to an OD_{600} of 0.1 and 100 µl were added to the charged and uncharged GaN surfaces. The cells were then vortexed loose from the surface of the GaN and diluted in the assay buffer, 25 µl of which was added to the wells of a 96-well plate. 25 µl of hydrogen peroxide (H_2O_2) was then added to each well and left to incubate at room temperature for 30 min. 25 µl of the provided substrate and horseradish peroxidase (HRP) was then added and left to incubate further for 15 min. The HRP and substrate react to form a pink solution. The 96-well plate was then read spectrophotometrically at OD_{560}. An increase in catalase activity is

seen by the decrease in the pinkness of the samples, which indicates a decrease in the amount of H_2O_2. The number of units of catalase present in each sample was calculated by plotting onto the standard curve. Each unit of catalase corresponds to the decomposition of one micromole of H_2O_2 per minute at room temperature.

Statistical Analysis: All statistical analysis was carried out using a significance level of $p< 0.05$.

III.2.vi. GaN Substrates

GaN substrates were manufactured as previously described[208]. To photoactivate these surfaces 5mm x 5mm pieces of GaN were irradiated under a UV lamp for 30 minutes to induce persistent photoconductivity. The samples were kept in the dark for at least 24 hours prior to experimentation.

III.3. Results and Discussion

During the attachment of bacteria to a surface and subsequent biofilm formation, bacteria interact with the extracellular environment using a variety of surface structures notably fimbriae, curli, flagella, and the LPS[278]. In this study, I used deletions mutations of genes that are critical for the formation of these structures[34] to identify their requirement for the PPC response (Table 2). I hypothesized that the presence of surface charge generated by the PPC would have a direct effect upon the adhesion of the bacteria.

Flagella are involved in motility, but also seek out crevices for adhesion [307,308]. Fimbriae are thin, rigid, polar filaments that protrude from the surface of bacteria;

Fimbriae are composed of the long-chained protein, pilin, and are critical for forming the initial stable cell-surface attachments [23,2]. Alteration to the structure of the fimbriae changes the adhesive potential of these bacteria [310,311]. Curli are thin, intrinsic components of the outer membrane that are associated with biofilm formation and cellular aggregation [92,99]. Curli production is highly regulated and helps make the transition from a predominantly flagellar-based motile lifestyle to a curli-enhanced adhesive lifestyle during the initial adhesion stage of biofilm formation[98]. Unlike fimbriae, there is no relationship between the number of curli and adhesion. The bacterial flagellar filament is a long tubular helix composed of a single type of protein, flagellin; flagella have critical roles in motility and in the mechanosensation of surfaces [301,312]. Bacteria like *E. coli* interact and transduce mechanical signals from their extracellular environment through their cell wall which is composed of a complex matrix known as the lipopolysaccharide complex (LPS)[105]. LPS have also been known to elicit inflammatory and virulence responses in animals. Its structure is composed of an oligosaccharide O-antigen, inner core and the lipid layer, lipid-A.

The deletion mutations of three major fimbriae genes: *fimA, fimB,* and *fimH,* were chosen to determine the contribution of the adhesion appendages upon the charged surfaces. *FimA* encodes the major repeating protein subunit of the fimbriae and deletion of the *FimA* gene results in the loss of fimbriae formation[85]. *FimB* encodes a transcriptional regulator *FimA* and loss of *FimB* function results in a loss of *FimA* production[313]. I examined the deletions of two genes associated with curli formation: *csgG* and *csgD*. The *csgG* encodes a protein that controls the stability and secretion of the

major curli structural protein curli *CsgA* and *CsgB* [90], while *csgD* encodes a transcriptional activator that regulates the expression of the curli operons [95]. Therefore, it controls the number of curli produced, and thereby offers control over the initial bacterial adhesion dynamics. Curli may be involved only during initial adhesion, and then silenced as the Cpx and Rcs pathways switch on during biofilm formation[314,90]. I also examined deletions of two major flagellar genes: *fliC,* which encodes flagellin, the major structural component of flagella[315,316], and *flgE*, which encodes the hook connection for the flagella protein to the cell body[74,315]. Lastly, I examined the deletion mutants of two genes that encode enzymes essential for the proper secretion of the LPS: *gmhB* and *rfaH* [34,317,318]. The deletion of both genes has been shown to alter *E. coli* adhesion[34].

Table 3.2 E. coli Surface Morphology Surface Structure/Function Characterization

gene	Bacterial Component/function	Zeta potential	% hydrophobicity
wildtype		-15.2 ± 0.49	5±0.04
ΔfimA	Fimbriae/ major repeating subunit	-13.8±0.92	10.53 ±0.09#
ΔfimB	Fimbriae/ transcriptional regulator of *fimA*	-15.7±0.93	2.83 ±5.72#
ΔfimH	Fimbriae/ a minor protein component that recognizes mannosyl residues	-16.6±0.25*	5.72 ±0.05
ΔcsgD	Curli/DNA-binding transcriptional activator in 2-component regulatory system	-15.7±0.8	26.3 ±0.14#
ΔcsgG	Curli/outer-membrane lipoprotein required for curli subunit secretion	-20.2±0.64**	9.45 ±0.05#
ΔFliC	Flagella/main structural subunit	-16.8±0.72*	10.99 ±0.12#
ΔFlgE	Flagella/connects filament to main bacterial body	-15.4±1.57	3.84±0.03#
ΔgmhB	LPS/enzyme required for LPS-synthesis	-15.3±0.35	6±0.09
ΔrfaH	LPS/ core synthesis and O-antigen attachment	14.2±0.42	2.82±0.02#

* P<0.05, ** P<0.001, # P <0.05

III.3.i. *E. coli* Adhesion to Inactivated and Photoactivated GaN Substrates

To determine the interactions of *E. coli* surface morphology mutants, I incubated Syto9-labeled *E. coli* cells on irradiated and non-irradiated GaN substrates. I observed a reduction of cell-substrate adhesion with wild type *E. coli* cells on GaN that have been photoactivated by UV light (Figure 11). This result is similar to the interaction of other microbes such as the budding yeast *Saccharomyces cerevisiae* and the Gram-negative bacteria *Pseudomonas aeruginosa* with photoactivated GaN surfaces [207,208]. Whether this is due to the physical alteration of the local environment such as a reduction in positive charge or due to active response from the bacteria remain unclear.

I observed a uniform alteration to the bacterial adhesive behavior on uncharged GaN. In some cases, there was a reduction (*fimA*, *fimB*, and *flgE*) in binding compared to WT and a lack of response to changes in surface charge. Comparing the adhesion trends of the strains on uncharged and charged surfaces, only the WT and *ΔfliC* strains show a significant decrease in the total retention of bacteria. Several other mutants (*fimH*, *csgG, csgD, gmhB, rfaH*) show the opposite response, an increased binding to charged GaN surfaces when compared to WT. There was a 4-fold increase of retention of Δ*fimH*, 5-fold of *ΔcsgG* and a 3-fold increase of Δ*gmhB*. An overall increase in adhesion of all the strains of bacteria was seen when grown on a UV charged surface. *FimH* encodes an essential component of the fimbria that mediates the adhesion strength, as deletions of *fimH* result in bacteria that do not form stable adhesion [319].

The results shown here support the hypothesis that the phenomenon of persistent photoconductivity on charged GaN surfaces would have a direct effect on the ability of WT bacteria to adhere. The structural adhesion appendages of the bacteria were shown to be involved in the adhesion process as evidenced by the deviation in adhesion by the mutants from the WT when placed on charged GaN substrates.

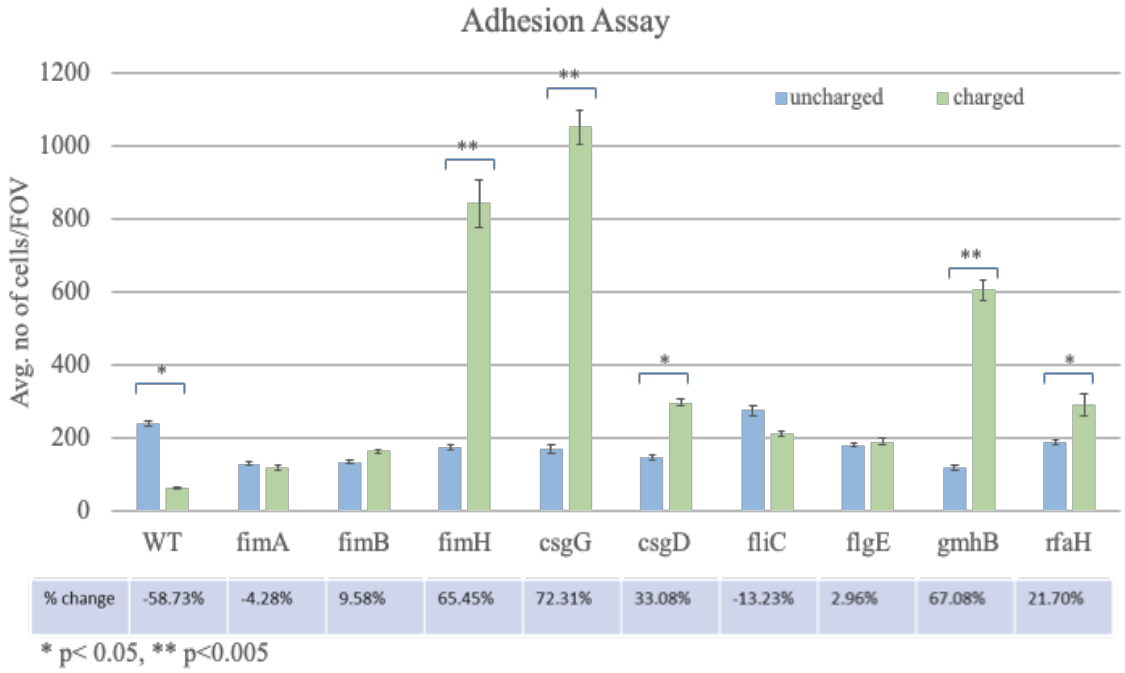

Figure 3.1 Adhesion Assay of E. coli Mutants Performed on Charged and Uncharged GaN Substrates

III.3.ii. GaN PPC Reduces *E. coli* Motility

The WT bacteria showed a great deal of change in their motility depending on the charge of the surface: the WT bacteria were immobile on the charged GaN whereas they showed regular movement on the uncharged surfaces.

This has been observed as an interesting aside during studies conducted for using photoelectric current as a disinfectant on surfaces. Cells that were identified as "Out of plane cellular orientation" (cells standing straight) were indicative of reversible attachment[320]. My preliminary results align with this observation. This property has not been studied in detail, but it warrants further investigation especially in the light of employing such properties for bioelectronics communication. The alteration of adhesion

and the bacterial mobility that arises when the bacteria cell is in contact with a GaN surface that has been UV activated is an important observation that supports the use of PPC in bioelectronics, because these are clear physiological alterations that are directly controlled by the surface condition.. The current working explanation is that the orientation of the bacteria feeds highly into its adhesive state, i.e. greater surface area contributes to a greater number of adhesive organelles in play.

A possible explanation could involve the pili. pili are known to control twitching and swimming motion[86], and these structures are regulated by the proton motive force (pmf). Reduction of pmf leads to slower pili action and therefore, slow bacteria. The charge generated by the PPC could affect the regulation of charge between the inside and outside of the bacteria, thereby halting the process of proton motive force. The abrupt halting of bacterial motion was an expected result for the flagellar mutants as it is known that flagella are primarily dependent on pmf[321]. Pmf is important in bacteria due to their involvement in pili biogenesis[75,322], virulence activity, and locomotion by driving bacterial flagellar motility[323], cell division[324], outer membrane protein transport and catabolism[325]. All these functions make it an indispensable phenomenon when studying the electrophysiology of bacteria. When the flagella sense a surface, flagellar motor function ceases immediately. Inhibiting flagellar rotation increases the pmf due to the non-utilization of the protons generated by the Electron Transport Chain (ETC)[312]. The flagellar deletion mutants behaved as expected. Similarly, the retraction speed and motion of pili are controlled by the pmf[86].

This is concurrent with previously reported data that showed a difference in the adhesion behavior of bacteria in response to the polarization of the substrate: increased adhesion upon an increase of negative potential to the surface (from -100 to -300mV) [308,202]. The rate of adhesion increases with the application of negative potential and vice-versa with positive potential[202].

I speculated whether this result was indicative of extracellular electron transfer leading to membrane depolarization and further to a decrease in adhesion rate. Extracellular electron transfer is a type of mechanosensation[18]. It is a biochemical process where electrons are transferred across the bacterial cell membrane and be induced by the Persistent photoconductivity of group III semiconductor materials[194]. The energy transfer could have polarized the cell and therefore created a similar positive charge on the cell membrane and the surface. This could have led to the repulsion of the positively charged surface and the now polarized and positively charged bacteria. The UV activation may also have caused the deletion mutants to open previously covered porins/pathways, thereby creating an electron/proton gradient. I decided to test this hypothesis by measuring the membrane potential of the *E. coli* WT as a means of better understanding the influence of externally provided electrons upon adhesion.

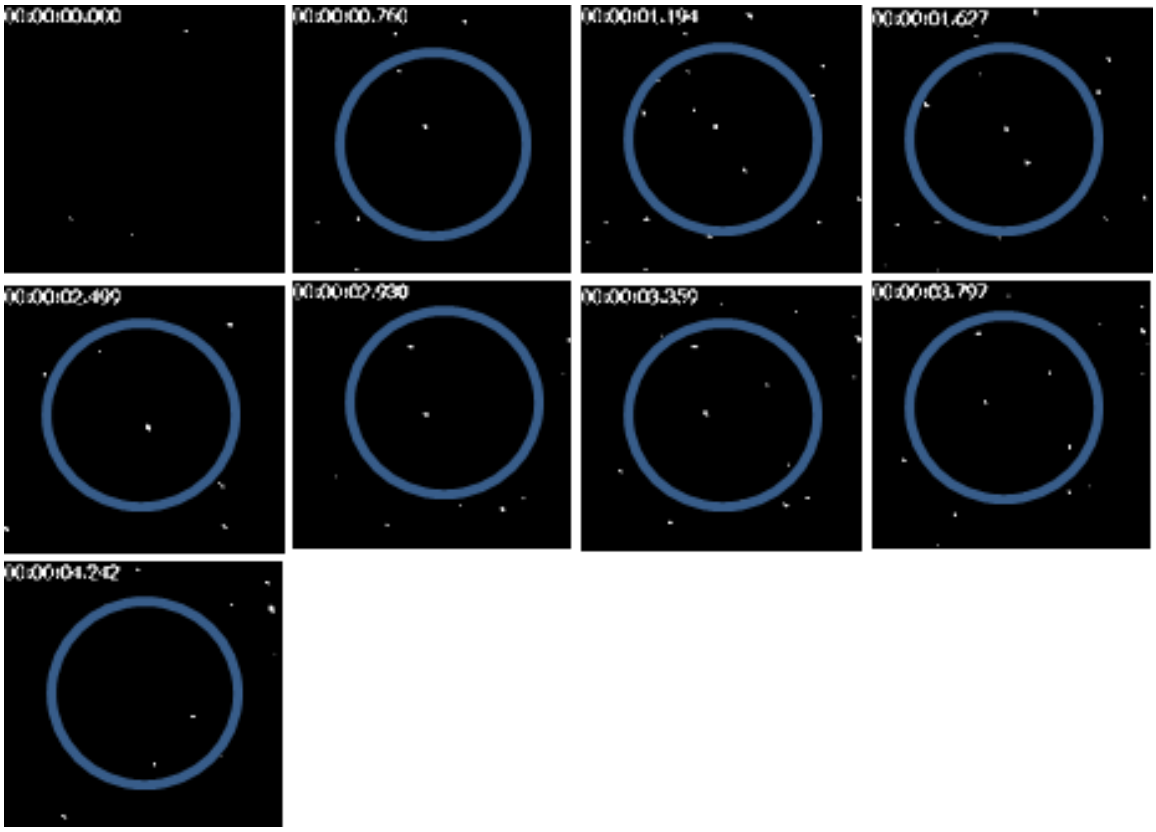

Figure 3.2 Time Lapse of Cellular Motility on Uncharged GaN Substrates over 5 Minutes

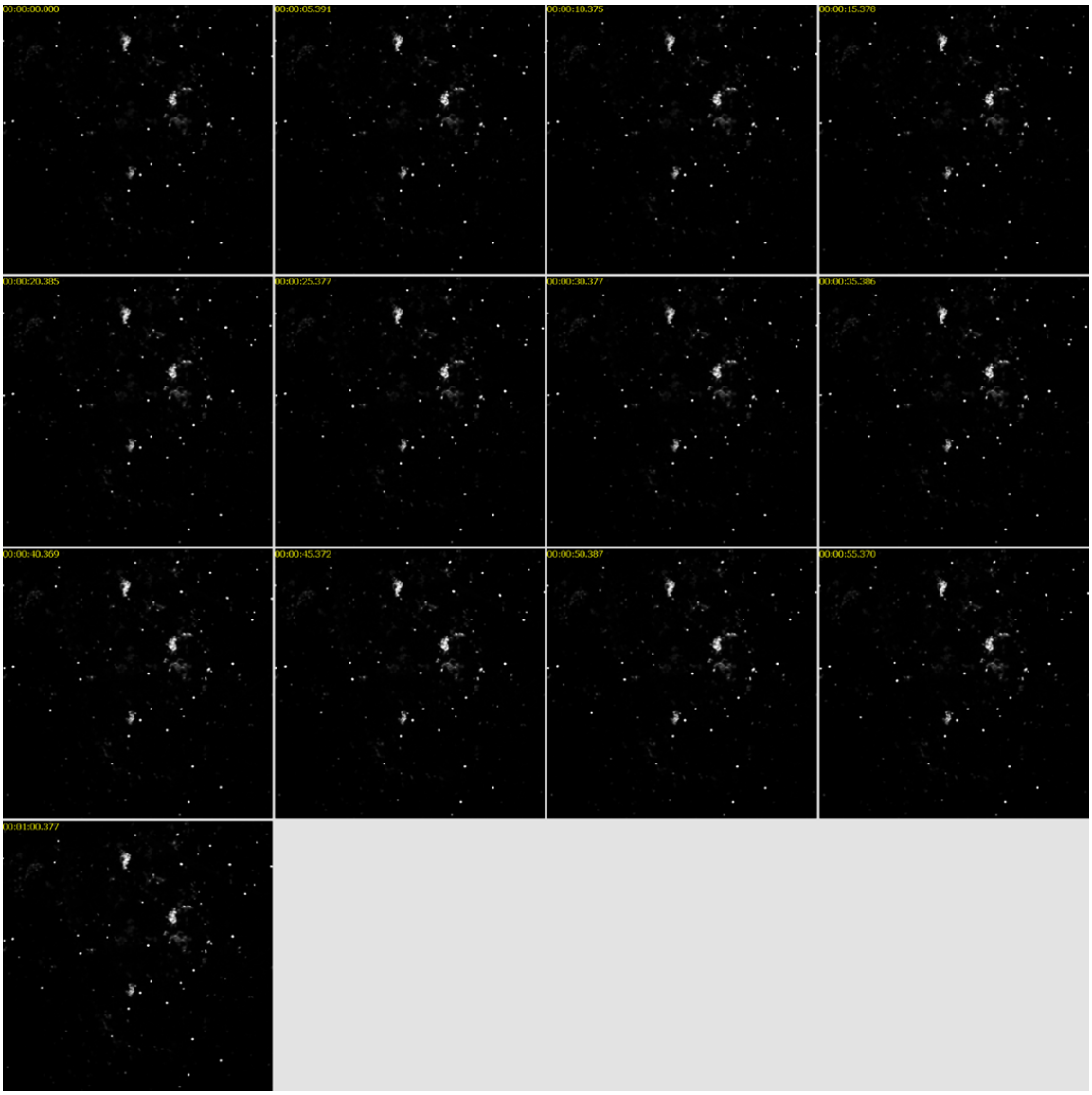

Figure 3.3 Time Lapse of Cellular Immobility on Charged GaN Substrates over 1 Minute

III.3.iii. Plasma Membrane Potential of *E. coli* Adhesion in Response to Photoactivated GaN Substrates

To test whether the changes in adhesive behavior of the bacteria when placed on a charged photoconductive GaN substrate were due to an imbalance of the proton gradient, I quantified changes in bacterial membrane potential.

To quantify any changes in membrane potential ($\Delta\Psi$), I used the ratiometric dye DiOC(3) on bacteria exposed to activated and non-activated GaN surfaces. The DiOC(3) dye is sequestered in cells with normal proton motive force (pmf); if the membrane potential is altered, there will be a shift from green to red fluorescence[326]. The ratio of the green to red fluorescence was calculated for wild type *E. coli* bacteria. Higher ratiometric values correspond to lower membrane potential (Ψ). I analyzed whether there were any changes in adhesion of the wild type *E. coli* bacteria that were grown on both uncharged and charged GaN surfaces. A radical change in membrane potential was seen in the wild type *E. coli* bacteria , supporting our hypothesis .

Studies related to mechanosensation have shown that bacterial adhesion and biofilm formation are primarily dependent on cell surface structures: flagella, pili, curli [86,224,327,328]. To see what effect each has on photoconductive surfaces, I chose deletion mutants pertaining to the bacterial cell surface structures (Table 1). Single-gene deletion mutants of non-essential genes of *E. coli* were obtained from the Keio library[38]. I repeated the experiment using the *E coli* bacteria that were mutants for genes encoding the structural and surface coating proteins to determine whether these mutant bacteria respond to GaN surfaces in the same way as the wild type. If mutant *E. coli* bacteria does

not respond as the wildtype bacteria, then we can conclude that the gene encodes a protein that is involved in a process or mechanism that is essential for this response.

I showed that the membrane potentials of all the mutant strains grown on the uncharged surfaces were lower than that of the wild type *E. coli*. This could have been due to a depolarization effect. A proton ionophore, Carbonyl Cyanide m-Chlorophenylhydrazine (CCCP) was used as a positive control to account for this possibility; it reduces the membrane potential by dissipating the proton motive force.

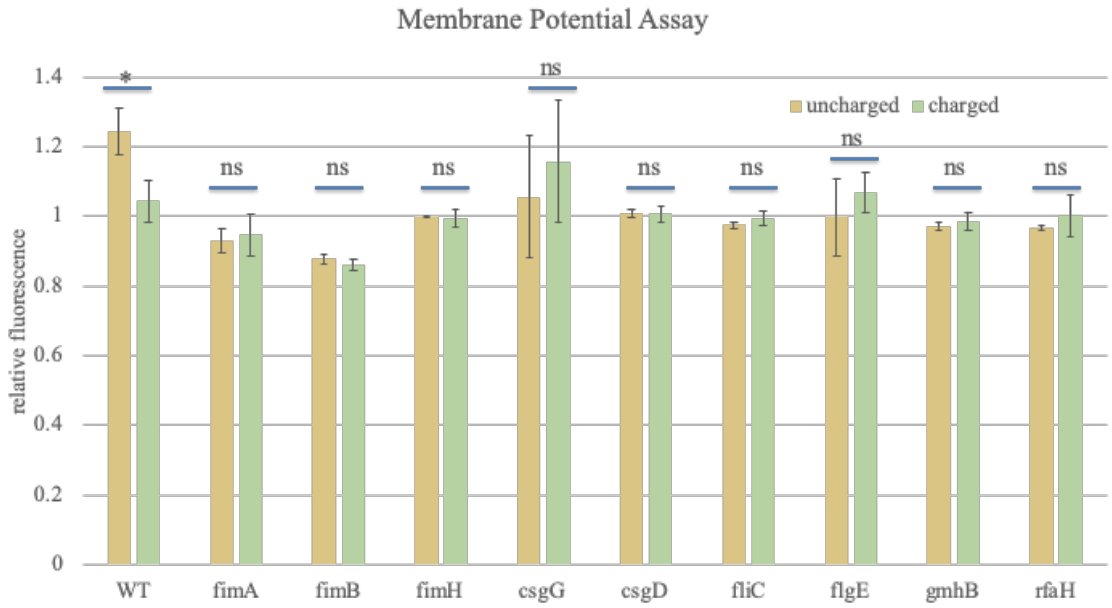

Figure 3.4 Membrane Potential Assay. The ratiometric dye DiOC(3) was used to determine the relative membrane potentials of all the bacterial strains grown on plain and UV-irradiated GaN surfaces. Lower relative fluorescence values indicate higher membrane potential. The WT bacteria grown upon plain and UV irradiated surfaces was significantly different. There is a net increase in the membrane potential after exposing the bacteria to UV irradiated GaN surfaces exhibiting PPC. The proton ionophore CCCP was used as the positive control to reduce the membrane potential to zero. All the data was obtained by ratiometrically profiling images obtained from a spinning disc confocal microscope set at 40x magnification.

Using the results obtained as baseline membrane potentials for the individual strains, I compared their membrane potential to that when grown on the charged surfaces. In stark contrast to the ΔΨ of the WT, all the mutant strains showed little to no change in membrane potentials upon the comparison of their growth on charged and uncharged surfaces. i.e. there was no charge difference between the outside and inside of the cells. This disproved the hypothesis that membrane potentials were changed during the process of PPC and could be linked directly to a decrease in mobility. The membrane potentials of the bacteria that carry deletion mutation in genes encoding proteins that are components of surface adhesion structures or cell wall components remained constant even in the presence of a charge GaN substrate. Membrane potential is an important requirement for bacterial cell division[324]. Keeping the number of adhered bacteria constant on a bioelectronic interface can eliminate any bias caused by bacterial reproduction. Since the membrane potential of the wild type *E. coli* changed in response to the UV activation of the GaN substrate, I considered that perhaps membrane potential was not the only factor influenced through PPC. It is possible that extracellular electron transport pathways [329–332] could have been disrupted by the application of an external PPC charge. We have previously shown that bacterial internal processes are disrupted when incubated on GaN surfaces that have been activated via UV irradiation by quantifying intracellular Ca^{2+} concentration[208]. Combining this with the observations made in this present study, I conclude that although internal processes were affected by the PPC, it did not change the overall membrane potentials. In a different study, it was shown that the blocking of voltage and calcium flux altered mechanosensation[333]. It is not

unreasonable to think that perhaps all these bacteria (from their studies and ours, share the same mechanism, excluding the possibility of change in membrane potential being the sole driving force). The change of the plasma member of the wild type *E. coli* cell in response to GaN activation, but not any of the mutants *E. coli*, which alter a diverse array of structural components in the cell, demonstrates the complexity of maintaining property membrane potential, i.e. no single system is responsible for the response.

The next step was to see whether the charge that forms between the surface of the the bacterial cells and the liquid media could have had anything to do with their reactions to the charge. To measure this, I examined the zeta potential of the bacterial cells from each of the strains used in this study. To determine how the genetic/structural changes influence the surface properties of the *E. coli* cell, I determined the surface charge (zeta potential) and relative hydrophobicity of these cells. I found that only three mutations *(ΔfimH, Δ csgG, ΔcsgD*, and *ΔFliC*) had significantly altered surface potentials.

When comparing the values of zeta potential and the adhesion behavior of the strains, I noticed a trend. Mutant bacterials cells that had zeta potentials lower than the WT exhibited an increase in the adhesion to UV irradiated GaN surfaces. Following the trend, I expected to see increased adhesion in all the following strains: Δ*fimB*, Δ*fimH*, *ΔcsgG, ΔcsgD, ΔfliC*, Δ*flgE,* and Δ*gmhB*. I found that for the most part, only 3 mutations (*ΔfimH, ΔcsgG,* and Δ*fliC*) exhibited significant changes to their zeta potential when compared to wild type *E. coli* cells. Large zeta potential values indicate a more stable dispersion of particles. This change in zeta potential values indicated that the genetic loss of the structures from in these mutant cells changed their surface physicochemical

properties to foster a greater degree of cell-cell aggregation. Δ*fliC* and Δ*gmhB* seemed to be the only exceptions to this finding; *ΔfliC E. coli* had reduced adhesion and *ΔgmhB* had an increased number of cells on activated GaN surfaces. The *ΔfliC* result could mean the flagella, which are missing in *ΔfliC* cells are required for adhesion and for controlling surface charge; and that surface charge alone is not sufficient for controlling the binding to the GaN surface. it is also possible that the increased adhesion properties of Δ*fimH* and Δ*csgG* were influenced by their inherent tendency to aggregate, as evidenced by their zeta potentials (Graph 1 and Table 1). However, this possibility can be disregarded when the binding of the Δ*fimH* and Δ*csgG E. coli* cells to charged surfaces was no different than uncharged surfaces.

Another possible explanation of the adhesion variances between wild type *E. coli cells* and the *E. coli* mutant cells on UV charged GaN surfaces is that chemical moieties may have become more accessible due to the deletions. The alteration in the adhesion of mutant *E. coli* may be due to steric attraction/repulsion. Bacteria are inherently negatively charged since their outermost layer is made of peptidoglycan, a mixture of carboxyl and amine groups and loss of structures like pili or components of the LPS may provide access to this charged surface to UV-activated GaN materials.

The hydrophobicity of these strains was also measured using a standard MATH assay. Fimbriae and LPS are required for the co-aggregation of bacteria [334], which was corroborated by the data I had obtained. These results suggest that neither zeta potential nor hydrophobicity not directly affect bacterial adhesion but may be involved in the process by contributing to the roles that the adhesion appendages play.

III.3.iv. Catalase Activity

Organisms under stress produce reactive oxygen species (ROS). ROS are generated in the mitochondria in response to environmental disturbances such an attack by macrophages. It can cause internal cellular injury. Hydrogen peroxide (H_2O_2) is amongst the most commonly found ROS. The enzymes catalase and superoxide dismutase are involved in the cell's defense mechanism of converting the harmful ROS species into inert products.

To test whether persistent photoconductivity induced a stress response within the bacterial cell, I performed an assay to measure ROS activity. I hypothesized that if the bacteria were experiencing environmental stress from PPC, there would be an increase in the ROS produced within the cell.

The measurement of catalase can act as an indirect indicator of oxidative stress. Catalases are enzymes that catalyze hydrogen peroxide[335] decomposition into water and oxygen. If the bacterial cell experiences stress when placed on a charged photoconductive surface and produces the ROS hydrogen peroxide, it should produce the enzyme catalase to catalyze that reaction. Thus, the amount of catalase produced with the cell can be correlated to the among of exposure to ROS the higher the catalase activity the greater the exposure to ROS. We found that wild type *E. coli* bacteria demonstrate a robust increase in catalase activity when exposed to an activated GaN substrate. Previous work has shown that activated GaN produces ROS[1]. All mutant *E. coli* used in this study, except FimA show enhanced catalase activity, suggesting that all are exposed to greater levels of ROS, perhaps produced as defects in their electron transport chain due to their

loss of gene function. However, in most cases there is an increase in catalase activity in response to the activated GaN surface. This is not true for the bacteria with mutations in genes that encode fimbrial FimA which showed a lowered response to activated GaN exposure, suggesting that fimbriae are necessary for the ROS response on GaN materials. These results also suggest that ROS can be used as activators of certain bacterial pathways and that fimbriae are

The wild type bacteria were found to be more sensitive to persistent photoconductivity than the adhesion mutants. Only some of the mutants, *ΔfliC, ΔgmhB,* and *ΔrfaH,* showed stress responses as measured by quantifying the catalase production. There was 11.51% increase in the amount of catalase generated by the Wild Type bacteria (See Figure 8). An increase in catalase activity indicates ROS concentration at the interface. I repeated this experiment using the bacterial mutants mentioned above. *ΔfliC, ΔgmhB,* and *ΔrfaH* mutants showed 15.82%, 17.4% and 19.52 % respective increases in their catalase production. The *ΔgmhB* and *ΔrfaH* mutants do not have key components required to produce lipopolysaccharide (LPS)[34] and the *ΔfliC* does not have flagella components[336].

I have shown from this assay that their removal causes an increase in catalase activity within the cell. The LPS are outer membrane components of Gram-negative bacteria primarily involved in triggering an immune response within the cell[105]. Interestingly, both the LPS and flagellin, a key component of flagella, are associated with microbe-associated molecular pattern (MAMP), which induce innate immunity within the cell[337]. All the other strains had no significant differences in catalase activity before and

after charging the GaN. This non-reactivity is perhaps the most important result of this experiment. All the fimbrial mutants, curli mutants, and *ΔflgE* did not display any catalase activity in response to the photoelectric current, implying their importance in detecting ROS species on WT. This implies their importance in responding to reactive oxygen species present at the interface. The electrical stimulation of semiconductor surfaces inevitably produces reactive oxygen species. In hopes of mitigating the toxicity of ROS to the bacteria, understanding the role of the extracellular adhesion appendages of bacteria and their responses to electrogenic stimulation is important.

In summary, I found that persistent photoconductivity of GaN semiconductor surfaces can be used to influence specific bacterial responses: immobility, inhibition of cellular replication and catalase production in the presence of external charges. I also determined through our analysis of the adhesion knockouts, that bacterial adhesion can be controlled on charged surfaces. While the exact mechanism is not evident from the data I have collected thus far, further investigation using double-gene knockouts is bound to reveal the mechanisms involved. I suggest that the PPC property of GaN materials can be useful in the context of bioelectronics and biosensors, where an external charge elicits specific biological responses at the interface. It's short duration and gradual dissipation work in favor of its use in biosensors. components of this response system.

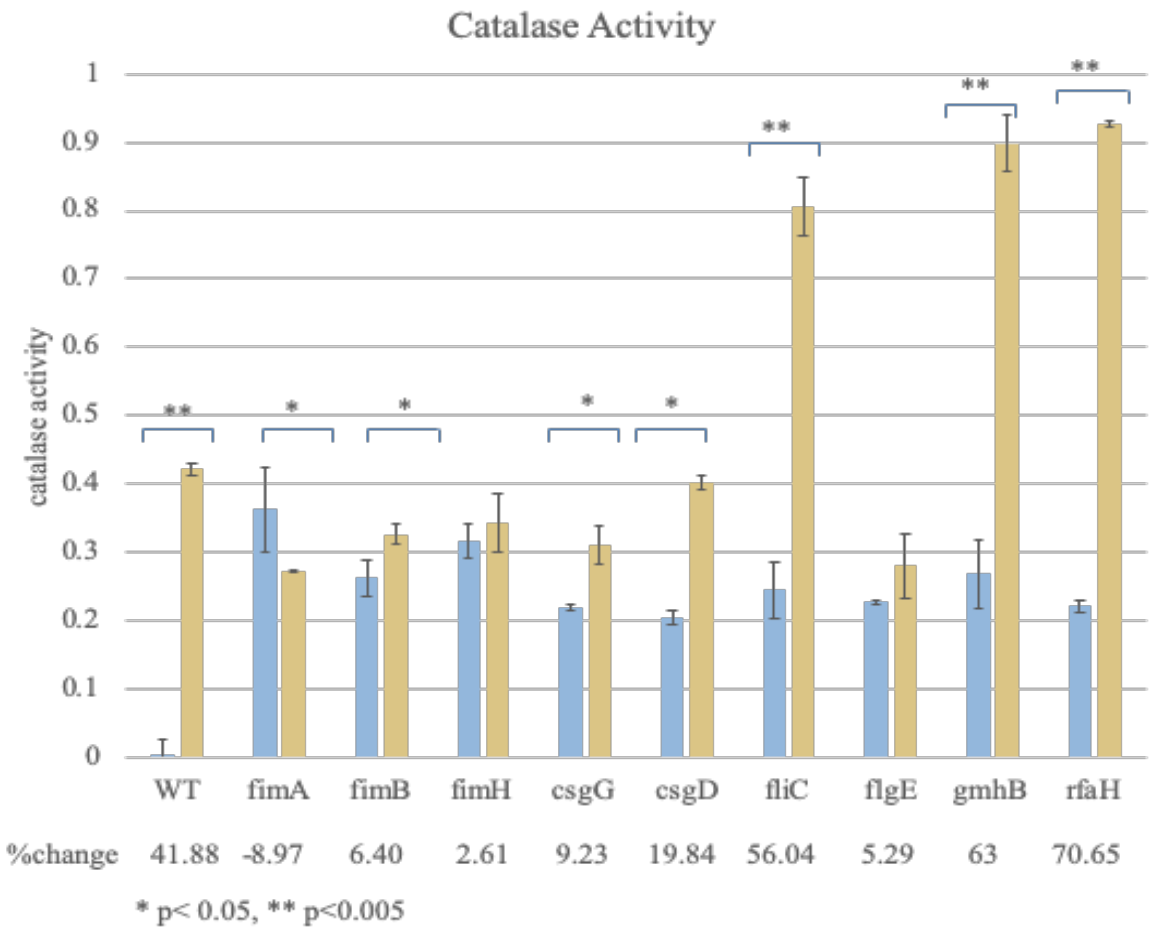

Figure 3.5 Catalase Assay. ROS activity as measured through the production of the enzyme catalase and table indicating the percentage change of membrane potential after charging the GaN surfaces using UV.

III.4. Conclusion

I conducted a preliminary analysis of the effects of persistent photoconductivity upon *E. coli* adhesion mutants in an effort to understand how bacteria can be controlled using PPC. The well-characterized GaN Group III semiconductor was used in this analysis. UV illuminated GaN substrates had a remarkable effect on wild type *E. coli* bacterial adhesion and motility: there was an increase in the number of adherent bacteria and a complete immobilization upon contact with the photoconductive substrate. *E. coli* adhesion mutants were similarly tested and compared to the wild type bacteria. UV charging of the substrate substantially increased the adhesion of the mutants. I measured membrane potentials of all the strains upon both the charged and uncharged surfaces. Surprisingly, only the WT showed a significant change in the membrane potential indicating that PPC does not affect the chosen bacterial appendages. Additionally, I tested to see if PPC would influence the ROS activity of the chosen mutants. A change was seen only in the WT, *ΔfliC, ΔgmhB* and *ΔrfaH* adhesion mutants demonstrating that these particular appendages are important for stress management against PPC. These results provide us with evidence proving that bacteria use their adhesion appendages to adjust to the presence of PPC.

III.5. Supplementary Information

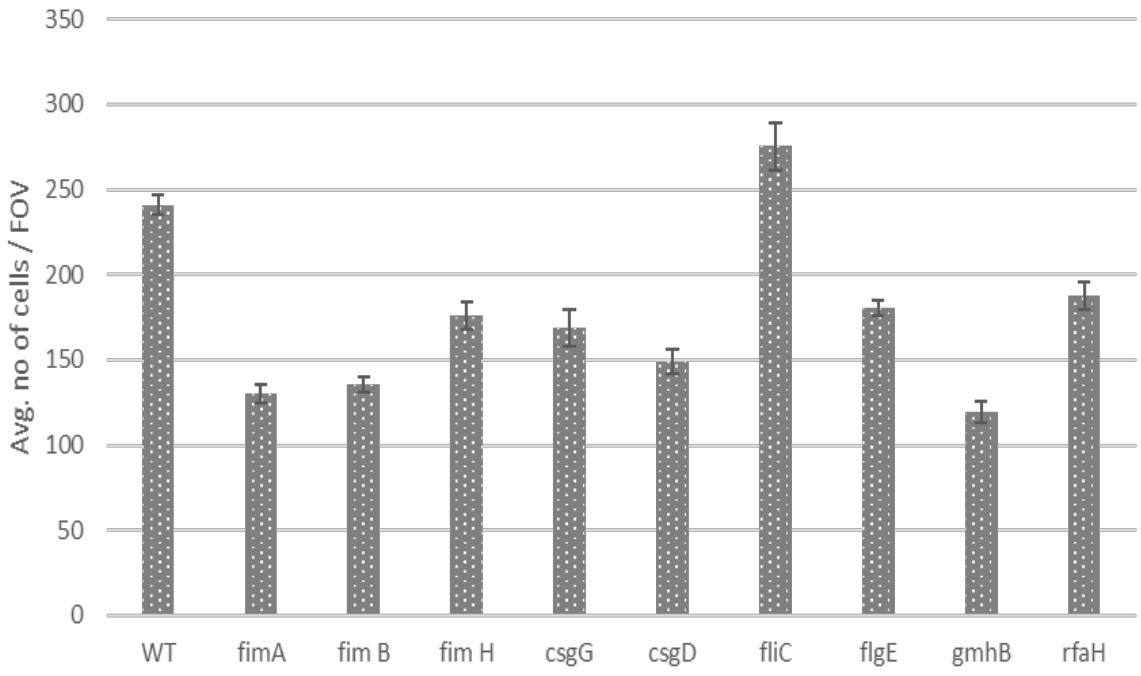

Supplementary Figure 3.1 Adhesion of the E. coli Mutants on Inactivated GaN Surfaces (Plain). All the mutants have diminished adhesion compared to the WT except for fliC.

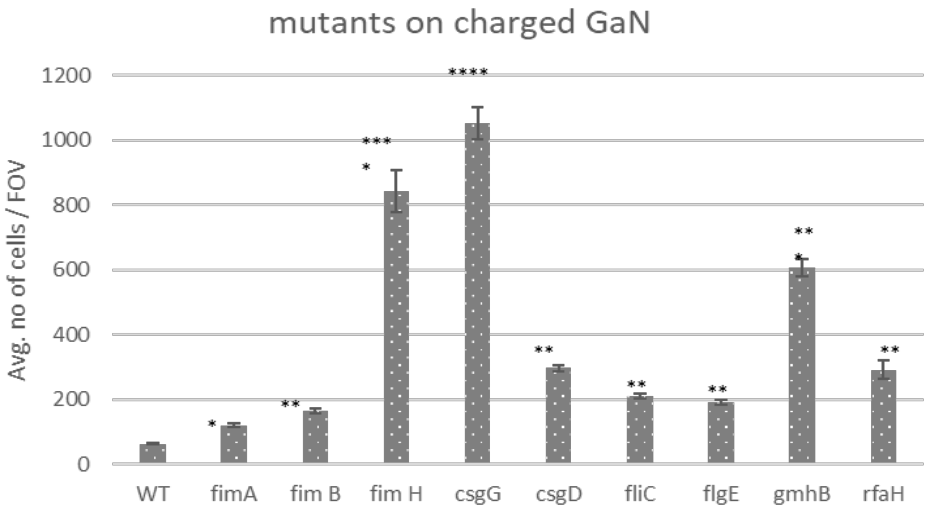

mutant	WT	fimA	fim B	fim H	csgG	csgD	fliC	flgE	gmhB	rfaH
avg. no of	188	358	492	2528	3155	889	633	574	1817	875
std dev	2.536116	5.523655	6.31967	63.48329	48.72518	9.396549	6.474468	8.024228	27.53968	28.33257
p-value		0.0000022	0.0000000	0.0000005	0.0000000	0.0000000	0.0000000	0.0000002	0.0000000	0.0002640

Supplementary Figure 3.2 Bacterial Knockout Adhesion onto UV Photoactivated GaN Substrates. All the strains show increased adhesion to WT. fimH and csgG show the highest numbers.

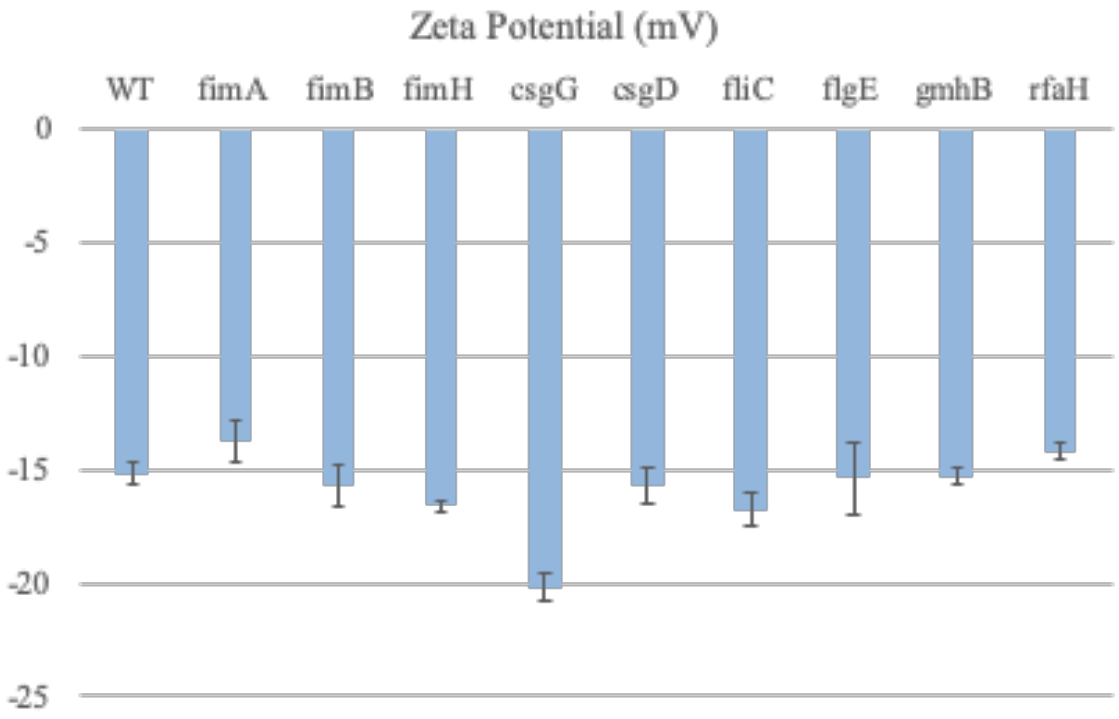

Supplementary Figure 3.3 Zeta Potential Measurements of the Bacterial Strains taken on a Malvern Zeta Sizer.

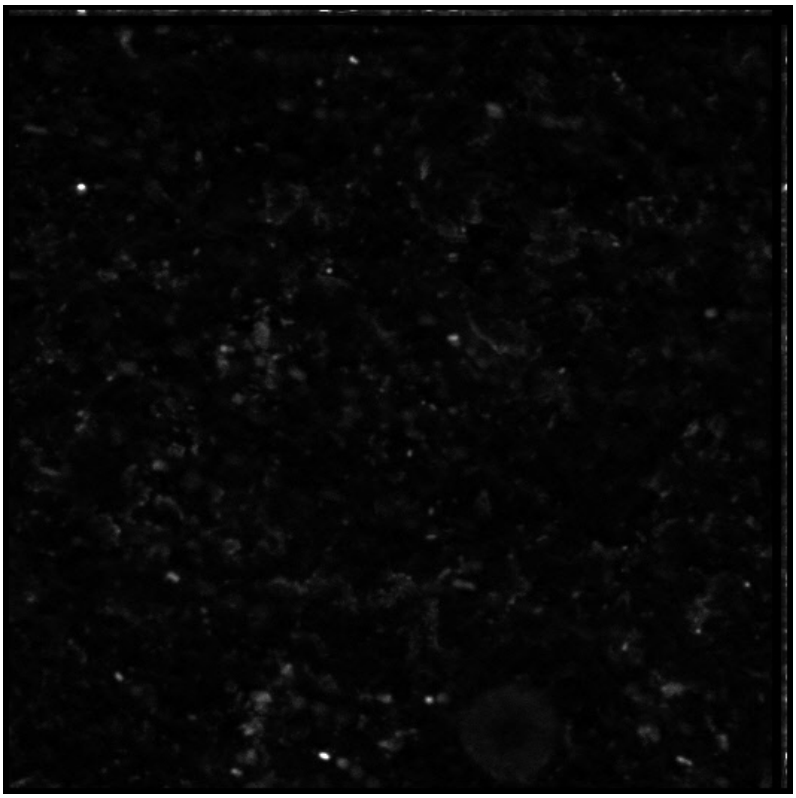

Supplementary Figure 3.4 Gif of Bacteria Moving on the Inactivated GaN Substrate

CHAPTER IV

POLYACRYLAMIDE GEL STIFFNESS INFLUENCES THE ADHESION OF BACTERIAL MUTANTS

IV.1. Introduction

Shortly after their discovery, microorganisms were found to be the root source of infections and illnesses. Their most extreme form, antibiotic-resistant persister cells exist deep within biofilms, which are complex communities of bacteria found at the air-water interface[2]. About 71% of the earth is covered with water and the human body itself is composed of 60% water. This offers microorganisms an enormous number of surfaces to colonize and propagate. In an effort to eradicate biofilms from medical instruments and commercial pipes alike, early researchers studied bacteria in as much excruciating detail as possible[146]. What they failed to notice was the role the substrates played in this process. Surface chemistry[142,338,339], wettability[124,125,129,340], and topography[10,131,341] are some material properties that have been directly linked to inducing specific bacterial responses. Mechanical properties of bacteria control every aspect of their existence[108]: morphology, changing their growth rate and divisibility in response to stressful environments. A biological perspective upon how material properties, such as stiffness influence the bacterial adhesion could prove invaluable.

Material stiffness may affect initial bacterial attachment to surfaces, which is an important step in the process of biofilm formation. I predict that if *E. coli* can sense different stiffnesses, then when they are placed on soft, medium and hard substrates, they will exhibit a decreasing trend of adhesiveness. Our preliminary experiment demonstrates this hypothesis; bacteria do sense change in stiffness of the substrate. The manner in which bacteria sense and respond to changes in the stiffness of the substrate, however, is unknown. Numerous reports suggest that bacteria use adhesion appendages (pili, curli, flagella, and LPS) to sense their environment[42,52,342]. For instance, it has been reported that flagella can sense crevices and nooks in the environment to provide bacteria with a sense of direction and orientation[301]. The flagella stop rotating when it encounters a surface and proceeds to activate the pili, which promotes cell-cell adhesion and initial biofilm formation[87]. However, the mechanism of bacterial sensing of mechanical properties such as stiffness has not been thoroughly studied. We hypothesize that if bacteria use adhesion appendages (pili, curli, flagella, and LPS) to sense this change in stiffness, then bacteria lacking functional adhesion appendages will fail to properly sense the surface stiffness as shown by a deviation from wild type response. Here, we examine the role stiffness plays on influencing initial bacterial adhesion and begin to unravel their underlying mechanisms.

IV.2. Materials and Methods

IV.2.i. Bacterial Strains and Growth Conditions

9 single deletion mutants and the parent strain were chosen from the Keio library[38]- a collection of 3895 single-gene mutants of *E. coli* BW25113 and obtained from the Yale *E. coli* genetic stock center. The list of strains has been described in Table 1. The bacterial cells were grown overnight in Lysogeny Broth (LB) media in a shaker incubator set to 37°C. The strains arrived as lyophilized powders which were struck upon LB agar plates for overnight growth at 37°C. The mutants were selected as Kanamycin resistant colonies. The bacteria were stored at -80°C for long-term storage. For immediate use, the bacteria were stored at 4°C for up to 2 weeks and re-plated to a maximum subculture of 4.

IV.2.ii. Preparing Polyacrylamide Gels of Different Stiffnesses

The polyacrylamide hydrogels used in our experiments were prepared using a derivative of the protocol by Tse et al[343]. Briefly, 40% Acrylamide (monomer) was mixed with a 2% bis-acrylamide (cross-linker) solution in the volumes mentioned in table 2. The appropriate amount of distilled water was added to the tubes to obtain a final volume of 1 ml. tetramethylethylenediamine (*TEMED*) was added at a final concentration of 0.2%. 6 µl of a 20% w/v solution of ammonium persulfate (APS) was added to each tube and the solutions were mixed thoroughly. 20 µl of the solution was drop casted between 20x20 square glass coverslips. The top coverslip was coated with a silanizing agent before use to facilitate easy removal. This method of sandwiching the hydrogel between coverslips

enabled all the hydrogels to have a uniform thickness. The coverslips were kept in petri dishes with the lid on to prevent oxygen exposure. After 20 min, the top coverslip was removed, and the gels were ready. The gels were then incubated in water for 10 minutes, followed by media to reduce the toxicity of the polyacrylamide gels.

Table 4.1 List of Keio Library E. coli Mutants and their Functions

No	Bacterial Component	Role	Protein Name	KEIO library No.	function
1	WT	**BW 25113**			
2	Flagella	Filament	**FliC**	JW1908-1	main structural subunit
3	Flagella	Hook	**FlgE**	JW1063-1	connects filament to main bacterial body
4	Curli		**csgD**	JW1023-1	DNA-binding transcriptional activator in 2-component regulatory system
5	Curli		**csgG**	JW1020-1	outer membrane lipoprotein required for curli subunit secretion
6	Pili		**fimA**	JW4277-1	major repeating subunit
7	Pili		**fimB**	JW4275-1	promoting primarily on/off inversion regulator fimA
8	Pili		**fimH**	JW4283-3	minor component that recognizes mannosyl residues present at the surface
9	LPS	core	**rfaH**	JW3818-1	LPS core synthesis and O-antigen attachment
10	LPS	enzyme D,D-heptose 1,7-biphosphate phosphatase	**gmhB**	JW0196-2	catalyzes 3rd essential step of LPS-synthesis

IV.2.iii. Material Characterization: Determining the Modulus of Elasticity

To determine Young's modulus, a proportionately higher volume (5 ml) was poured into a 3D printed dog bone shape made according to ASTM standards[344] for plastic 1. They were then covered with a glass plate and allowed to polymerize for 20 minutes. All the hydrogels were made at room temperature. The Young's modulus was then measured using an Instron. The values we obtained have been displayed in Table 2. Tension tests were performed at room temperature according to the ASTM D-638 03 at a crosshead speed of 10 mm/min and gauge length 33.52 mm using an Instron 3384.

Table 4.2 Compositions of Soft, Medium and Hard Hydrogels to Make 1 ml of Polyacrylamide Gel Solution. 2 µl TEMED (catalyst) and 6 µl APS (polymerizing agent) were added to polymerize the gels. To make 10 ml, add the proportionate amounts (shown below) in ml instead of µl.

gel stiffness	40% acrylamide (µl)	2% bis acrylamide (µl)	Young's modulus (kPa)
soft	2	1.32	17.32
medium	2	2.4	28.907
hard	6	4	1547.4

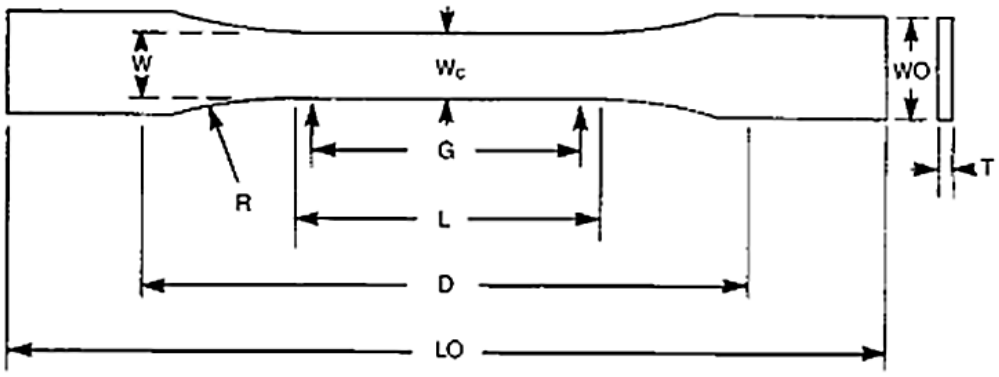

TYPES I, II, III & V

Dimensions (see drawings)	Type III
W—Width of narrow section[E,F]	19 [0.75]
L—Length of narrow section	57 [2.25]
WO—Width overall, min[G]	29 [1.13]
WO—Width overall, min[G]	...
LO—Length overall, min[H]	246 [9.7]
G—Gage length[I]	50 [2.00]
G—Gage length[I]	...
D—Distance between grips	115 [4.5]
R—Radius of fillet	76 [3.00]
RO—Outer radius (Type IV)	...

Figure 4.1 Dog Bone Structure for Type III Plastic as Shown in the ASTM[344]. A 3D printed mold was cast in these dimensions to mold the gels into the appropriate shape for tensile testing.

IV.2.iv. Adhesion Assay

A standard bacterial adhesion assay was performed on a Zeiss inverted spinning disc confocal microscope. Bacterial cells were grown overnight in a shaker incubator at 37°C. 100 µl of the overnight culture of bacterial cells were incubated with SYTO9 in the dark at room temperature (~23°C) for 20 minutes and brought up to a final volume of 1ml using PBS. 200 µl of this culture was drop cast onto a polyacrylamide gel-covered glass coverslip. The gels were then dipped into a small water bath to wash off non-adherent cells. The number of bacterial cells was counted per FOV at 40x magnification on the confocal microscope. At least 10 images were taken per sample with three experimental repetitions.

IV.2.v. Statistical Analysis

The data was run through a one-way ANOVA analysis prior to performing standard t-tests.

IV.3. Results

IV.3.i. Wild Type Bacteria

The Young's modulus is measured as a ratio of the stress of a material against the strain it experiences. It is the relationship between the deformation of a material and the force required to deform it. The Young's moduli of the soft, medium and hard polyacrylamide hydrogels were 17.32 kPa, 28.9 kPa, and 1547.69 kPa respectively.

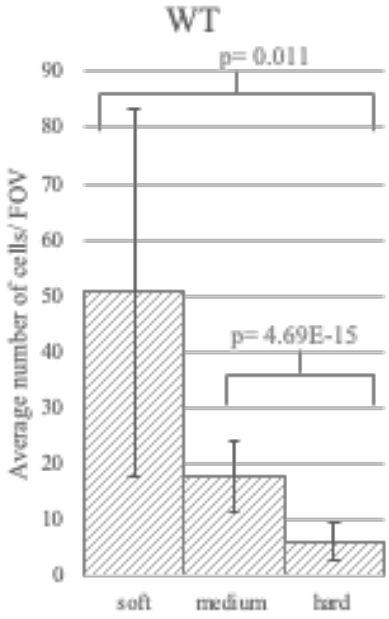

Figure 4.2 Wild Type E. coli Cell Adhesion on Soft, Medium and Hard Hydrogels.

The wild type (WT) *E. coli* strain was grown in LB media and incubated for 5 minutes on polyacrylamide hydrogels of different stiffnesses (figure 38 confocal images). The direct counting method on the AxioVision 4.8 software was used to determine the total number of attached cells. The average attachment of wild type *E. coli* bacteria was 50 ± 32.8, 17 ± 5.09 and 6 ± 3.49 cells/cm^2 on the soft, medium and hard polyacrylamide hydrogels respectively. There is a clear marked decrease in the total number of cells attached to each polyacrylamide gel with increasing stiffness. Our findings support our initial hypothesis that material stiffness influences bacterial attachment. To show that bacterial viability was not affected by the chemical composition of the material i.e. the monomer, cross-linker, TEMED or APS ($p < 0.05$) a one-way ANOVA analysis was performed, confirming that change in the bacterial behavior was not due to the chemistry of the surfaces.

IV.3.ii. Adhesion Trends Based on the Adhesive Activity of the Deletion Mutants

IV.3.ii.A. Adhesion Trends for Fimbrial Mutants

Three fimbrial deletion mutants, *ΔfimA, ΔfimB*, and *ΔfimH* were chosen for this experiment. Fimbriae, also known as pili, are small, thin proteinaceous filaments present on the outermost layer of bacteria. These structures are built from pilin subunits. FimA and FimH subunits are necessary for the assembly of the pili[346]. FimA is the main structural subunit building the pilus rod and FimB is a regulatory protein that controls the function of FimA. The FimH subunit is an adhesin, present at the distal tip of the fimbriae[37].

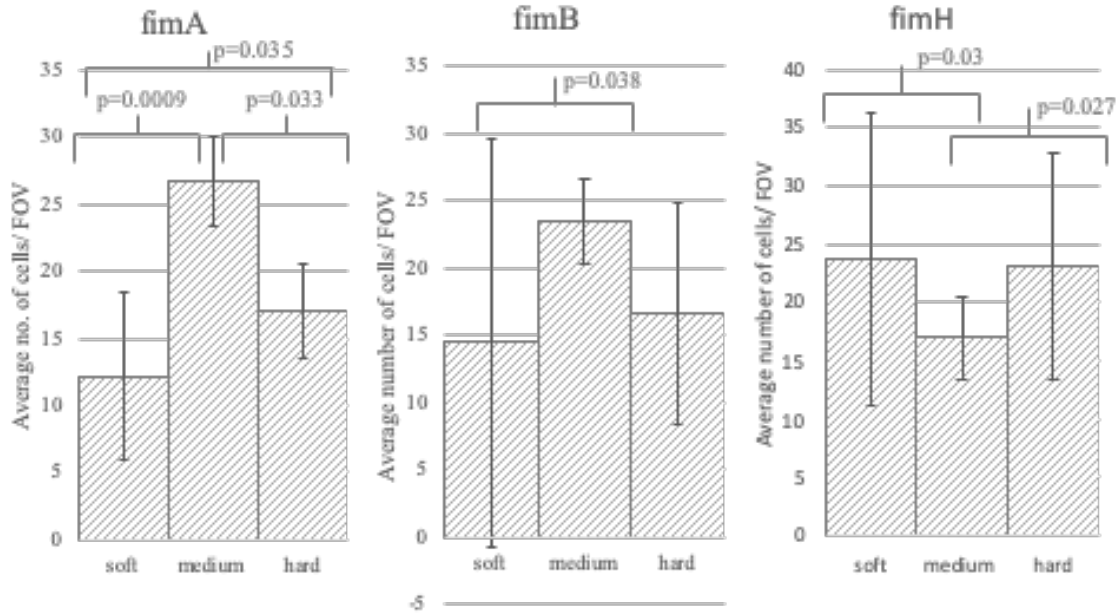

Figure 4.3 Adhesion Assay of Fimbrial Deletion Mutants. fimA, fimB and fimH, on Soft, Medium and Hard Polyacrylamide Hydrogels.

ΔfimA and *ΔfimB* followed the same adhesive trend: lowest bacterial adhesion on the soft surface followed by the hard surface and then the medium PA surface retaining the greatest number of bacteria. Although the average cell counts per stiffness were different for *ΔfimA* and *ΔfimB* mutants, they were in the same range (between 12 and 30 cells). *ΔfimH* mutants adhered the most on the soft and hard surfaces with no significant difference. The medium polyacrylamide gel retained the fewest number of Δ*fimH* cells. As fimB directly regulates the production of fimA, our result was in line with our expectations. Mutations in fimA have been reported to have an effect on fimH expression[346] and could possibly explain the variances in adhesive performance.

IV.3.ii.B. Adhesion Trends for Curli Mutants

Curli are extracellular fibers present on the cell wall of some Gram-negative bacteria. They are involved in cell-cell and cell-substrate aggregation. Curli promote community behavior within a biofilm and are found abundantly in the biofilm matrix[97,347]. Curli are produced by a delicate machinery of proteins composed of the outer membrane protein CsgG and the accessory proteins CsgE and CsgF[347,348]. The CsgD protein regulates the function of CsgG, thereby influencing curli synthesis[92,100,349].

ΔcsgG mutants adhered to the medium surface the most while *ΔcsgD* mutants preferred adhesion to the soft gel. The adhesion levels of the *ΔcsgG* for soft and hard hydrogels were roughly the same, between 7 and 28 cells/FOV. The *ΔcsgD* cells on the medium and hard polyacrylamide gels were also roughly the same, between 5-29 cells/ FOV. The use of *Δcsg*G and *ΔcsgD* knockouts has revealed the importance of curli in

adhesion. *ΔcsgD* mutants, which are responsible for controlling the synthesis of the CsgG subunit, adhered to the soft hydrogels in greater numbers than any of the other mutants. This result implies that although CsgD is required to produce major subunit CsgG, the bacterial cell must use other methods to compensate for its loss.

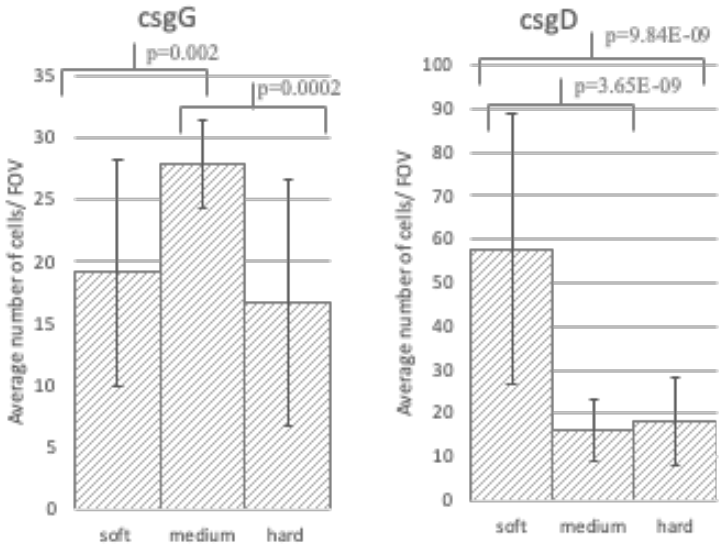

Figure 4.4 Adhesion Assay of Curli Deletion Mutants. csgG and csgD, on Soft, Medium and Hard Polyacrylamide Hydrogels.

IV.3.ii.C. Adhesion Trends for Flagellar Mutants

The bacterial flagella are slender tail-like bacterial appendages that allow movement in bacteria[307]. The flagellar structure comprises a basal body, a hook, and hook-filament proteins. We chose the flagellar mutant *ΔflgE* for its role in synthesizing the hook which serves as an anchor for the assembly of the other flagellar assembly proteins. *ΔfliC* was chosen as it is the knockout of the bacterium that does not have the machinery to produce the fliC subunits of the filament. We hypothesized that removal of the genes that encode for the basal assembly and filament assembly would decrease

overall adhesion. The *ΔfliC* mutants adhered the least onto the medium surface. It showed a high degree of adhesion (~55/ FOV) on the soft polyacrylamide hydrogel and hard hydrogels (~45 cells/FOV). The *ΔflgE* mutants adhered mostly to the soft surface, followed by the medium and hard hydrogels. The *ΔflgE* mutants were the only ones to show a similar trend of decreasing adhesion to the WT. Its function has been directly related to the flagellar motor function and assembly[350].

As both the mutants regulate the movement of the bacteria, we had predicted that their loss would result in increased adhesion at a single location. This was, in fact, what we saw (as represented in fig 5).

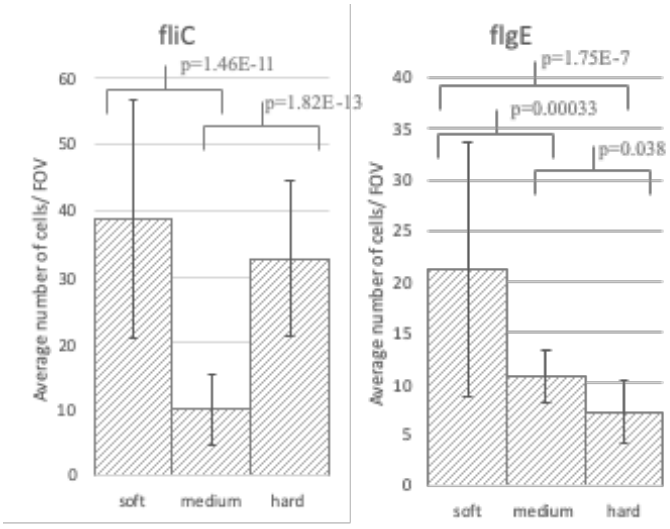

Figure 4.5 Adhesion Assay of Flagellar Deletion Mutants. fliC and flgE, on Soft, Medium and Hard Polyacrylamide Hydrogels.

IV.3.ii.D. Adhesion Trends for LPS Mutants

The lipopolysaccharide layer is the outermost layer of Gram-negative bacteria. It is a protective barrier that can alter its shape to accommodate changes. It is composed of a lipid layer, O-antigen, and polysaccharide. We chose the deletion mutant *ΔgmhB* since it is a knockout of the LPS biosynthetic enzyme D-R,β-D-Heptose-1,7-bisphosphate Phosphatase (GmhB)[34,317]. *ΔrfaH* was chosen since it is a knockout of the transcription factor rfaH, which is involved in RNA synthesis[34,105].

The *ΔgmhB* mutants adhered to the polyacrylamide hydrogels in the following order (from greatest to least): medium, soft and then hard. The number of bacteria on the hard gel was markedly low (~7 cells/FOV). The bacteria on the medium surface adhered in very high numbers (~45 cells/FOV). *ΔrfaH* mutants adhered from greatest to least in the following order: soft, hard and then medium.

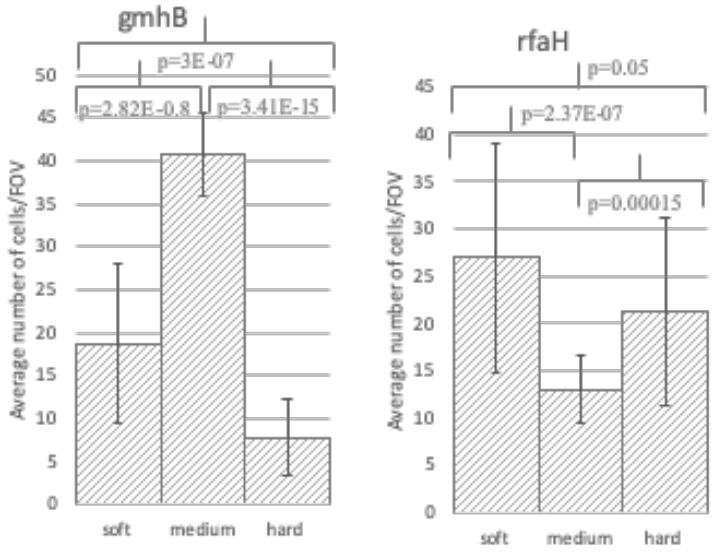

Figure 4.6 Adhesion Assay of LPS Deletion Mutants. gmhB and rfaH, on Soft, Medium and Hard Polyacrylamide Hydrogels.

IV.3.iii. Overall Comparison of Bacterial Adhesion

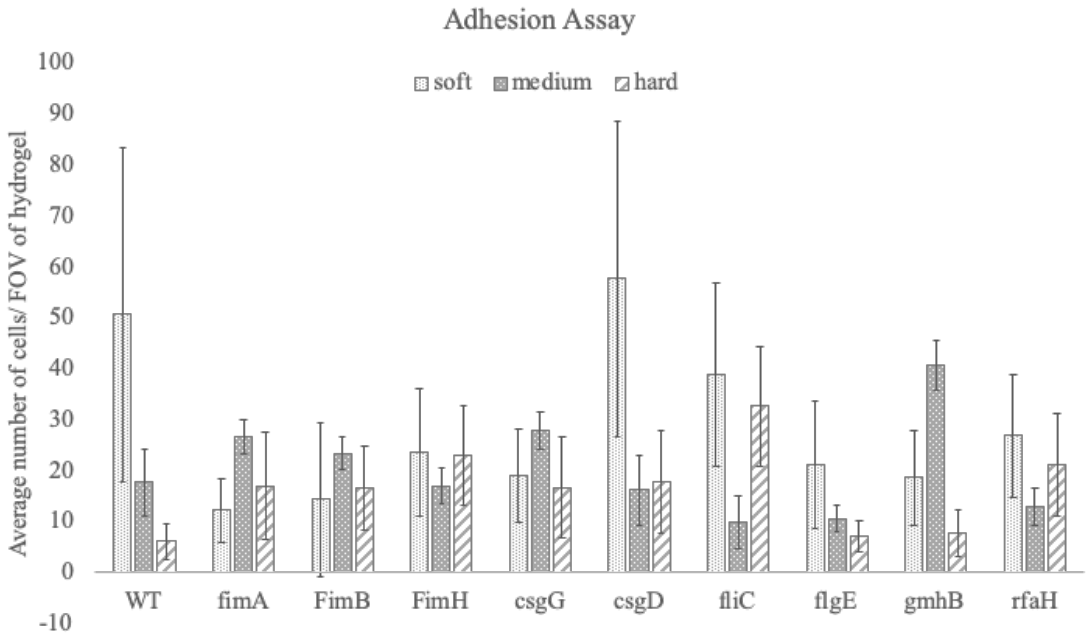

Figure 4.7 Adhesion Assay of E. coli Mutants on Soft, Medium and Hard Polyacrylamide Hydrogels.

When the adhesion patterns were compared overall, we noticed the following:

Soft > medium > hard: WT and *ΔflgE*

Medium > soft > hard: *ΔfimA, ΔfimB, ΔcsgG and ΔgmhB*

Soft > hard > medium: *ΔfimH, ΔcsgD, ΔfliC and ΔrfaH*

IV.3.iv. Comparison of Bacterial Adhesion Based on the Stiffness of the Substrate

To study the adhesion depicted in the figure above, we simplified the analysis by separating adhesion trends based on the stiffness of the substrate.

IV.3.iv.A. Comparison of the Adhesion of the Mutant Bacterial Strains to the WT on the Soft Surfaces (17 kPa)

The soft hydrogels retained more *ΔcsgD* bacteria than all the other strains, with adhesion values similar to WT. The adhesive behavior of all the other strains was lower than the WT. The soft surfaces retained *ΔfimA* the least, followed by *ΔfimB*. The *ΔfimA* and *ΔfimB* mutants had low average counts that were statistically significant when compared to the WT ($p<0.05$). This could indicate the role of fimbriae during the initial adhesion of *E. coli* onto soft polyacrylamide hydrogel surfaces.

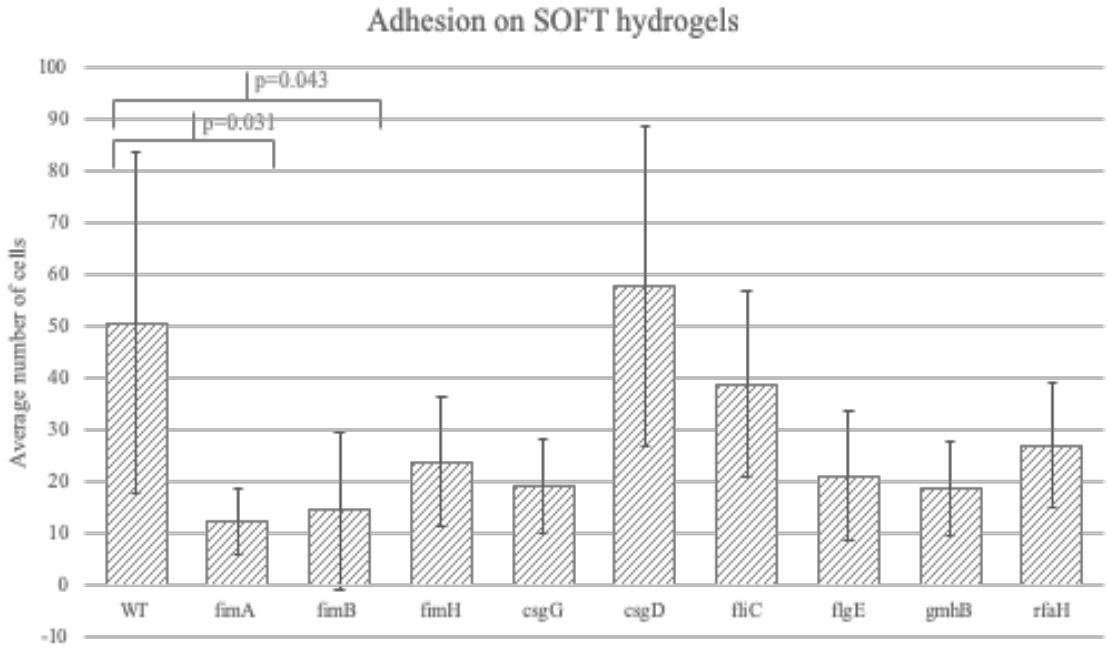

Groups	Count	Sum	Average	Std. Deviation	std. error
WT	30	1519	50.6333333	32.89	17.01098248
fimA	30	366	12.2	6.30	1.151111407
fimB	30	433	14.4333333	15.11	2.758345053
fimH	30	712	23.7333333	12.51	2.284346197
csgG	30	573	19.1	9.19	1.676991011
csgD	30	1732	57.7333333	31.02	5.663745021
fliC	30	1165	38.8333333	17.99	3.285315056
flgE	30	635	21.1666667	12.56	2.292458066
gmhB	30	560	18.6666667	9.30	1.697417466
rfaH	30	807	26.9	12.06	2.201540735

ANOVA						
Source of Variation	*SS*	*df*	*MS*	*F*	*P-value*	*F crit*
Between Groups	65360.0533	9	7262.22815	6.68358488	0.00000001064	1.91223587
Within Groups	315107.267	290	1086.57678			
Total	380467.32	299		F>Fcrit		

Figure 4.8 Adhesion Trends on Soft Polyacrylamide Hydrogels.

IV.3.iv.B. Comparison of the Adhesion of the Mutant Bacterial Strains to the WT on the Medium Surfaces (29 kPa)

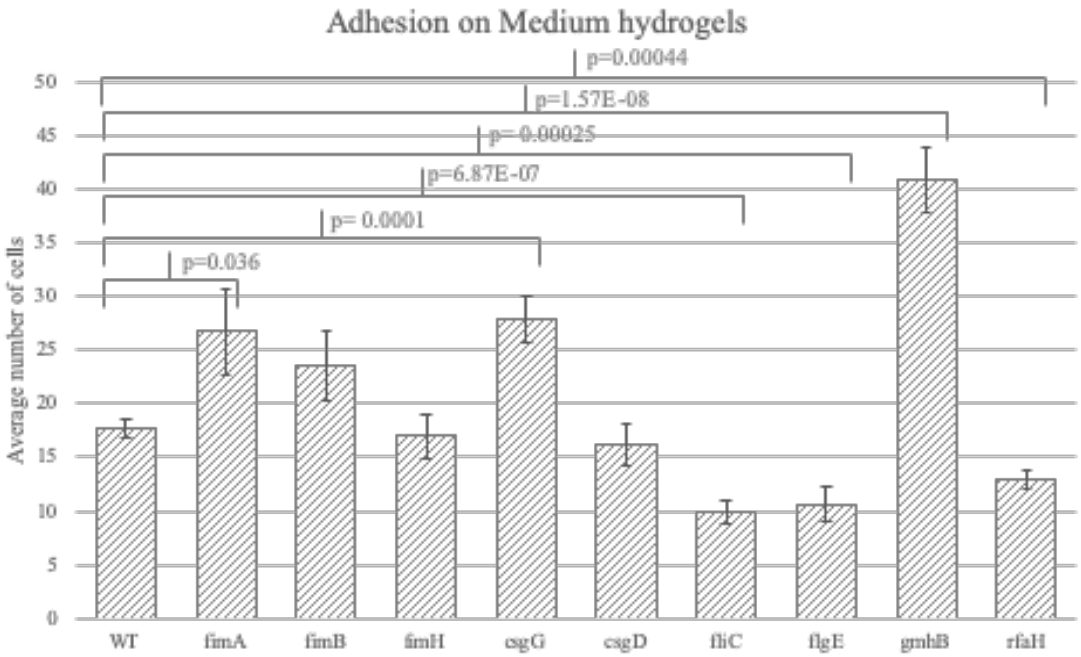

Groups	Count	Sum	Average	Std. Deviation	std. error
WT	30	531	17.7	4.94	0.901021132
fimA	30	802	26.7333333	22.07	0.891230895
fimB	30	704	23.4666667	17.77	0.844820549
fimH	30	509	16.9666667	11.11	0.930310484
csgG	30	837	27.9	12.28	17.70463485
csgD	30	485	16.1666667	10.62	17.72380899
fliC	30	298	9.93333333	5.81	18.35695919
flgE	30	319	10.6333333	8.43	19.04091705
gmhB	30	1225	40.8333333	16.49	19.77363191
rfaH	30	389	12.9666667	4.92	20.56499617

ANOVA						
Source of Variation	*SS*	*df*	*MS*	*F*	*P-value*	*F crit*
Between Groups	24612.8967	9	2734.7663	16.9290433	2.14968E-22	1.91223587
Within Groups	46847.4333	290	161.542874			
				F>Fcrit		
Total	71460.33	299				

Figure 4.9 Adhesion Trends on Medium Polyacrylamide Hydrogels.

IV.3.iv.C. Comparison of the Adhesion of the Mutant Bacterial Strains to the WT on the Hard Surfaces (1547 kPa)

The adhesion values of the bacterial strains grown on the medium-stiff hydrogels were mostly in the same range (between 10 – 30 cells/FOV). *ΔfliC, ΔflgE,* and *ΔrfaH* mutants showed lower adhesion levels on medium-stiff surfaces than the WT. *ΔfimA, ΔcsgG,* and *ΔgmhB* displayed increased adhesion levels. *ΔfimB, ΔfimH,* and *ΔcsgD* did not have statistically different adhesion values to the WT. The low adhesive levels of *ΔfliC* and *ΔflgE* are noteworthy here; their low values could indicate that the cells are mobile on the medium stiffness surface.

Wild type, *ΔflgE,* and *ΔgmhB E. coli* bacter*ia* all adhered in very small numbers onto the hard hydrogels. The greatest number of cells growing on hard hydrogels was seen on *ΔfliC.* It is interesting to note the contrasting adhesion levels between *ΔfliC* and *ΔflgE,* both of which are involved in the process of forming flagella. We were unable to discern any patterns based on this global analysis.

In summary, *E. coli* BW25113 parent strains preferred to adhere to soft surfaces, followed by medium and hard surfaces. All the genetic knockout strains exhibited similar levels of adhesion on surfaces of all stiffnesses except for *ΔcsgD*, *ΔfliC,* and *ΔgmhB*. The fewest number of bacterial cells were found on the hard hydrogels; specifically, the wild type, *ΔflgE*, and *ΔgmhB*.

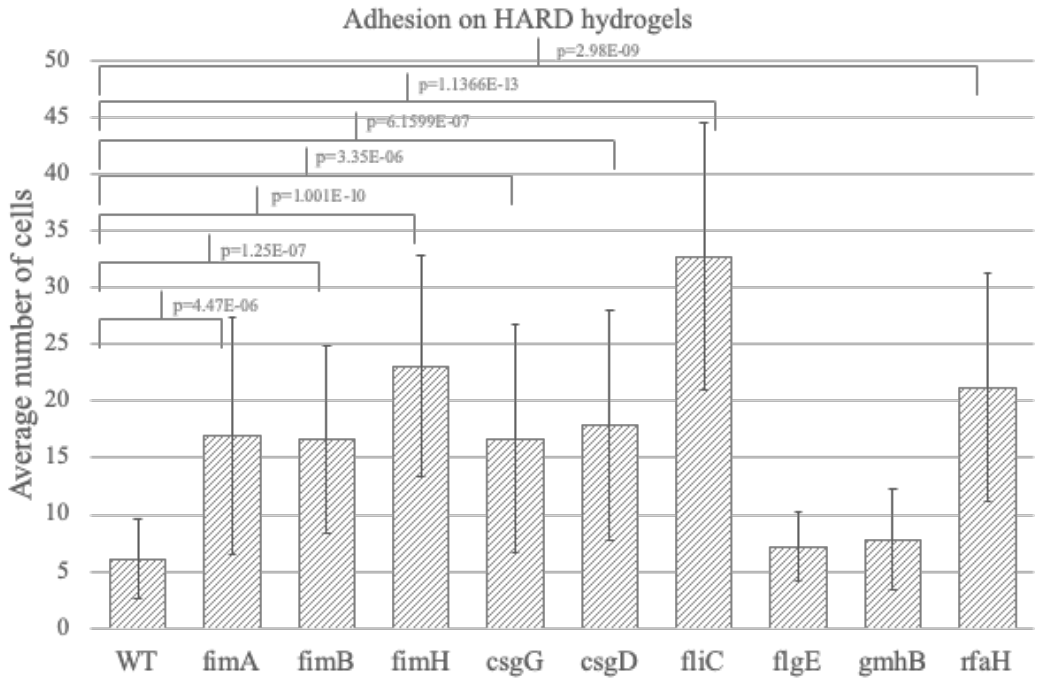

Groups	Count	Sum	Average	Std. Dev	std error
WT	30	183	6.1	3.49	0.64
fimA	30	510	17	10.45	1.90703477
fimB	30	498	16.6	8.22	1.49988505
fimH	30	692	23.0666667	9.74	1.7778544
csgG	30	501	16.7	9.99	1.82331642
csgD	30	537	17.9	10.12	1.84724088
fliC	30	982	32.7333333	11.75	2.14579693
flgE	30	215	7.16666667	3.05	0.55725793
gmhB	30	233	7.76666667	4.45	0.81322875
rfaH	30	636	21.2	10.01	1.82725219

ANOVA						
Source of Variation	*SS*	*df*	*MS*	*F*	*P-value*	*F crit*
Between Groups	18071.47	9	2007.94111	26.6610417	2.31471E-33	1.91223587
Within Groups	21840.9667	290	75.3136782			
				F>Fcrit		
Total	39912.4367	299				

Figure 4.10 Adhesion Trends on Hard Polyacrylamide Hydrogels.

IV.4. Discussion

The effect of material properties such as topography, roughness, surface chemistry, and hydrophobicity have been studied in great detail. The effects of stiffness, however, are less understood. A study conducted by Lichter et al[297] noting the adhesion trends of *Escherichia coli* and *Staphylococcus epidermis* on polyelectrolyte multilayer films showed the same trend of bacterial adhesion that we noticed: bacteria adhere more to softer substrates. More recently, this same trend was reported by Song et al, who performed a similar analysis on PDMS substrates of different stiffnesses[222] (See Table in Figure 38, Figure 38B). In stark contrast to these observations, Kolawe et al reported an increase in bacterial adhesion with increase in the stiffness of PEGDMA and agar gels[220] (see Table in figure 38 and Figure 38C). Both Song and Kolawe performed tests using *Escherichia coli* bacteria. Song repeated his experiments with *Pseudomonas aeruginosa* and confirmed that the increase in stiffness of the PDMS gels results in a decrease in bacterial adhesion. Kolewe also repeated his experiments, this time with *Staphylococcus aureus* and reconfirmed his observations of less adhesion on softer hydrogels[220]. Differences in experimental procedures could possibly explain these differences. For example, the thickness and stiffness of hydrogels have also been reported to influence bacterial adhesion[223]. The comparison of our results to that of Song's and Kolewe's has been shown in the table of figure 38. These results are different from ours, but one must consider the following: the order of magnitude for all the experiments was vastly different, along with the material chosen and the thickness of the substrates. It is possible that some or one of these features influenced bacterial adhesion. We recommend the

standardization of a protocol to study the individual effects of material properties on bacteria.

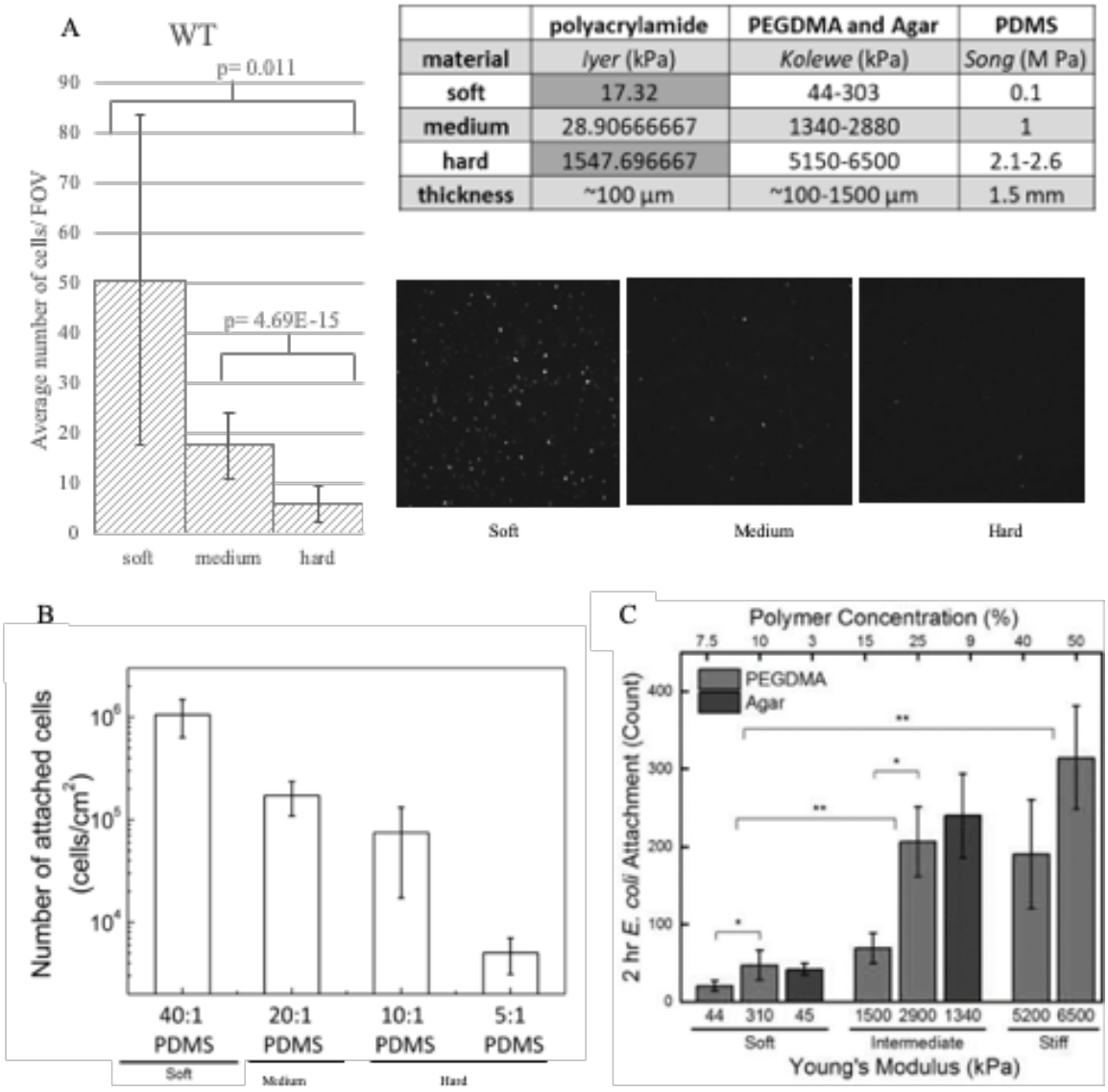

	polyacrylamide	PEGDMA and Agar	PDMS
material	*Iyer* (kPa)	*Kolewe* (kPa)	*Song* (M Pa)
soft	17.32	44-303	0.1
medium	28.90666667	1340-2880	1
hard	1547.696667	5150-6500	2.1-2.6
thickness	~100 µm	~100-1500 µm	1.5 mm

Figure 4.11 Background of Material Stiffness and its Effects on Bacteria. A: Adhesion assay performed in this paper: Comparison of the number of WT E. coli BW25113 cells on polyacrylamide gels of varied stiffnesses. B. As reported by Song et al. on PDMS substrate: decrease in adhesion with an increase in stiffness C. As reported by Kolawe et al on PEGDMA and agar substrates: increase in adhesion with an increase in stiffness. All stiffness data have been compared in the adjoining table.

In this study, I created adhesion profiles for 9 *E. coli* adhesion mutants and their parent wild type strain. Our preliminary results regarding the adhesion of the wild type *E. coli* strain align with other similar studies: increased bacterial retention upon softer hydrogels. We chose polyacrylamide gels in this study as a tunable substrate to study the effects of stiffness upon bacterial adhesion. We varied the amounts of the monomer acrylamide and cross-linker bis-acrylamide as described by a protocol by Tse et al. Polyacrylamide is essentially uncharged and since all the gels were made from the same materials, we mitigated the effects of electrostatic forces. A dynamic mechanical analysis was then performed to ascertain Young's modulus of the surfaces. In this test, the material is stretched between two heavy loads until it reaches its breaking point. Hydrogels of three different stiffnesses were obtained in this manner. A simple analysis of the hydrogels' hydrophobicity indicated that all the surfaces were superhydrophobic. We performed a live/dead cell assay (not shown) which confirmed that the cells did not die during this adhesion process. All the adhesion assays were performed within 5 minutes of adding the bacteria to the substrates, enabling us to visualize and quantify the early adhesion process of biofilm formation.

After our initial assay confirmed that stiffness affected bacterial adhesion of the wild type bacteria (*E. coli* BW25113), we chose adhesion deletion mutants for further assays to see if the deletion of key surface appendages influenced bacterial adhesion. We found that this was the case, although no patterns were immediately identifiable. A one-way ANOVA analysis confirmed that the datasets were significantly different ($p << 0.05$). We determined that the datasets were too large for global analysis and that a stepwise

analysis would be a better option at this initial stage. The adhesive activity of the bacteria was categorized based on their class (i.e. flagella, pili, etc) and based on the collective response of the mutants to the different stiffnesses.

The mutant strains of *E. coli* that we employed did not exhibit the same decreasing trend in adhesion as the wild type bacteria, except for *ΔflgE*. This suggests that bacteria find ways to adapt to external stresses even when physically limited. This leads us to believe that multiple signaling pathways must be at work. The response of the mutants, except for *ΔflgE*, to the change in stiffnesses was vastly different from that of the wild type bacteria, lending support to our hypothesis that bacteria use adhesion appendages to sense the stiffness of the surfaces they encounter. For the most part, there were different responses by the mutants of the same class. For example, the adhesive patterns of *ΔfimA* and *ΔfimB* in contrast to *ΔfimH.* Such non-homogenous responses support the notion that the bacteria adapt quickly and find alternative ways to survive whichever environmental stress they have been subjected to.

The response of the fimbrial mutants and the flagellar mutants warrants extra attention. There is an increasing dependency on both the pili and flagella on these surfaces. The increase in flagellar activity could indicate a need for locomotion and an increase in the pili activity points to increased cellular activity. If the stiffness is desirable, the bacteria cease their flagellar motion and start growing biofilm. As pili are responsible for cell-cell adhesion and communication, we posit that this activity points to an increase in initial attachment required for biofilm formation. The softer surfaces were

more conducive to fimbrial activity than the harder surfaces. In summary, pili and fimbriae are important during the initial mechanosensation process.

It is interesting to note that as the modulus of elasticity of the substrates increased, more appendage mutants seem to be involved in surface sensing. It could be that the *E.coli* put increasing amounts of effort during their contact with the increase in stiffness of the surfaces. We can surmise that bacteria do use adhesion appendages to sense the stiffness of the surface but that single bacterial appendages/knockouts are not solely responsible for mechanosensation of the stiffness of surfaces. We infer that mechanosensation of stiffness relies on a combination of factors, some of which may even be chemical in nature. As a part of our ongoing work, we are looking to identify these factors using mutants and double mutants of important genes. It will be interesting to test whether the stiffness of the bacterial membrane also shifts in relation to the substrate they encounter. We also predict that these bacteria secrete different ECM components depending on the stiffness of the surface. These are part of our ongoing studies.

IV.5. Supplementary Information

Supplementary Table 4.1 ANOVA: Single Factor Analysis for Wild Type Bacteria

SUMMARY

Groups	*Count*	*Sum*	*Average*	*Variance*	*std error*
Soft	30	1519	50.63333	8681.206	17.01098
medium	30	531	17.7	24.35517	0.901021
hard	30	183	6.1	12.16207	0.636712

ANOVA

Source of Variation	*SS*	*df*	*MS*	*F*	*P-value*	*F crit*
Between Groups	32023.82	4	8005.956	2.691727	0.036345	2.479015
Within Groups	252814	85	2974.282			
Total	284837.8	89				

Supplementary Table 4.2 t-test: fimA

t-Test: Two-Sample Assuming Unequal Variances		
	soft fimA	*medium fimA*
Mean	12.2	26.73333
Variance	39.75172	487.1678
Observations	30	30
df	34	
t Stat	-3.4678	
P(T<=t) one-tail	0.000722	
t Critical one-tail	1.690924	
P(T<=t) two-tail	0.001443	
t Critical two-tail	2.032245	
	soft fimA	*hard fimA*
Mean	12.2	17
Variance	39.75172	109.1034
Observations	30	30
df	48	
t Stat	-2.15486	
P(T<=t) one-tail	0.018109	
t Critical one-tail	1.677224	
P(T<=t) two-tail	0.036219	
t Critical two-tail	2.010635	
	medium fimA	*hard fimA*
Mean	26.73333	17
Variance	487.1678	109.1034
Observations	30	30
df	41	
t Stat	2.183234	
P(T<=t) one-tail	0.017399	
t Critical one-tail	1.682878	
P(T<=t) two-tail	0.034798	
t Critical two-tail	2.019541	

Supplementary Table 4.3 t-test: fimB

t-Test: Two-Sample Assuming Unequal Variances		
	soft fimB	*medium fimB*
Mean	14.43333333	23.46666667
Variance	228.254023	315.6367816
Observations	30	30
df	57	
t Stat	-2.121547723	
P(T<=t) one-tail	0.019117933	
t Critical one-tail	1.672028888	
P(T<=t) two-tail	0.038235865	
t Critical two-tail	2.002465459	
	soft fimB	*hard fimB*
Mean	14.43333	16.6
Variance	228.254	67.48966
Observations	30	30
df	45	
t Stat	-0.69007	
P(T<=t) one-tail	0.246846	
t Critical one-tail	1.679427	
P(T<=t) two-tail	0.493692	
t Critical two-tail	2.014103	
	medium fimB	*hard fimB*
Mean	23.46666667	16.6
Variance	315.6367816	67.48966
Observations	30	30
df	41	
t Stat	1.921478515	
P(T<=t) one-tail	0.030820788	
t Critical one-tail	1.682878002	
P(T<=t) two-tail	0.061641575	
t Critical two-tail	2.01954097	

Supplementary Table 4.4 t-test: fimH

t-Test: Two-Sample Assuming Unequal Variances		
	soft fimH	*medium fimH*
Mean	23.73333333	16.96666667
Variance	156.5471264	123.4816092
Observations	30	30
df	57	
t Stat	2.214797939	
P(T<=t) one-tail	0.015393283	
t Critical one-tail	1.672028888	
P(T<=t) two-tail	0.030786565	
t Critical two-tail	2.002465459	
	soft fimH	*hard fimH*
Mean	23.73333	23.06667
Variance	156.5471	94.82299
Observations	30	30
df	55	
t Stat	0.23031	
P(T<=t) one-tail	0.409353	
t Critical one-tail	1.673034	
P(T<=t) two-tail	0.818705	
t Critical two-tail	2.004045	
	medium fimH	*hard fimH*
Mean	16.96666667	23.06667
Variance	123.4816092	94.82299
Observations	30	30
df	57	
t Stat	-2.261304365	
P(T<=t) one-tail	0.013786827	
t Critical one-tail	1.672028888	
P(T<=t) two-tail	0.027573655	
t Critical two-tail	2.002465459	

Supplementary Table 4.5 t-test: csgG

t-Test: Two-Sample Assuming Unequal Variances		
	soft csgG	*medium csgG*
Mean	19.1	27.9
Variance	84.36897	150.9206897
Observations	30	30
df	54	
t Stat	-3.14226	
P(T<=t) one-tail	0.001361	
t Critical one-tail	1.673565	
P(T<=t) two-tail	0.002721	
t Critical two-tail	2.004879	
	soft csgG	*hard csgG*
Mean	19.1	16.7
Variance	84.36897	99.73448
Observations	30	30
df	58	
t Stat	0.968815	
P(T<=t) one-tail	0.16833	
t Critical one-tail	1.671553	
P(T<=t) two-tail	0.33666	
t Critical two-tail	2.001717	
	medium csgG	*hard csgG*
Mean	27.9	16.7
Variance	150.9206897	99.73448
Observations	30	30
df	56	
t Stat	3.874719912	
P(T<=t) one-tail	0.000141091	
t Critical one-tail	1.672522303	
P(T<=t) two-tail	0.000282182	
t Critical two-tail	2.003240719	

Supplementary Table 4.6 t-test: csgD

t-Test: Two-Sample Assuming Unequal Variances		
	soft csgD	*medium csgD*
Mean	57.73333	16.16667
Variance	962.3402	112.8333
Observations	30	30
df	36	
t Stat	6.94331	
P(T<=t) one-tail	1.95E-08	
t Critical one-tail	1.688298	
P(T<=t) two-tail	3.9E-08	
t Critical two-tail	2.028094	
	soft csgD	*hard csgD*
Mean	57.73333	17.9
Variance	962.3402	102.369
Observations	30	30
t Stat	6.686391	
P(T<=t) one-tail	4.87E-08	
t Critical one-tail	1.689572	
P(T<=t) two-tail	9.74E-08	
t Critical two-tail	2.030108	
	medium csgD	*hard csgD*
Mean	16.16667	17.9
Variance	112.8333	102.369
Observations	30	30
df	58	
t Stat	-0.64717	
P(T<=t) one-tail	0.260037	
t Critical one-tail	1.671553	
P(T<=t) two-tail	0.520074	
t Critical two-tail	2.001717	

Supplementary Table 4.7 t-test: fliC

t-Test: Two-Sample Assuming Unequal Variances		
	soft fliC	*medium fliC*
Mean	38.83333	9.933333
Variance	323.7989	33.71954
Observations	30	30
df	35	
t Stat	8.371616	
P(T<=t) one-tail	3.57E-10	
t Critical one-tail	1.689572	
P(T<=t) two-tail	7.13E-10	
t Critical two-tail	2.030108	
	soft fliC	*hard fliC*
Mean	38.83333	32.73333
Variance	323.7989	138.1333
Observations	30	30
df	50	
t Stat	1.554538	
P(T<=t) one-tail	0.063182	
t Critical one-tail	1.675905	
P(T<=t) two-tail	0.126364	
t Critical two-tail	2.008559	
	medium fliC	*hard fliC*
Mean	9.933333	32.73333
Variance	33.71954	138.1333
Observations	30	30
df	42	
t Stat	-9.52614	
P(T<=t) one-tail	2.34E-12	
t Critical one-tail	1.681952	
P(T<=t) two-tail	4.68E-12	
t Critical two-tail	2.018082	

Supplementary Table 4.8 t-test: flgE

t-Test: Two-Sample Assuming Unequal Variances		
	soft flgE	*medium flgE*
Mean	21.16667	10.63333
Variance	157.6609	71.13678
Observations	30	30
df	51	
t Stat	3.814175	
P(T<=t) one-tail	0.000185	
t Critical one-tail	1.675285	
P(T<=t) two-tail	0.00037	
t Critical two-tail	2.007584	
	soft flgE	*hard flgE*
Mean	21.16667	7.166667
Variance	157.6609	9.316092
Observations	30	30
df	32	
t Stat	5.934175	
P(T<=t) one-tail	6.57E-07	
t Critical one-tail	1.693889	
P(T<=t) two-tail	1.31E-06	
t Critical two-tail	2.036933	
	medium flgE	*hard flgE*
Mean	10.63333333	7.166667
Variance	71.13678161	9.316092
Observations	30	30
df	36	
t Stat	2.116907744	
P(T<=t) one-tail	0.020622902	
t Critical one-tail	1.688297714	
P(T<=t) two-tail	0.041245805	
t Critical two-tail	2.028094001	

Supplementary Table 4.9 t-test: gmhB

t-Test: Two-Sample Assuming Unequal Variances		
	soft gmhB	*medium gmhB*
Mean	18.66667	40.83333
Variance	86.43678	272.0057
Observations	30	30
df	46	
t Stat	-6.41285	
P(T<=t) one-tail	3.47E-08	
t Critical one-tail	1.67866	
P(T<=t) two-tail	6.95E-08	
t Critical two-tail	2.012896	
	soft gmhB	*hard gmhB*
Mean	18.66667	7.766667
Variance	86.43678	19.84023
Observations	30	30
df	42	
t Stat	5.791185	
P(T<=t) one-tail	3.96E-07	
t Critical one-tail	1.681952	
P(T<=t) two-tail	7.93E-07	
t Critical two-tail	2.018082	
	medium gmhB	*hard gmhB*
Mean	40.83333	7.766667
Variance	272.0057	19.84023
Observations	30	30
df	33	
t Stat	10.60167	
P(T<=t) one-tail	1.84E-12	
t Critical one-tail	1.69236	
P(T<=t) two-tail	3.67E-12	
t Critical two-tail	2.034515	

Supplementary Table 4.10 t-test: rfaH

t-Test: Two-Sample Assuming Unequal Variances		
	soft rfaH	*medium rfaH*
Variance	145.4034483	24.17126437
Observations	30	30
df	38	
t Stat	5.860505927	
P(T<=t) one-tail	4.42269E-07	
t Critical one-tail	1.68595446	
P(T<=t) two-tail	8.84537E-07	
t Critical two-tail	2.024394164	
	soft rfaH	*hard rfaH*
Mean	26.9	21.2
Variance	145.4034483	100.1655172
Observations	30	30
df	56	
t Stat	1.992272511	
P(T<=t) one-tail	0.025612367	
t Critical one-tail	1.672522303	
P(T<=t) two-tail	0.051224733	
t Critical two-tail	2.003240719	
	medium rfaH	*hard rfaH*
Mean	12.96666667	21.2
Variance	24.17126437	100.1655172
Observations	30	30
df	42	
t Stat	-4.044236226	
P(T<=t) one-tail	0.000109862	
t Critical one-tail	1.681952357	
P(T<=t) two-tail	0.000219723	
t Critical two-tail	2.018081703	

CHAPTER V

CONCLUSION AND FUTURE PERSPECTIVES

V.1. Conclusions

In this thesis, we peruse the effects of three material properties, nanotopographies, persistent photoconductivity and stiffness upon *E. coli* bacteria. The data we collected supports the overarching hypothesis that bacteria detect substrate changes through mechanosensation and adapt to these changes in a physiological manner. The model organism, *Escherichia coli* was chosen for this work due to its genetic accessibility. It is the most studied and well-understood organism on this planet with a fully sequenced genome. *E. coli* is a Gram-negative bacterium commonly found in the gut but has the capability of surviving outside the body. Aside from having a fully sequenced genome, its rapid rate of reproduction and ability to survive in variable growth conditions makes it an ideal candidate for study.

In Chapter 2, we investigated how changing the nanotopographies of seven polymeric materials would affect early bacterial adhesion and physiology. The polymeric surfaces (all started as flat materials) were altered through an oxygen plasma etch process to produce the following patterns: tent, crater, popcorn, and grass. We hypothesized that these topographical features would delay the formation of biofilm by preventing proper deposition (conditioning phase of biofilm formation), cell viability and adhesiveness. The changes in bacterial adhesive behavior and viability could not be related directly to

specific topographical patterns. We analyzed other factors that could be influencing the changes. Material composition was shown to play a vital role and statistical analyses revealed that contact angle (hydrophobicity) does not influence the adhesion of bacteria onto the nanostructured polymers. We determined that bacterial adhesion is not influenced by a single surface property and is instead a product of multiple material properties working in concert with each other. Further analyses at the 24 h time point revealed that bacteria overcome the obstacles provided by the change in topographical patterns and form a robust biofilm.

In chapter 3, we analyzed how the unique phenomenon, persistent photoconductivity effect of Group III semiconductors, affects the mechanosensation of bacteria. To do this, we used nine single-deletion mutants of *E. coli* BW25113 obtained from the Keio collection. The mutants were selected based on their importance to mechanosensation: pili (*fimA, fimB, fimH*), curli (*csgG, csgD*), flagella (*fliC, flgE*) and LPS (*gmhB, rfaH*). Non-functionalized GaN, a previously characterized Group III semiconductor that exhibits persistent photoconductivity upon UV illumination, was used as a substrate for these tests. We hypothesized that charged photoconductive substrates would have a direct effect on bacterial adhesion and that by using the single-deletion mutants, we would be able to systematically elucidate the contribution of the structural elements. We showed that charged GaN substrates inhibited bacterial motility and immobilized all the strains. The use of the genetic knockouts revealed the relative importance of fimbriae in bacterial mechanosensation upon charged GaN. Analysis of the catalase activity within the mutants revealed the importance of the fimbriae, curli and the

flgE genes in sensing reactive oxygen species. We predicted that the membrane potential of the bacteria was responsible for the immobilization of the bacteria. However, our hypothesis was not supported as we found no change in membrane potential activity of the mutant strains. The findings of this preliminary research take us one step closer to developing a generalized model regarding the pathways involved in mechanosensation of PPC. We visualize this information being used to develop the next generation of bioelectronics, with bacteria as the living computer system that transmits encoded information. It would be interesting to analyze any quorum sensing molecules secreted by the bacteria on the photoconductive surface. We predict that molecules such as flavin may be involved in transmitting extracellular signals to communicate with other bacteria not directly in contact with the UV activated surface. It would also be of interest to see if electrically stimulated surfaces also induce a similar response in bacteria or if our observations are limited to persistent photoconductivity effects.

In chapter 4, we investigated the role stiffness of a substrate plays upon bacterial adhesion. The adhesive roles of WT *E. coli* and 9 of its isogenic mutants were compared on soft, medium and hard fabricated polyacrylamide substrates. We hypothesized that bacteria lacking functional appendages would fail to sense the stiffness of the substrate as evidenced by its deviation from the WT response. We have only just begun understanding the role-specific bacterial appendages play in sensing change in stiffness of the substrate. The pathways used by bacteria to sense and respond to changes in the stiffness of the substrate is still unknown. We expect further genetic analyses to lend us more information. To further understand how stiffness affects bacterial

mechanosensation, we propose microfluidic experiments utilizing shear flow as a factor that would both affect such environmental sensing and provide a more realistic model. It would also be helpful to generalize the parameters for the studies, thereby bringing researchers to the same level playing field enabling comparison and critique of work.

This research provides a basic framework to expand upon for genetic analyses of the bacterial responses. It remains to be understood how these genes play a role in mechanosensation.

V.2. Future Perspectives

V.2.i. Initial Conditioning

Bacteria release proteins when in the media as a part of the initial conditioning, to make the environment more suitable for inhabitation It would be productive to analyze the protein deposition phase of surface conditioning different nanotopographical surface. We hypothesize that the material composition, nanostructure and exposed functional groups influence will protein deposition.

V.2.ii. Cell-cell Communication Between Bacteria

We propose to measure quorum sensing molecules secreted by the bacteria to provide us insight into cell-cell communication. What kind of molecules are released by the bacteria when they interact with these surfaces? We recommend measuring flavin and peptide release, which can also be used as analytes in biosensing applications. Certain peptoids have been known to prevent biofilms and flavins have recently been shown to be

important for cell-cell communication between bacteria (even if they are in different biofilms).

We further recommend co-culture studies (more than one kind of bacteria in the culture). An analysis of whether PPC promotes or inhibits commensal growth would be interesting. (For example, *C. albicans* and MRSA have a unique relationship)

V.2.iii. Analyses Under Flow Conditions

Analysis of bacterial adhesion and deposition would prove valuable if done under dynamic conditions. We propose using a microfluidic device to provide more realistic environmental conditions, which would also allow control over the flow rate and bacterial density.

V.2.iv.Study the Forces Required for Adhesion

As we have shown in this dissertation, bacteria adhere differently to substrates with different material properties. We propose an analysis of the strength of adhesion between bacteria and the substrate using TIRF microscopy. Lower adhesive forces should be easier to remove biofilms.

V.2.v. Immune Response to Material-Influenced Bacterial Cells

It would be interesting to see how immune cells (t-cells, macrophages, etc.) respond to bacteria that have been exposed to altered material properties. Does it promote engulfing the bacteria? Will there be an increase in bacterial dispersion? Will the rate of

bacterial multiplication exceed the ability of the immune cells to respond? Does it change the morphology of the immune cell? And if so, how would that affect its response to bacterial infections? These are some of the questions we look forward to finding the answers to.

REFERENCES

1. Zhurina M V., Gannesen A V., Zdorovenko EL, Plakunov VK. Composition and functions of the extracellular polymer matrix of bacterial biofilms. *Microbiology*. 2014;83(6):713-722. doi:10.1134/S002626171406023X
2. Flemming H-C, Wingender J, Szewzyk U, Steinberg P, Rice SA, Kjelleberg S. Biofilms: an emergent form of bacterial life. *Nat Rev Microbiol*. 2016;14(9):563-575. doi:10.1038/nrmicro.2016.94
3. Bos R, van der Mei HC, Busscher HJ. Physico-chemistry of initial microbial adhesive interactions – its mechanisms and methods for study. *FEMS Microbiol Rev*. 1999;23(2):179-230. doi:10.1111/j.1574-6976.1999.tb00396.x
4. Donlan RM. Biofilms: microbial life on surfaces. *Emerg Infect Dis*. 2002;8(9):881-890. doi:10.3201/eid0809.020063
5. Galié S, García-Gutiérrez C, Miguélez EM, Villar CJ, Lombó F. Biofilms in the food industry: Health aspects and control methods. *Front Microbiol*. 2018;9(MAY):1-18. doi:10.3389/fmicb.2018.00898
6. Costerton JW, Stewart PS, Greenberg EP. Bacterial biofilms: a common cause of persistent infections. *Science*. 1999;284(5418):1318-1322. doi:10.1126/SCIENCE.284.5418.1318
7. SHARPPS Program N. Overview of Healthcare-Associated Infections in North Carolina. 2013. http://epi.publichealth.nc.gov/cd/hai/figures/hai_may2017_annual_v2.pdf. Accessed November 28, 2017.
8. Cassini A, Högberg LD, Plachouras D, et al. Attributable deaths and disability-adjusted life-years caused by infections with antibiotic-resistant bacteria in the EU and the European Economic Area in 2015: a population-level modelling analysis. *Lancet Infect Dis*. 2019;19(1):56-66. doi:10.1016/S1473-3099(18)30605-49.
   Klevens RM, Edwards JR, Richards CL, et al. Estimating health care-associated infections and deaths in U.S. hospitals, 2002. *Public Health Rep*. 2007;122(2):160-166. doi:10.1177/003335490712200205
10. Nguyen DHK, Pham VTH, Truong VK, et al. Role of topological scale in the differential fouling of *Pseudomonas aeruginosa* and *Staphylococcus aureus* bacterial cells on wrinkled gold-coated polystyrene surfaces. *Nanoscale*. 2018. doi:10.1039/C7NR08178B
11. de la Fuente-Núñez C, Reffuveille F, Haney EF, et al. Broad-Spectrum Anti-biofilm Peptide That Targets a Cellular Stress Response. Parsek MR, ed. *PLoS Pathog*. 2014;10(5):e1004152. doi:10.1371/journal.ppat.1004152
12. de la Fuente-Núñez C, Reffuveille F, Fernández L, Hancock RE. Bacterial biofilm development as a multicellular adaptation: antibiotic resistance and new therapeutic strategies. *Curr Opin Microbiol*. 2013;16(5):580-589.

13. doi:10.1016/J.MIB.2013.06.01313. Flemming HC, Wingender J. The biofilm matrix. *Nat Rev Microbiol*. 2010;8(9):623-633. doi:10.1038/nrmicro2415
14. Mazza MG. The Physics of Biofilms -- An Introduction. 2016. doi:10.1088/0022-3727/49/20/203001
15. Tuson HH, Weibel DB. Bacteria–surface interactions. *Soft Matter*. 2013;9(17):4368. doi:10.1039/c3sm27705d
16. Sadovskaya I. Exopolysaccharide Quantification. In: Humana Press, New York, NY; 2014:347-357. doi:10.1007/978-1-4939-0473-0_29
17. Seviour T, Derlon N, Dueholm MS, et al. Extracellular polymeric substances of biofilms: Suffering from an identity crisis. *Water Res*. 2019;151:1-7. doi:10.1016/j.watres.2018.11.020
18. Xiao Y, Zhang E, Zhang J, et al. Extracellular polymeric substances are transient media for microbial extracellular electron transfer. 2017;(July):1-9.
19. David G. Davies, Matthew R. Parsek JPP, Barbara H. Iglewski, J. W. Costerton EPG. *The Involvement of Cell-to-Cell Signals in the Development of a Bacterial Biofilm*. http://science.sciencemag.org/. Accessed April 2, 2019.
20. Miller MB, Bassler BL. *QUORUM SENSING IN BACTERIA*. Vol 12.; 2001. www.annualreviews.org.
21. Waters CM, Bassler BL. QUORUM SENSING: Cell-to-Cell Communication in Bacteria. *Annu Rev Cell Dev Biol*. 2005;21(1):319-346. doi:10.1146/annurev.cellbio.21.012704.131001
22. Martínez E, Cosnahan RK, Wu M, et al. Oxylipins mediate cell-to-cell communication in Pseudomonas aeruginosa. *Commun Biol*. 2019;2(1):66. doi:10.1038/s42003-019-0310-0
23. Ahmed SAKS, Rudden M, Smyth TJ, Dooley JSG, Marchant R, Banat IM. Natural quorum sensing inhibitors effectively downregulate gene expression of Pseudomonas aeruginosa virulence factors. *Appl Microbiol Biotechnol*. March 2019:1-15. doi:10.1007/s00253-019-09618-0
24. Garrett TR, Bhakoo M, Zhang Z. Bacterial adhesion and biofilms on surfaces. *Prog Nat Sci*. 2008;18(9):1049-1056. doi:10.1016/j.pnsc.2008.04.001
25. Stewart PS, Costerton JW. Antibiotic resistance of bacteria in biofilms. *Lancet*. 2001;358(9276):135-138. doi:10.1016/S0140-6736(01)05321-1
26. Mah TFC, O'Toole GA. Mechanisms of biofilm resistance to antimicrobial agents. *Trends Microbiol*. 2001;9(1):34-39. doi:10.1016/S0966-842X(00)01913-2
27. Del Pozo J, Patel R. The Challenge of Treating Biofilm - associated Bacterial Infections. doi:10.1038/sj.clpt.6100247
28. France E, Al. *Spatial Structure Facilitates the Accumulation and Persistence of Antibiotic-resistant Mutants in Biofilms*.; 2018. doi:10.1111/eva.12728
29. Barrett TC, Mok WWK, Murawski AM, Brynildsen MP. Enhanced antibiotic resistance development from fluoroquinolone persisters after a single exposure to antibiotic. *Nat Commun*. 2019;10(1):1177. doi:10.1038/s41467-019-09058-4
30. Brown DR, Silhavy TJ. Nitrogen Starvation Induces Persister Cell Formation in Escherichia coli. *jb.asm.org 1 J Bacteriol*. 2019;201:622-640. doi:10.1128/JB.00622-18

31. Chen X, Li G, Liao X, et al. A switch in the poly(dC)/RmlB complex regulates bacterial persister formation. *Nat Commun*. 2019;10(1):27. doi:10.1038/s41467-018-07861-z
32. Mah T-F. Biofilm-specific antibiotic resistance. *Future Microbiol*. 2012;7(9):1061-1072. doi:10.2217/fmb.12.76
33. Beenken KE, Dunman PM, Mcaleese F, et al. Global Gene Expression in Staphylococcus aureus Biofilms. *J Bacteriol*. 2004;186:4665-4684. doi:10.1128/JB.186.14.4665-4684.2004
34. Niba ETE, Naka Y, Nagase M, Mori H, Kitakawa M. A Genome-wide Approach to Identify the Genes Involved in Biofilm Formation in *E. coli*. *DNA Res*. 2008;14(6):237-246. doi:10.1093/dnares/dsm024
35. Ren A Bedzyk S M Thomas R W Ye T K Wood DL. Escherichia coli biofilms. *Appl Microbiol Biotechnol*. 2004;64:515-524. doi:10.1007/s00253-003-1517-y
36. Sauer K. *The Genomics and Proteomics of Biofilm Formation*.; 2003. http://genomebiology.com/2003/4/6/219. Accessed July 26, 2018.
37. Schembri MA, Kjaergaard K, Klemm P. Global gene expression in Escherichia coli biofilms. *Mol Microbiol*. 2003;48(1):253-267. doi:10.1046/j.1365-2958.2003.03432.x
38. Baba T, Ara T, Hasegawa M, et al. Construction of Escherichia coli K-12 in-frame, single-gene knockout mutants: the Keio collection. *Mol Syst Biol*. 2006. doi:10.1038/msb4100050
39. Ivanova K, Ramon E, Hoyo J, Tzanov T. Innovative Approaches for Controlling Clinically Relevant Biofilms: Current Trends and Future Prospects. *Curr Top Med Chem*. 2017:1889-1914. doi:10.2174/1568026617666170105
40. Gordon VD, Davis-Fields M, Kovach K, Rodesney CA. Biofilms and mechanics: a review of experimental techniques and findings. *J Phys D Appl Phys*. 2017;50(22):223002. doi:10.1088/1361-6463/aa6b83
41. Dunne WM. Bacterial adhesion: seen any good biofilms lately? *Clin Microbiol Rev*. 2002;15(2):155-166. http://www.ncbi.nlm.nih.gov/pubmed/11932228.
42. Hori K, Matsumoto S. Bacterial adhesion: From mechanism to control. *Biochem Eng J*. 2010;48:424-434. doi:10.1016/j.bej.2009.11.014
43. Boks NP, Norde W, van der Mei HC, Busscher HJ. Forces involved in bacterial adhesion to hydrophilic and hydrophobic surfaces. *Microbiology*. 2008;154(10):3122-3133. doi:10.1099/mic.0.2008/018622-0
44. Carpentier B, Cerf O. Biofilms and their consequences, with particular reference to hygiene in the food industry. *J Appl Bacteriol*. 1993;75(6):499-511. http://www.ncbi.nlm.nih.gov/pubmed/8294303. Accessed January 10, 2018.
45. Pratt LA, Kolter R. Genetic analysis of Escherichia coli biofilm formation: Roles of flagella, motility, chemotaxis and type I pili. *Mol Microbiol*. 1998;30(2):285-293. doi:10.1046/j.1365-2958.1998.01061.x
46. Houdt R Van, Michiels CW. Role of bacterial cell surface structures in Escherichia coli biofilm formation. *Res Microbiol*. 2005;156:626-633. doi:10.1016/j.resmic.2005.02.005

47. Wu S, Zhang B, Liu Y, Suo X, Li H. *The Influence of Surface Topography on Bacterial Adhesion: A Review : The Influences of Material Surfaces on Bacterial Adhesion*.https://avs.scitation.org/doi/ampdf/10.1116/1.5054057
48. Boland T, Latour RA, Stutzenberger FJ. Molecular Basis of Bacterial Adhesion. https://pdfs.semanticscholar.org/0962/a689070f79499e390d3b4f40b35977775d6e.pdf.
49. Prüß BM. Involvement of Two-Component Signaling on Bacterial Motility and Biofilm Development. 2017. doi:10.1128/JB.00259-17
50. Chaban B, Hughes HV, Beeby M. The flagellum in bacterial pathogens: For motility and a whole lot more. *Semin Cell Dev Biol*. 2015;46:91-103. doi:10.1016/j.semcdb.2015.10.032
51. Duvernoy M-C, Mora T, Ardré M, et al. Asymmetric adhesion of rod-shaped bacteria controls microcolony morphogenesis. *Nat Commun*. 2018;9(1):1120. doi:10.1038/s41467-018-03446-y
52. Berne C, Ellison CK, Ducret A, Brun Y V. Bacterial adhesion at the single-cell level. *Nat Rev Microbiol*. 2018. doi:10.1038/s41579-018-0057-5
53. Mohit V, Culley A, Lovejoy C, Bouchard F, Vincent WF. Hidden biofilms in a far northern lake and implications for the changing Arctic. *npj Biofilms Microbiomes*. 2017;3(1):17. doi:10.1038/s41522-017-0024-3
54. Smith HJ, Schmit A, Foster R, Littman S, Kuypers MM, Foreman CM. Biofilms on glacial surfaces: hotspots for biological activity. *npj Biofilms Microbiomes*. 2016;2(1):16008. doi:10.1038/npjbiofilms.2016.8
55. Galdiero S, Falanga A, Cantisani M, et al. Microbe-host interactions: structure and role of Gram-negative bacterial porins. *Curr Protein Pept Sci*. 2012;13(8):843-854. doi:10.2174/138920312804871120
56. Delcour AH. Electrophysiology of Bacteria. 2013. doi:10.1146/annurev-micro-092412-155637
57. Long Z, Quaife B, Salman H, Oltvai ZN. Cell-cell communication enhances bacterial chemotaxis toward external attractants. *Sci Rep*. 2017;7(1):12855. doi:10.1038/s41598-017-13183-9
58. Albert LS, Brown DG. Variation in bacterial ATP concentration during rapid changes in extracellular pH and implications for the activity of attached bacteria. *Colloids Surfaces B Biointerfaces*. 2015;132:111-116. doi:10.1016/J.COLSURFB.2015.05.020
59. Szczesny M, Beloin C, Ghigo J-M. Increased Osmolarity in Biofilm Triggers RcsB-Dependent Lipid A Palmitoylation in Escherichia coli. 2018. doi:10.1128/mBio.01415-18
60. Otto K, Silhavy TJ. Surface sensing and adhesion of Escherichia coli controlled by the Cpx-signaling pathway. *Proc Natl Acad Sci U S A*. 2002;99(4):2287-2292. doi:10.1073/pnas.042521699
61. Guest RL, Wang J, Wong JL, Raivio TL, Dirita VJ. A Bacterial Stress Response Regulates Respiratory Protein Complexes To Control Envelope Stress Adaptation. *jb.asm.org 1 J Bacteriol March*. 2017;199:153-170. doi:10.1128/JB

62. Jani S, Seely AL, Peabody GL, Jayaraman A, Manson MD. Chemotaxis to self-generated AI-2 promotes biofilm formation in Escherichia coli. doi:10.1099/mic.0.000567
63. Jain R, Faith NG, Milkowski A, et al. Using Chemoattractants to Lure Bacteria to Contact-Killing Surfaces. 2016:5698-5702. doi:10.1002/anie.201510813
64. Haswell ES, Phillips R, Rees DC. Mechanosensitive Channels: What Can They Do and How Do They Do It? *Structure*. 2011;19(10):1356-1369. doi:10.1016/J.STR.2011.09.005
65. Boris Martinac. Mechanosensitive ion channels An evolutionary and scientific tour de force in mechanobiology. 2012. doi:10.1126/sci
66. Kung C. A possible unifying principle for mechanosensation. *Nat Rev*. 2005. doi:10.1038/nature03896
67. Ian R. Booth, Michelle D. Edwards, Susan Black US, and Samantha Miller. Mechanosensitive channels in bacteria: signs of closure? 2007. doi:10.1038/nrmicro1659
68. Si F, Li B, Margolin W, Sun SX. Bacterial growth and form under mechanical compression. *Nat Publ Gr*. 2015. doi:10.1038/srep11367
69. Sukharev SI, Blount P, Martinac B, Kung C. *MECHANOSENSITIVE CHANNELS OF ESCHERICHIA COLI: The MscL Gene, Protein, and Activities*. Vol 59.; 1997. www.annualreviews.org.
70. Park Y, Kim Y, Lim S. Locomotion of a single-flagellated bacterium. *J Fluid Mech*. 2019;859:586-612. doi:10.1017/jfm.2018.799
71. Friedlander RS, Vogel N, Aizenberg J. Role of Flagella in Adhesion of Escherichia coli to Abiotic Surfaces. 2015. doi:10.1021/acs.langmuir.5b00815
72. Conrad JC. Physics of bacterial near-surface motility using flagella and type IV pili: implications for biofilm formation. 2012. doi:10.1016/j.resmic.2012.10.016
73. Persat A. Bacterial mechanotransduction. *Curr Opin Microbiol*. 2017;36:1-6. doi:10.1016/j.mib.2016.12.002
74. Minamino T, Imada K. The bacterial flagellar motor and its structural diversity. *Trends Microbiol*. 2015;23(5):267-274. doi:10.1016/j.tim.2014.12.011
75. Hospenthal MK, Costa TRD, Waksman G. *Pilus Biogenesis at the Inner and Outer Membranes of Gram-Negative Bacteria*.; 2017. http://discovery.ucl.ac.uk/1557577/1/Hospenthal et al %28NRM%29_Accepted %28002%29.pdf.
76. Ellison CK, Kan J, Dillard RS, et al. Obstruction of pilus retraction stimulates bacterial surface sensing. *Science*. 2017;358(6362):535. doi:10.1126/SCIENCE.AAN5706
77. Francis VI, Stevenson EC, Porter SL, Biosciences †, Building GP. Two-component systems required for virulence in Pseudomonas aeruginosa. *FEMS Microbiol Lett*. 2017;364:104. doi:10.1093/femsle/fnx104
78. Berne C, Ducret A, Hardy GG, Brun Y V. Adhesins involved in attachment to abiotic surfaces by Gram- negative bacteria. doi:10.1128/microbiolspec.MB-0018-2015

79. Ribbe J, Baker AE, Euler S, O'Toole GA, Maier B. Role of Cyclic Di-GMP and Exopolysaccharide in Type IV Pilus Dynamics. 2017;199(8):1-10.
80. Persat A, Inclan YF, Engel JN, Stone HA, Gitai Z. Type IV pili mechanochemically regulate virulence factors in Pseudomonas aeruginosa. *Proc Natl Acad Sci U S A*. 2015;112(24):7563-7568. doi:10.1073/pnas.1502025112
81. Buensuceso RNC, Daniel-Ivad M, Kilmury SLN, et al. Cyclic AMP-Independent Control of Twitching Motility in Pseudomonas aeruginosa. *J Bacteriol*. 2017;199(16):e00188-17. doi:10.1128/JB.00188-17
82. Busch A, Waksman G. Chaperone–usher pathways: diversity and pilus assembly mechanism. *Philos Trans R Soc B Biol Sci*. 2012;367(1592):1112. doi:10.1098/RSTB.2011.0206
83. Werneburg GT, Thanassi DG. Pili Assembled by the Chaperone/Usher Pathway in Escherichia coli and Salmonella. *EcoSal Plus*. 2018;8(1). doi:10.1128/ecosalplus.ESP-0007-2017
84. Otto K, Norbeck J, Larsson † Thomas, Karlsson K-A, Hermansson M. Adhesion of Type 1-Fimbriated Escherichia coli to Abiotic Surfaces Leads to Altered Composition of Outer Membrane Proteins. *J Bacteriol*. 2001;183(8):2445-2453. doi:10.1128/JB.183.8.2445-2453.2001
85. Schwan WR, Shibata S, Aizawa S-I, Wolfe AJ. The Two-Component Response Regulator RcsB Regulates Type 1 Piliation in Escherichia coli. *J Bacteriol*. 2007;189(19):7159-7163. doi:10.1128/JB.00705-07
86. Zhang R, Ni L, Jin Z, Li J, Jin F. Bacteria slingshot more on soft surfaces. *Nat Commun*. 2014;5(1):5541. doi:10.1038/ncomms6541
87. Maier B, Wong GCL. How Bacteria Use Type IV Pili Machinery on Surfaces. *Trends Microbiol*. 2015;23(12):775-788. doi:10.1016/J.TIM.2015.09.002
88. Verstraeten N, Braeken K, Debkumari B, et al. Living on a surface: swarming and biofilm formation. *Trends Microbiol*. 2008;16(10):496-506. doi:10.1016/j.tim.2008.07.004
89. Ford KM, Antani JD, Nagarajan A, Johnson MM, Lele PP. Switching and Torque Generation in Swarming *E. coli*. *Front Microbiol*. 2018;9:2197. doi:10.3389/FMICB.2018.02197
90. Barnhart MM, Chapman MR. Curli biogenesis and function. *Annu Rev Microbiol*. 2006;60:131-147. doi:10.1146/annurev.micro.60.080805.142106
91. Brombacher E, Dorel C, Zehnder AJB, Landini P. The curli biosynthesis regulator CsgD co-ordinates the expression of both positive and negative determinants for biofilm formation in Escherichia coli. *Microbiology*. 2003;149(10):2847-2857. doi:10.1099/mic.0.26306-0
92. Prigent-Combaret C, Brombacher † Eva, Vidal O, et al. Complex Regulatory Network Controls Initial Adhesion and Biofilm Formation in Escherichia coli via Regulation of the csgD Gene. *J Bacteriol*. 2001;183(24):7213-7223. doi:10.1128/JB.183.24.7213-7223.2001
93. Jubelin G, Vianney A, Beloin C, et al. CpxR/OmpR Interplay Regulates Curli Gene Expression in Response to Osmolarity in Escherichia coli. *J Bacteriol*. 2005;187(6):2038-2049. doi:10.1128/JB.187.6.2038-2049.2005

94. Kimkes TEP, Heinemannid M. Reassessing the role of the Escherichia coli CpxAR system in sensing surface contact. 2018. doi:10.1371/journal.pone.0207181
95. Ogasawara H, Yamada K, Kori A, Yamamoto K, Ishihama A. Regulation of the Escherichia coli csgD promoter: interplay between five transcription factors. 2010. doi:10.1099/mic.0.039131-0
96. Dunbar M, Debenedictis E, Keten S. Dimerization energetics of curli fiber subunits CsgA and CsgB. doi:10.1038/s41524-019-0164-5
97. Evans ML, Chapman MR. Curli biogenesis: Order out of disorder. *Biochim Biophys Acta - Mol Cell Res*. 2014;1843(8):1551-1558. doi:10.1016/J.BBAMCR.2013.09.010
98. Pesavento C, Becker G, Sommerfeldt N, et al. Inverse regulatory coordination of motility and curli-mediated adhesion in Escherichia coli. 2008. doi:10.1101/gad.475808
99. Gualdi L, Tagliabue L, Bertagnoli S, Ieranò T, De Castro C, Landini P. Cellulose modulates biofilm formation by counteracting curli-mediated colonization of solid surfaces in Escherichia coli. 2008. doi:10.1099/mic.0.2008/018093-0
100. Brombacher E, Baratto A, Dorel C, Landini P. Gene Expression Regulation by the Curli Activator CsgD Protein: Modulation of Cellulose Biosynthesis and Control of Negative Determinants for Microbial Adhesion. *J Bacteriol*. 2006;188(6):2027-2037. doi:10.1128/JB.188.6.2027-2037.2006
101. Steimle A, Autenrieth IB. Structure and function: Lipid A modifications in commensals and pathogens. *Int J Med Microbiol*. 2016;306(5):290-301. doi:10.1016/J.IJMM.2016.03.001
102. Startek JB, Boonen B, Talavera K, Meseguer V. TRP Channels as Sensors of Chemically-Induced Changes in Cell Membrane Mechanical Properties. *Int J Mol Sci*. 2019;20(2). doi:10.3390/ijms20020371
103. Startek JB, Talavera K, Voets T, Alpizar YA. Differential interactions of bacterial lipopolysaccharides with lipid membranes: implications for TRPA1-mediated chemosensation OPEN. *Sci RepoRts |*. 2018;8:12010. doi:10.1038/s41598-018-30534-2
104. Rosadini C V, Kagan JC. Early innate immune responses to bacterial LPS This review comes from a themed issue on Innate immunity. *Curr Opin Immunol*. 2017;44:14-19. doi:10.1016/j.coi.2016.10.005
105. Klein G, Raina S. Regulated Assembly of LPS, Its Structural Alterations and Cellular Response to LPS Defects. *Int J Mol Sci*. 2019;20(2):356. doi:10.3390/ijms20020356
106. Chalabaev S, Chauhan A, Novikov A, et al. Biofilms Formed by Gram-Negative Bacteria Undergo Increased Lipid A Palmitoylation, Enhancing In Vivo Survival. 2014. doi:10.1128/mBio.01116-14
107. Cui M, Wang Z, Hu X, Wang X. Effects of lipopolysaccharide structure on lycopene production in Escherichia coli. *Enzyme Microb Technol*. 2019;124(May 2018):9-16. doi:10.1016/j.enzmictec.2019.01.009
108. Song F, Koo H, Ren D. Effects of Material Properties on Bacterial Adhesion and Biofilm Formation. 2015. doi:10.1177/0022034515587690

109. Dantas LC de M, Silva-Neto JP da, Dantas TS, Naves LZ, das Neves FD, da Mota AS. Bacterial Adhesion and Surface Roughness for Different Clinical Techniques for Acrylic Polymethyl Methacrylate. *Int J Dent*. 2016;2016:1-6. doi:10.1155/2016/8685796
110. Yuan Y, Hays MP, Hardwidge PR, Kim J. Surface characteristics influencing bacterial adhesion to polymeric substrates †. 2017. doi:10.1039/c7ra01571b
111. Yoda I, Koseki H, Tomita M, et al. *Effect of Surface Roughness of Biomaterials on Staphylococcus Epidermidis Adhesion*.; 2014. doi:10.1186/s12866-014-0234-2
112. Wu S, Altenried S, Zogg A, Zuber F, Maniura-Weber K, Ren Q. Role of the Surface Nanoscale Roughness of Stainless Steel on Bacterial Adhesion and Microcolony Formation. 2018. doi:10.1021/acsomega.8b00769
113. Liu L, Ercan B, Sun L, Ziemer KS, Webster TJ. Understanding the Role of Polymer Surface Nanoscale Topography on Inhibiting Bacteria Adhesion and Growth. 2015. doi:10.1021/acsbiomaterials.5b00431
114. Wu S, Zuber F, Maniura-Weber K, Brugger J, Ren Q. Nanostructured surface topographies have an effect on bactericidal activity. *J Nanobiotechnology*. 2018;16(1):20. doi:10.1186/s12951-018-0347-0
115. Cheng Y, Feng G, Moraru CI. Micro- and Nanotopography Sensitive Bacterial Attachment Mechanisms: A Review. *Front Microbiol*. 2019;10:191. doi:10.3389/fmicb.2019.00191
116. Bazaka K, Jacob M V., Crawford RJ, Ivanova EP. Efficient surface modification of biomaterial to prevent biofilm formation and the attachment of microorganisms. *Appl Microbiol Biotechnol*. 2012;95(2):299-311. doi:10.1007/s00253-012-4144-7
117. Riedewald F. Bacterial Adhesion to Surfaces : The Influence of Surface Roughness. 2016;(July).
118. Vadillo-Rodríguez V, Guerra-García-Mora AI, Perera-Costa D, Gónzalez-Martín ML, Fernández-Calderón MC. Bacterial response to spatially organized microtopographic surface patterns with nanometer scale roughness. *Colloids Surfaces B Biointerfaces*. 2018;169:340-347. doi:10.1016/j.colsurfb.2018.05.038
119. Ammar Y, Swailes D, Bridgens B, Chen J. Influence of surface roughness on the initial formation of biofilm. *Surf Coat Technol*. 2015. doi:10.1016/j.surfcoat.2015.07.062
120. Song F. Effects of substrate stiffness on bacterial biofilm formation. 2016. http://surface.syr.edu/etd.
121. Hossain MR, Jiang M, Wei Q, Leff LG, Mohammed Hossain CR. Microplastic surface properties affect bacterial colonization in freshwater. 2018. doi:10.1002/jobm.201800174
122. Katsikogianni M, Missirlis YF. Concise review of mechanisms of bacterial adhesion to biomaterials and of techniques used in estimating bacteria-material interactions. *Eur Cells Mater*. 2004;8(January):37-57. doi:10.22203/eCM.v008a05
123. Sun M, Watson GS, Watson JA, et al. Wettability and adhesional differences on a natural template: The cicada wing. *Sci Adv Mater*. 2014;6(7). doi:10.1166/sam.2014.1805

124. Wiencek KM, Fletcher M. Effects of substratum wettability and molecular topography on the initial adhesion of bacteria to chemically defined substrata. *Biofouling*. 1997. doi:10.1080/08927019709378338
125. Spriano S, Sarath Chandra V, Cochis A, et al. How do wettability, zeta potential and hydroxylation degree affect the biological response of biomaterials? *Mater Sci Eng C*. 2017;74:542-555. doi:10.1016/J.MSEC.2016.12.107
126. Yuan Y, Lee TR. *Contact Angle and Wetting Properties*. Vol 38.; 2016. doi:10.1007/978-3-642-34243-1
127. Xiu Y, Zhu L, Hess DW, Wong CP. Hierarchical silicon etched structures for controlled hydrophobicity/ superhydrophobicity. *Nano Lett*. 2007;7(11):3388-3393. doi:10.1021/nl0717457
128. Hejda F, Solař P, Kousal J. *Surface Free Energy Determination by Contact Angle Measurements-A Comparison of Various Approaches*. https://pdfs.semanticscholar.org/e5a0/e7dc916cfeb7f0b4a3e24027cf7421d5d5e0.pdf. Accessed January 28, 2019.
129. Poncin-Epaillard F, Herry JM, Marmey P, Legeay G, Debarnot D, Bellon-Fontaine MN. Elaboration of highly hydrophobic polymeric surface - A potential strategy to reduce the adhesion of pathogenic bacteria? *Mater Sci Eng C*. 2013;33(3):1152-1161. doi:10.1016/j.msec.2012.12.020
130. Nguyen SH, Webb HK, Crawford RJ, Ivanova EP. Natural antibacterial surfaces. In: *Antibacterial Surfaces*. ; 2015. doi:10.1007/978-3-319-18594-1_2
131. Li X, Cheung GS, Watson GS, et al. The nanotipped hairs of gecko skin and biotemplated replicas impair and/or kill pathogenic bacteria with high efficiency. *Nanoscale*. 2016;8(45):18860-18869. doi:10.1039/C6NR05046H
132. Han Z, Mu Z, Li B, et al. Active Antifogging Property of Monolayer SiO2 Film with Bioinspired Multiscale Hierarchical Pagoda Structures. *ACS Nano*. 2016;10(9):8591-8602. doi:10.1021/acsnano.6b03884
133. Kayes MI, Galante AJ, Stella NA, Haghanifar S, Shanks RMQ, Leu PW. Stable lotus leaf-inspired hierarchical, fluorinated polypropylene surfaces for reduced bacterial adhesion. *React Funct Polym*. 2018;128:40-46. doi:10.1016/J.REACTFUNCTPOLYM.2018.04.013
134. Bixler GD, Bhushan B. Biofouling: lessons from nature. *Philos Trans A Math Phys Eng Sci*. 2012;370(1967):2381-2417. doi:10.1098/rsta.2011.0502
135. Marine J, Myers CP, Picquet GA, Zaidel LA, Wu D, Uhrich KE. Reduction of bacterial attachment on hydroxyapatite surfaces: Using hydrophobicity and chemical functionality to enhance surface retention and prevent attachment. *Colloids Surfaces B Biointerfaces*. 2018;167:531-537. doi:10.1016/J.COLSURFB.2018.04.045
136. Bandara CD, Singh S, Afara IO, et al. Bactericidal Effects of Natural Nanotopography of Dragonfly Wing on Escherichia coli. *ACS Appl Mater Interfaces*. 2017;9(8):6746-6760. doi:10.1021/acsami.6b13666
137. Alexander MR, Williams P. Water contact angle is not a good predictor of biological responses to materials. *Cit Biointerphases*. 2017;12:2-201. doi:10.1116/1.4989843

138. Hoek EMV, Agarwal GK. Extended DLVO interactions between spherical particles and rough surfaces. *J Colloid Interface Sci*. 2006;298(1):50-58. doi:10.1016/j.jcis.2005.12.031
139. Xu L-C, Siedlecki CA. *Staphylococcus epidermidis* adhesion on hydrophobic and hydrophilic textured biomaterial surfaces. *Biomed Mater*. 2014;9(3):035003. doi:10.1088/1748-6041/9/3/035003
140. Yea-Ling Ong †, Anneta Razatos ‡, George Georgiou, ‡ A, Mukul M. Sharma* †. Adhesion Forces between *E. coli* Bacteria and Biomaterial Surfaces. 1999;(10):2719-2725. doi:10.1021/LA981104E
141. Staphylococcus epidermidis adhesion on hydrophobic and hydrophilic textured biomaterial surfaces. 2014. doi:10.1088/1748-6041/9/3/035003
142. Oh JK, Yegin Y, Yang F, et al. The influence of surface chemistry on the kinetics and thermodynamics of bacterial adhesion. doi:10.1038/s41598-018-35343-1
143. Hä H, Vargas JN, Jung M, et al. Adhesion Properties of Freestanding Hydrophobin Bilayers. 2018;34:8549. doi:10.1021/acs.langmuir.8b00575
144. Yuan Y, Hays MP, Hardwidge PR, Kim J. Surface characteristics influencing bacterial adhesion to polymeric substrates †. 2017. doi:10.1039/c7ra01571b
145. Grivet M, Morrier JJ, Benay G, Barsotti O. Effect of hydrophobicity on in vitro streptococcal adhesion to dental alloys. *J Mater Sci Mater Med*. 2000;11(10):637-642. doi:10.1023/A:1008913915399
146. Elbourne A, Chapman J, Gelmi A, Cozzolino D, Crawford RJ, Truong VK. Bacterial-nanostructure interactions: The role of cell elasticity and adhesion forces. *J Colloid Interface Sci*. 2019;546:192-210. doi:10.1016/J.JCIS.2019.03.050
147. Terada A, Okuyama K, Nishikawa M, Tsuneda S, Hosomi M. The effect of surface charge property on Escherichia coli initial adhesion and subsequent biofilm formation. *Biotechnol Bioeng*. 2012;109(7):1745-1754. doi:10.1002/bit.24429
148. France RM, Short RD. Plasma Treatment of Polymers: The Effects of Energy Transfer from an Argon Plasma on the Surface Chemistry of Polystyrene, and Polypropylene. A High-Energy Resolution X-ray Photoelectron Spectroscopy Study. *Langmuir*. 1998;14(17):4827-4835. doi:10.1021/la9713053
149. Mozeti M, Primc G, Vesel A, - al, Mozetic M. To cite this article: Alenka Vesel and Miran Mozetic. *J Phys D Appl Phys*. 2017;50:21. doi:10.1088/1361-6463/aa748a
150. Abernathy G. Determination of Polymer Surface Properties Before and After Oxygen Plasma Etching. 2016.
151. Tsougeni K, Vourdas N, Tserepi A, Gogolides E, Cardinaud C. Mechanisms of Oxygen Plasma Nanotexturing of Organic Polymer Surfaces: From Stable Super Hydrophilic to Super Hydrophobic Surfaces. *Langmuir*. 2009;25(19):11748-11759. doi:10.1021/la901072z
152. Parreira P, Magalhã es A, Gonçalves IC, et al. Effect of surface chemistry on bacterial adhesion, viability, and morphology. 2011. doi:10.1002/jbm.a.33178
153. Wang B, Li X, Wu B, et al. Recent developments in smart antibacterial surfaces to inhibit biofilm formation and bacterial infections. *Artic J Mater Chem B*. 2018;6:4274. doi:10.1039/c8tb01245h

154. Zwitterionic Cellulose Carbamate with Regioselective Substitution Pattern: A Coating Material Possessing Antimicrobial Activity. 2016. doi:10.1002/mabi.201500349
155. Busscher HJ, Van Der Mei RBHC. Initial microbial adhesion is a determinant for the strength of biofilm adhesion. *FEMS Microbiol Lett*. 1995;128(3):229-234. doi:10.1016/0378-1097(95)00103-C
156. Moreira J, Gomes L, Whitehead KA, Lynch S. Effect of surface conditioning with cellular extracts on Escherichia coli adhesion and initial biofilm formation. 2017. doi:10.1016/j.fbp.2017.03.008
157. Speranza G, Gottardi G, Pederzolli C, et al. Role of chemical interactions in bacterial adhesion to polymer surfaces. *Biomaterials*. 2004;25:2029-2037. doi:10.1016/j.biomaterials.2003.08.061
158. Wang Y, Lee SM, Dykes G. The physicochemical process of bacterial attachment to abiotic surfaces: Challenges for mechanistic studies, predictability and the development of control strategies. *Crit Rev Microbiol*. 2015;41(4):452-464. doi:10.3109/1040841X.2013.866072
159. Hermansson M. *The DLVO Theory in Microbial Adhesion*. Vol 14.; 1999. www.elsevier.nl/locate/colsurfb. Accessed December 19, 2018.
160. Van Oss CJ. *Energetics of Cell-Cell and Cell-Biopolymer Interactions*. Vol 1.; 1989. https://link.springer.com/content/pdf/10.1007/BF02797387.pdf.
161. Algburi A, Comito N, Kashtanov D, Dicks LMT, Chikindas ML. Control of Biofilm Formation: Antibiotics and Beyond. 2017. doi:10.1128/AEM.02508-16
162. Romaniuk JAH, Cegelski L. Bacterial cell wall composition and the influence of antibiotics by cell-wall and whole-cell NMR. *Philos Trans R Soc Lond B Biol Sci*. 2015;370(1679). doi:10.1098/rstb.2015.0024
163. Prasetyoputri A, Jarrad AM, Cooper MA, Blaskovich MAT. The Eagle Effect and Antibiotic-Induced Persistence: Two Sides of the Same Coin? *Trends Microbiol*. 2019;27(4):339-354. doi:10.1016/J.TIM.2018.10.007
164. Worthington RJ, Richards JJ, Melander C. Small molecule control of bacterial biofilms. doi:10.1039/c2ob25835h
165. Ishii S, Fukui K, Yokoshima S, et al. High-throughput Screening of Small Molecule Inhibitors of the Streptococcus Quorum-sensing Signal Pathway. doi:10.1038/s41598-017-03567-2
166. Battesti A, Majdalani N, Gottesman S. The RpoS-Mediated General Stress Response in Escherichia coli *. *Annu Rev Microbiol*. 2011;65:189-213. doi:10.1146/annurev-micro-090110-102946
167. Wang Y, Zeng Y, Wang Y, et al. Antimicrobial peptide GH12 targets Streptococcus mutans to arrest caries development in rats. *J Oral Microbiol*. 2018;11(1):1549921. doi:10.1080/20002297.2018.1549921
168. Luo J, Hein C, Mücklich F, Solioz M. Killing of bacteria by copper, cadmium, and silver surfaces reveals relevant physicochemical parameters. *Biointerphases*. 2017;12(2):020301. doi:10.1116/1.4980127
169. Alexander JW. History of the Medical Use of Silver*. http://www.silveredgehealth.com/pdf/history.pdf.

170. Roe D, Karandikar B, Bonn-Savage N, Gibbins B, Roullet J-B. Antimicrobial surface functionalization of plastic catheters by silver nanoparticles. *J Antimicrob Chemother*. 2008;61(4):869-876. doi:10.1093/jac/dkn034
171. Eckhardt S, Brunetto PS, Gagnon J, Priebe M, Giese B, Fromm KM. Nanobio Silver: Its Interactions with Peptides and Bacteria, and Its Uses in Medicine. 2013. doi:10.1021/cr300288v
172. Stevens KNJ, Crespo-Biel O, Van Den Bosch EEM, et al. The relationship between the antimicrobial effect of catheter coatings containing silver nanoparticles and the coagulation of contacting blood. 2009. doi:10.1016/j.biomaterials.2009.03.054
173. Graves JL, Tajkarimi M, Cunningham Q, et al. Rapid evolution of silver nanoparticle resistance in Escherichia coli. *Front Genet*. 2015;6:42. doi:10.3389/fgene.2015.00042
174. Codiţă I, Caplan DM, Drăgulescu E-C, et al. Antimicrobial activity of copper and silver nanofilms on nosocomial bacterial species. *Roum Arch Microbiol Immunol*. 69(4):204-212. http://www.ncbi.nlm.nih.gov/pubmed/21462835. Accessed November 22, 2017.
175. Sánchez MC, Toledano-Osorio M, Bueno J, et al. Antibacterial effects of polymeric PolymP-n Active nanoparticles. An in vitro biofilm study. *Dent Mater*. 2019;35(1):156-168. doi:10.1016/J.DENTAL.2018.11.015
176. Banerjee I, Pangule RC, Kane RS. Antifouling Coatings: Recent Developments in the Design of Surfaces That Prevent Fouling by Proteins, Bacteria, and Marine Organisms. *Adv Mater*. 2011;23(6):690-718. doi:10.1002/adma.201001215
177. Keskin D, Mergel O, Van Der Mei HC, Busscher HJ, Van Rijn P. Inhibiting Bacterial Adhesion by Mechanically Modulated Microgel Coatings. 2018. doi:10.1021/acs.biomac.8b01378
178. Antoci V, King SB, Jose B, et al. Vancomycin covalently bonded to titanium alloy prevents bacterial colonization. *J Orthop Res*. 2007;25(7):858-866. doi:10.1002/jor.20348
179. Francolini I, Vuotto C, Piozzi A, Donelli G. Antifouling and antimicrobial biomaterials: an overview. *APMIS*. 2017;125(4):392-417. doi:10.1111/apm.12675
180. Spengler C, Thewes N, Jung P, Bischoff M, Jacobs K. Determination of the nano-scaled contact area of staphylococcal cells. *Nanoscale*. 2017;9(28):10084-10093. doi:10.1039/C7NR02297B
181. Watson GS, Watson JA, Cribb BW. Diversity of Cuticular Micro- and Nanostructures on Insects: Properties, Functions, and Potential Applications. *Annu Rev Entomol*. 2017;62(1):185-205. doi:10.1146/annurev-ento-031616-035020
182. Hasan J, Crawford RJ, Ivanova EP. Antibacterial surffaces: the quest for a new generation of biomaterials. *Trends Biotechnol*. 2013;31(5):295.
183. Nowlin K, Boseman A, Covell A, LaJeunesse D. Adhesion-dependent rupturing of Saccharomyces cerevisiae on biological antimicrobial nanostructured surfaces. *J R Soc Interface*. 2014;12(102):20140999-20140999. doi:10.1098/rsif.2014.0999

184. Kelleher SM, Habimana O, Lawler J, et al. Cicada Wing Surface Topography: An Investigation into the Bactericidal Properties of Nanostructural Features. *ACS Appl Mater Interfaces*. 2016;8(24):14966-14974. doi:10.1021/acsami.5b08309
185. Krasowska A, Sigler K. How microorganisms use hydrophobicity and what does this mean for human needs? *Front Cell Infect Microbiol*. 2014;4(August):1-7. doi:10.3389/fcimb.2014.00112
186. Ivanova EP, Hasan J, Webb HK, et al. Natural bactericidal surfaces: Mechanical rupture of pseudomonas aeruginosa cells by cicada wings. *Small*. 2012;8(16):2489-2494. doi:10.1002/smll.201200528
187. Ivanova EP, Hasan J, Webb HK, et al. Bactericidal activity of black silicon. *Nat Commun*. 2013;4:2838. doi:10.1038/ncomms3838
188. Bhadra CM, Khanh Truong V, Pham VTH, et al. Antibacterial titanium nano-patterned arrays inspired by dragonfly wings. *Sci Rep*. 2015;5:16817. doi:10.1038/srep16817
189. Linklater DP, Juodkazis S, Ivanova EP. Nanofabrication of mechano-bactericidal surfaces. *Nanoscale*. 2017. doi:10.1039/C7NR05881K
190. Bazaka K, Jacob M V., Crawford RJ, Ivanova EP. Plasma-assisted surface modification of organic biopolymers to prevent bacterial attachment. *Acta Biomater*. 2011;7(5):2015-2028. doi:10.1016/j.actbio.2010.12.024
191. Armentano I, Arciola CR, Fortunati E, et al. The interaction of bacteria with engineered nanostructured polymeric materials: a review. *ScientificWorldJournal*. 2014;2014:410423. doi:10.1155/2014/410423
192. Modaresifar K, Azizian S, Ganjian M, Fratila-Apachitei LE, Zadpoor AA. Bactericidal effects of nanopatterns: A systematic review. *Acta Biomater*. 2019;83:29-36. doi:10.1016/j.actbio.2018.09.059
193. Mimee M, Nadeau P, Hayward A, et al. Gastrointestinal Health. 2018;918(May):915-918.
194. White GF, Edwards MJ, Gomez-Perez L, Richardson DJ, Butt JN, Clarke TA. Mechanisms of Bacterial Extracellular Electron Exchange. *Adv Microb Physiol*. 2016. doi:10.1016/bs.ampbs.2016.02.002
195. White GF, Edwards MJ, Gomez-Perez L, Richardson DJ, Butt JN, Clarke TA. *Shewanella Electron Transfer. Mechanisms of Bacterial Extracellular Electron Exchange*. https://core.ac.uk/download/pdf/41993713.pdf.
196. Zou L, Huang Y-H, Long Z-E, Qiao Y. On-going applications of Shewanella species in microbial electrochemical system for bioenergy, bioremediation and biosensing. *World J Microbiol Biotechnol*. 2019;35(9):9. doi:10.1007/s11274-018-2576-7
197. Humphries J, Xiong L, Liu J, et al. Species-Independent Attraction to Biofilms through Electrical Signaling. *Cell*. 2017;168:200-209.e12. doi:10.1016/j.cell.2016.12.014
198. Trushin M V. *The Possible Role of Electromagnetic Fields in Bacterial Communication*. Vol 36.; 2003. http://nghl-ntge.s3.amazonaws.com/JMicrobiolImmunolInfect2003_36_153-160.

199. Huan-Hsuan L(, Hsu), Deng P, Zhang Y, Nguyen HN, Jiang X. Nanostructured interfaces for probing and facilitating extracellular electron transfer. *J Mater Chem B*. 2018;6:7144. doi:10.1039/c8tb01598h
200. Kato S. Microbial extracellular electron transfer and its relevance to iron corrosion. *Microb Biotechnol*. 2016. doi:10.1111/1751-7915.12340
201. Queisser HJ. Persistent Photoconductivity in Semiconductors. In: *Proceedings of the 17th International Conference on the Physics of Semiconductors*. New York, NY: Springer New York; 1985:1303-1308. doi:10.1007/978-1-4615-7682-2_295
202. Gall I, Herzberg M, Oren Y. The effect of electric fields on bacterial attachment to conductive surfaces †. *Soft Matter*. 2013. doi:10.1039/c2sm27270a
203. Chuo Ann L, Mahmud S, Khadijah S, et al. Enhanced photoconductivity and antibacterial response of rubber-grade ZnO upon UVA illumination. 2014. doi:10.4028/www.scientific.net/AMR.925.33
204. Petrofsky J, Laymon M, Chung W, Kelly D, Bs C, Yang T-N. *Effect of Electrical Stimulation on Bacterial Growth*.; 2008. https://pdfs.semanticscholar.org/b629/393775a98bf9cfc5d6e052c95076897869d0.pdf.
205. Berthelot R, Neethirajan S. Harnessing electrical energy for anti-biofilm therapies: effects of current on cell morphology and motility. *J Exp Nanosci*. 2017;12(1):197-207. doi:10.1080/17458080.2017.1296977
206. Snyder PJ, Kirste R, Collazo R, Ivanisevic A. Persistent Photoconductivity, Nanoscale Topography, and Chemical Functionalization Can Collectively Influence the Behavior of PC12 Cells on Wide Bandgap Semiconductor Surfaces. 2017. doi:10.1002/smll.201700481
207. Snyder PJ, Lajeunesse DR, Reddy P, Kirste R, Collazo R, Ivanisevic A. Bioelectronics communication: encoding yeast regulatory responses using nanostructured gallium nitride thin films. 2018;10:11506. doi:10.1039/c8nr03684e
208. Gulyuk A V, Lajeunesse DR, Collazo R, Ivanisevic A. Characterization of Pseudomonas aeruginosa Films on Different Inorganic Surfaces before and after UV Light Exposure. 2018. doi:10.1021/acs.langmuir.8b02079
209. Darnell M, Gu L, Mooney D. RNA-seq reveals diverse effects of substrate stiffness on mesenchymal stem cells. *Biomaterials*. 2018;181:182-188. doi:10.1016/j.biomaterials.2018.07.039
210. Engler AJ, Sen S, Lee Sweeney H, Discher DE. Matrix Elasticity Directs Stem Cell Lineage Specification. doi:10.1016/j.cell.2006.06.044
211. Li Y, Fanous MJ, Kilian KA, Popescu G. Quantitative phase imaging reveals matrix stiffness-dependent growth and migration of cancer cells. *Sci Rep*. 2019;9(1):248. doi:10.1038/s41598-018-36551-5
212. Zhu Y, Li X, Janairo RRR, et al. Matrix stiffness modulates the differentiation of neural crest stem cells in vivo. *J Cell Physiol*. 2019;234(5):7569-7578. doi:10.1002/jcp.27518
213. Li J, Han D, Zhao Y-P. Kinetic behaviour of the cells touching substrate: the interfacial stiffness guides cell spreading. *Sci Rep*. 2014;4:3910. doi:10.1038/srep03910

214. Jiang X, Georges PC, Li B, et al. *Cell Growth in Response to Mechanical Stiffness Is Affected by Neuron-Astroglia Interactions*. Vol 1.; 2007. https://benthamopen.com/contents/pdf/TONEURJ/TONEURJ-1-7.pdf.
215. Engler AJ, Griffin MA, Sen S, Bönnemann CG, Sweeney HL, Discher DE. Myotubes differentiate optimally on substrates with tissue-like stiffness: pathological implications for soft or stiff microenvironments. *J Cell Biol*. 2004;166(6):877-887. doi:10.1083/jcb.200405004
216. Jalali S, Tafazzoli-Shadpour M, Haghighipour N, Omidvar R, Safshekan F. Regulation of Endothelial Cell Adherence and Elastic Modulus by Substrate Stiffness. *Cell Commun Adhes*. 2015. doi:10.1080/15419061.2016.1265949org/10.1080/15419061.2016.1265949
217. Reimer M, Silviya •, Zustiak P, Sheth • Saahil, Joseph •, Schober M. Intrinsic Response Towards Physiologic Stiffness is Cell-Type Dependent. *Cell Biochem Biophys*. 2013;76:197-208. doi:10.1007/s12013-017-0834-1
218. Parandakh A, Anbarlou A, Tafazzoli-Shadpour M, Ardeshirylajimi A, Khani M-M. Substrate topography interacts with substrate stiffness and culture time to regulate mechanical properties and smooth muscle differentiation of mesenchymal stem cells. *Colloids Surfaces B Biointerfaces*. 2019;173:194-201. doi:10.1016/j.colsurfb.2018.09.066
219. Roeder RK. Mechanical Characterization of Biomaterials. 2013. doi:10.1016/B978-0-12-415800-9.00003-6
220. Kolewe KW, Peyton SR, Schiffman JD. Fewer Bacteria Adhere to Softer Hydrogels. 2015. doi:10.1021/acsami.5b04269
221. Guégan C, Garderes J, Le Pennec G, et al. Alteration of bacterial adhesion induced by the substrate stiffness. *Colloids Surfaces B Biointerfaces*. 2014;114:193-200. doi:10.1016/J.COLSURFB.2013.10.010
222. Song F, Ren D. Stiffness of cross-linked poly(dimethylsiloxane) affects bacterial adhesion and antibiotic susceptibility of attached cells. *Langmuir*. 2014;30(34):10354-10362. doi:10.1021/la502029f
223. Kolewe KW, Zhu J, Mako NR, Nonnenmann SS, Schi JD. Bacterial Adhesion Is A ff ected by the Thickness and Stiffness of Poly(ethylene glycol) Hydrogels. 2018. doi:10.1021/acsami.7b12145
224. Song F, Brasch ME, Wang H, Henderson JH, Sauer K, Ren D. How Bacteria Respond to Material Stiffness during Attachment: A Role of Escherichia coli Flagellar Motility. *ACS Appl Mater Interfaces*. 2017;9(27):22176-22184. doi:10.1021/acsami.7b04757
225. Ultee E, Ramijan K, Dame RT, Briegel A, Claessen D. *Stress-Induced Adaptive Morphogenesis in Bacteria*. Vol 74. Elsevier Ltd; 2019. doi:10.1016/bs.ampbs.2019.02.001
226. Baumgarten T, Sperling S, Seifert J, et al. Membrane vesicle formation as a multiple-stress response mechanism enhances pseudomonas putida DOT-T1E cell surface hydrophobicity and biofilm formation. *Appl Environ Microbiol*. 2012;78(17):6217-6224. doi:10.1128/AEM.01525-12

227. Boyce KJ, Andrianopoulos A. Fungal dimorphism: the switch from hyphae to yeast is a specialized morphogenetic adaptation allowing colonization of a host. Braus G, ed. *FEMS Microbiol Rev*. 2015;39(6):797-811. doi:10.1093/femsre/fuv035
228. Ryder VJ, Chopra I, O'Neill AJ. Increased Mutability of Staphylococci in Biofilms as a Consequence of Oxidative Stress. *PLoS One*. 2012;7(10). doi:10.1371/journal.pone.0047695
229. Meylan S, Andrews IW, Collins JJ. Review Targeting Antibiotic Tolerance , Pathogen by Pathogen. *Cell*. 2018;172(6):1228-1238. doi:10.1016/j.cell.2018.01.037
230. Serra DO, Hengge R. Stress responses go three dimensional - The spatial order of physiological differentiation in bacterial macrocolony biofilms. *Environ Microbiol*. 2014;16(6):1455-1471. doi:10.1111/1462-2920.12483
231. Sies H, Berndt C, Jones DP. Oxidative Stress. *Annu Rev Biochem*. 2017;86(1):715-748. doi:10.1146/annurev-biochem-061516-045037
232. Sikdar R, Simmons AR, Doerrler WT. Multiple Envelope Stress Response Pathways Are Activated in an Escherichia coli Strain with Mutations in Two Members of the DedA Membrane Protein Family. 2013. doi:10.1128/JB.00762-12
233. Rowlett VW, Mallampalli VKPS, Karlstaedt A, et al. Impact of Membrane Phospholipid Alterations in Escherichia coli on Cellular Function and Bacterial Stress Adaptation. 2017. doi:10.1128/JB
234. Davey ME, O'toole GA. Microbial Biofilms: from Ecology to Molecular Genetics. *Microbiol Mol Biol Rev*. 2000;64(4):847-867. doi:10.1128/MMBR.64.4.847-867.2000
235. O'Toole G, Kaplan HB, Kolter R. Biofilm Formation as Microbial Development. *Annu Rev Microbiol*. 2000;54(1):49-79. doi:10.1146/annurev.micro.54.1.49
236. Kanerva M, Ollgren J, Virtanen MJ, Lyytikäinen O. Estimating the annual burden of health care–associated infections in Finnish adult acute care hospitals. *Am J Infect Control*. 2009;37(3):227-230. doi:10.1016/J.AJIC.2008.07.004
237. Klevens RM, Edwards JR, Richards CL, et al. Estimating Health Care-associated infections and deaths in U.S. hospitals, 2002. https://journals.sagepub.com/doi/pdf/10.1177/003335490712200205.
238. Winkelstroter LK. Microbial Biofilms: The Challenge of Food Industry. *Biochem Mol Biol J*. 2015;01(01). doi:10.21767/2471-8084.100005
239. *Biofilms, Infection, and Antimicrobial Therapy*. http://loyce2008.free.fr/Microbiologie/Biofilms, Infection, and Antimicrobial Therapy - J. Pace - CRC Press, 2006.pdf#page=40. Accessed January 16, 2019.
240. Armbruster CR, Parsek MR. New insight into the early stages of biofilm formation. doi:10.1073/pnas.1804084115
241. Ae JP, Ae SF, Brooks J. Bacterial cell attachment, the beginning of a biofilm. doi:10.1007/s10295-007-0234-4
242. Wang L, Chen W, Terentjev E. Effect of micro-patterning on bacterial adhesion on polyethylene terephthalate surface. doi:10.1177/0885328214563998

243. De F, Macagnano A, Fabrizio S, et al. Featuring work from Dr As featured in: A study on the dependence of bacteria adhesion on the polymer nanofibre diameter. *Cite this Environ Sci Nano*. 2019;6:778. doi:10.1039/c8en01237g
244. Lorenzetti M, Dogs I, Stopar D, Kalin M, Kobe S. The Influence of Surface Modification on Bacterial Adhesion to Titanium-Based Substrates. 2014. doi:10.1021/am507148n
245. Aggarwal S, Poppele EH, Hozalski RM. Development and testing of a novel microcantilever technique for measuring the cohesive strength of intact biofilms. *Biotechnol Bioeng*. 2010;105(5):n/a-n/a. doi:10.1002/bit.22605
246. Mitik-Dineva N, Wang J, Truong VK, et al. Escherichia coli, Pseudomonas aeruginosa, and Staphylococcus aureus Attachment Patterns on Glass Surfaces with Nanoscale Roughness. *Curr Microbiol*. 2009;58(3):268-273. doi:10.1007/s00284-008-9320-8
247. Weibel DB, Diluzio WR, Whitesides GM. Microtechnology Microfabrication meets microbiology. *Nat Rev | Microbiol*. 2007;5. doi:10.1038/nrmicro1616
248. Linklater DP, Nguyen HKD, Bhadra CM, Juodkazis S, Ivanova EP. Influence of nanoscale topology on bactericidal efficiency of black silicon surfaces. *Nanotechnology*. 2017;28(24):245301. doi:10.1088/1361-6528/aa700e
249. Hazell G, May PW, Taylor P, Nobbs AH, Welch CC, Su B. Studies of black silicon and black diamond as materials for antibacterial surfaces †. *Cite this Biomater Sci*. 2018;6:1424. doi:10.1039/c8bm00107c
250. Elbourne A, Crawford RJ, Ivanova EP. Nano-structured antimicrobial surfaces: From nature to synthetic analogues. *J Colloid Interface Sci*. 2017;508:603-616. doi:10.1016/j.jcis.2017.07.021
251. L??decke C, Roth M, Yu W, Horn U, Bossert J, Jandt KD. Nanorough titanium surfaces reduce adhesion of Escherichia coli and Staphylococcus aureus via nano adhesion points. *Colloids Surfaces B Biointerfaces*. 2016;145:617-625. doi:10.1016/j.colsurfb.2016.05.049
252. Truong VK, Pham VTH, Medvedev A, et al. Self-organised nanoarchitecture of titanium surfaces influences the attachment of Staphylococcus aureus and Pseudomonas aeruginosa bacteria. *Appl Microbiol Biotechnol*. 2015;99(16):6831-6840. doi:10.1007/s00253-015-6572-7
253. Dickson MN, Liang EI, Rodriguez LA, Vollereaux N, Yee AF. Nanopatterned polymer surfaces with bactericidal properties. *Biointerphases*. 2015;10(2):021010. doi:10.1116/1.4922157
254. Nejadnik MR, van der Mei HC, Norde W, Busscher HJ. Bacterial adhesion and growth on a polymer brush-coating. *Biomaterials*. 2008;29(30):4117-4121. doi:10.1016/j.biomaterials.2008.07.014
255. Bazaka K, Jacob M V., Crawford RJ, Ivanova EP. Plasma-assisted surface modification of organic biopolymers to prevent bacterial attachment. *Acta Biomater*. 2011;7:2015-2028. doi:10.1016/j.actbio.2010.12.024
256. Petra Landsberger, Viola Boenke, Anna A. Gorbushina, et al. Bacterial attachment on poly[acrylonitrile-co-(2-methyl-2-propene-1-sulfonic acid)] surfaces. http://karo03.bplaced.net/karsten.rodenacker/Me/Misc_WWW/pdf/Poly4bio1.pdf.

257. Sjöström T, Nobbs AH, Su B. Bactericidal nanospike surfaces via thermal oxidation of Ti alloy substrates. *Mater Lett*. 2016;167:22-26. doi:10.1016/j.matlet.2015.12.140
258. Thomas P, Sekhar AC, Upreti R, Mujawar MM, Pasha SS. Optimization of single plate-serial dilution spotting (SP-SDS) with sample anchoring as an assured method for bacterial and yeast cfu enumeration and single colony isolation from diverse samples. *Biotechnol Reports*. 2015;8:45-55. doi:10.1016/J.BTRE.2015.08.003
259. Nedela O, Slepicka P, Švorcík V. Surface modification of polymer substrates for biomedical applications. *Materials (Basel)*. 2017;10(10). doi:10.3390/ma10101115
260. Hasan J, Chatterjee K. Recent advances in engineering topography mediated antibacterial surfaces. *Nanoscale*. 2015;7:15568. doi:10.1039/c5nr04156b
261. Bhadra CM. New Approaches in the fabrication of multidimensional smart materials for biotechnological applications. 2016.
262. Bazaka K, Jacob M V, Chrzanowski W, Ostrikov K. Anti-bacterial surfaces: natural agents, mechanisms of action, and plasma surface modification. 2015. doi:10.1039/c4ra17244b
263. Milella A, Mundo R Di, Palumbo F, Favia P, Fracassi F, Agostino R. Plasma Nanostructuring of Polymers : Different Routes to Superhydrophobicity. 2009:460-466. doi:10.1002/ppap.200930011
264. Wohlfart E, Fern Andez-Bl Azquez JP, Knoche E, et al. Nanofibrillar Patterns by Plasma Etching: The Influence of Polymer Crystallinity and Orientation in Surface Morphology. *Macromolecules*. 2010;43:9908-9917. doi:10.1021/ma101889s
265. Fernández-Blázquez JP, Fell D, Bonaccurso E, Del Campo A. Superhydrophilic and superhydrophobic nanostructured surfaces via plasma treatment. *J Colloid Interface Sci*. 2011;357:234-238. doi:10.1016/j.jcis.2011.01.082
266. Ikoma T, Kobayashi H, Tanaka J, Walsh D, Mann S. Microstructure, mechanical, and biomimetic properties of fish scales from Pagrus major. doi:10.1016/S1047-8477(03)00053-4
267. Strobel M, Lyons CS. An Essay on Contact Angle Measurements. doi:10.1002/ppap.201000041
268. Tomko J, Olson DH, Giri A, et al. Nanoscale wetting and energy transmission at solid-liquid interfaces. doi:10.1021/acs.langmuir.8b03675
269. Good RJ, Girifalco LA. *Energies of Solids from Contact Angle Data 561 A THEORY FOR ESTIMATION OF SURFACE AND INTERFACIAL ENERGIES. III. ESTIMATION OF SURFACE ENERGIES OF SOLIDS FROM CONTACT ANGLE DATA*.; 1960. https://pubs.acs.org/sharingguidelines.
270. Li B, Logan BE, Fe Cr -y-z. Bacterial adhesion to glass and metal-oxide surfaces. *Colloids Surfaces B Biointerfaces*. 2004;36:81-90. doi:10.1016/j.colsurfb.2004.05.006
271. Madows PS. *The Attachment of Bacteria to Solid Surfaces*. Vol 75. Springer-Verlag; 1971. https://link.springer.com/content/pdf/10.1007%2FBF00407699.pdf.

272. Park KD, Kim YS, Han DK, et al. Bacterial adhesion on PEG modified polyurethane surfaces. *Biomaterials*. 1998;19(7-9):851-859. doi:10.1016/S0142-9612(97)00245-7
273. Shi L, Günther S, Hübschmann T, Wick LY, Harms H, Müller S. Limits of propidium iodide as a cell viability indicator for environmental bacteria. *Cytom Part A*. 2007;71A(8):592-598. doi:10.1002/cyto.a.20402
274. Sharifian Gh M, Wilhelm MJ, Sheffield JB, Dai H-L. Living *E. coli* is Permeable to Propidium Iodide: A Study by Time-Resolved Second-Harmonic Scattering and Fluorescence Microscopy. *Biophys J*. 2015;108(2):148a-149a. doi:10.1016/j.bpj.2014.11.819
275. Stiefel P, Schmidt-Emrich S, Maniura-Weber K, Ren Q. Critical aspects of using bacterial cell viability assays with the fluorophores SYTO9 and propidium iodide. *BMC Microbiol*. 2015;15:36. doi:10.1186/s12866-015-0376-x
276. Davey HM, Hexley P. Red but not dead? Membranes of stressed Saccharomyces cerevisiae are permeable to propidium iodide. *Environ Microbiol*. 2011;13(1):163-171. doi:10.1111/j.1462-2920.2010.02317.x
277. Riccardi C, Nicoletti I. Analysis of apoptosis by propidium iodide staining and flow cytometry. *Nat Protoc*. 2006;1(3):1458-1461. doi:10.1038/nprot.2006.238
278. Tuson HH, Weibel DB. Bacteria-surface interactions Introduction to microbial surface sensing. 2013. doi:10.1039/C3SM27705D
279. Jaggessar A, Shahali H, Mathew A, Yarlagadda PKD V. Bio-mimicking nano and micro-structured surface fabrication for antibacterial properties in medical implants. *J Nanobiotechnology*. 2017;15. doi:10.1186/s12951-017-0306-1
280. Hsu LC, Fang J, Borca-Tasciuc DA, Worobo RW, Moraru CI. Effect of micro- and nanoscale topography on the adhesion of bacterial cells to solid surfaces. *Appl Environ Microbiol*. 2013;79(8):2703-2712. doi:10.1128/AEM.03436-12
281. Feng G, Cheng Y, Wang S-Y, Borca-Tasciuc DA, Worobo RW, Moraru CI. Bacterial attachment and biofilm formation on surfaces are reduced by small-diameter nanoscale pores: how small is small enough? *npj Biofilms Microbiomes*. 2015;1(1):15022. doi:10.1038/npjbiofilms.2015.22
282. Vatankhah-Varnosfaderani M, Daniel WFM, Everhart MH, et al. Mimicking biological stress-strain behaviour with synthetic elastomers. *Nature*. 2017;549(7673):497-501. doi:10.1038/nature23673
283. Yoshida S, Hagiwara K, Hasebe T, Hotta A. Surface modification of polymers by plasma treatments for the enhancement of biocompatibility and controlled drug release. 2013. doi:10.1016/j.surfcoat.2013.02.042
284. Gogolides E. Controlling roughness: from etching to nanotexturing and plasma-directed organization on organic and inorganic materials Related content. 2011. doi:10.1088/0022-3727/44/17/174021
285. Luan Y, Liu S, Pihl M, et al. Bacterial interactions with nanostructured surfaces. *Curr Opin Colloid Interface Sci*. 2018;38:170-189. doi:10.1016/J.COCIS.2018.10.007

286. Serrano C, García-Fern Andez L, Fern Andez-Bl Azquez JP, et al. Nanostructured medical sutures with antibacterial properties. 2015. doi:10.1016/j.biomaterials.2015.02.039
287. Rizzello L, Galeone A, Vecchio G, Brunetti V, Sabella S, Pompa PP. Molecular response of Escherichia coli adhering onto nanoscale topography. *Nanoscale Res Lett*. 2012;7(1):575. doi:10.1186/1556-276X-7-575
288. Tallawi M, Opitz M, Lieleg O. Modulation of the mechanical properties of bacterial biofilms in response to environmental challenges. *Biomater Sci*. 2017;5(5):887-900. doi:10.1039/C6BM00832A
289. Linklater DP, De Volder M, Baulin VA, et al. High Aspect Ratio Nanostructures Kill Bacteria via Storage and Release of Mechanical Energy. 2018. doi:10.1021/acsnano.8b01665
290. Ayazi M, Golshan Ebrahimi N, Jafari Nodoushan E. Bacterial adhesion reduction on the surface with a simulated pattern: An insight into extrand model. *Int J Adhes Adhes*. 2019;88:66-73. doi:10.1016/j.ijadhadh.2018.10.017
291. Watson GS, Green DW, Sun M, et al. The Insect (cicada) Wing Membrane Micro / Nano Structure – Nature ' s Templates for Control of Optics , Wetting , Adhesion , Contamination , Bacteria and Eukaryotic Cells. 2015;(December 2016).
292. Ren Y, Wang C, Chen Z, Allan E. Emergent Heterogeneous Micro-environments in Biofilms:Substratum Surface Heterogeneity and Bacterial Adhesion Force-sensing Development of an in-vitro model system for dental plaque biofilms View project Multiscale Surface Structures to Control the Infect. 2018. doi:10.1093/femsre/fuy001
293. French S, Côté J-P, Stokes JM, Truant R, Brown ED. Bacteria Getting into Shape: Genetic Determinants of *E. coli* Morphology. *MBio*. 2017;8(2):e01977-16. doi:10.1128/mBio.01977-16
294. Crawford RJ, Webb HK, Truong VK, Hasan J, Ivanova EP. Surface topographical factors influencing bacterial attachment. *Adv Colloid Interface Sci*. 2012;179-182:142-149. doi:10.1016/j.cis.2012.06.015
295. You Z, Pearce DJG, Sengupta A, Giomi L. Geometry and Mechanics of Microdomains in Growing Bacterial Colonies. 2018. doi:10.1103/PhysRevX.8.031065
296. Carniello V, Peterson BW, van der Mei HC, Busscher HJ. Physico-chemistry from initial bacterial adhesion to surface-programmed biofilm growth. *Adv Colloid Interface Sci*. 2018;261:1-14. doi:10.1016/j.cis.2018.10.005
297. Lichter JA, Thompson MT, Delgadillo M, Nishikawa T, Rubner MF, Van Vliet KJ. Substrata Mechanical Stiffness Can Regulate Adhesion of Viable Bacteria. *Biomacromolecules*. 2008. doi:10.1021/bm701430y
298. Harris LK, Theriot JA. Surface Area to Volume Ratio: A Natural Variable for Bacterial Morphogenesis. *Trends Microbiol*. 2018;26(10):815-832. doi:10.1016/J.TIM.2018.04.008
299. Eun Y-J, Weibel DB. Fabrication of Microbial Biofilm Arrays by Geometric Control of Cell Adhesion. 2009. doi:10.1021/la803985a

300. Dworkin J. Form equals function? Bacterial shape and its consequences for pathogenesism mi_7387 792..795. 2010. doi:10.1111/j.1365-2958.2010.07387.x
301. Friedlander RS, Vlamakis H, Kim P, Khan M, Kolter R, Aizenberg J. Bacterial flagella explore microscale hummocks and hollows to increase adhesion. 2013;2(14). doi:10.1073/pnas.1219662110
302. Bruzaud J, Tarrade J, Coudreuse A, et al. Flagella but not type IV pili are involved in the initial adhesion of Pseudomonas aeruginosa PAO1 to hydrophobic or superhydrophobic surfaces. *Colloids Surfaces B Biointerfaces*. 2015;131. doi:10.1016/j.colsurfb.2015.04.036
303. Reguera G, Tuominen M. Extracellular Electron Transfer Via Microbial Nanowires Ion conducting membranes for renewable energy View project. 2005. doi:10.1038/nature03661
304. Gorby YA, Yanina S, McLean JS, et al. *Electrically Conductive Bacterial Nanowires Produced by Shewanella Oneidensis Strain MR-1 and Other Microorganisms*.; 2006. www.pnas.orgcgidoi10.1073pnas.0604517103.
305. Lienemann M, Teravest MA, Pitk€ J-P, et al. Towards patterned bioelectronics: facilitated immobilization of exoelectrogenic Escherichia coli with heterologous pili. 2018. doi:10.1111/1751-7915.13309
306. Cheng Y, Feng G, Moraru CI. Micro- and Nanotopography Sensitive Bacterial Attachment Mechanisms: A Review. *Front Microbiol*. 2019;10(February):191. doi:10.3389/fmicb.2019.00191
307. Dahlquist FW. The Bacterial Flagellar Motor Continues to Amaze. 2018. doi:10.1016/j.bpj.2017.11.3786
308. Berg HC. The flagellar motor adapts, optimizing bacterial behavior. 2016. doi:10.1002/pro.3055
309. Zoueki CW, Tufenkji N, Ghoshal S. A modified microbial adhesion to hydrocarbons assay to account for the presence of hydrocarbon droplets. *J Colloid Interface Sci*. 2010;344(2):492-496. doi:10.1016/J.JCIS.2009.12.043
310. Sokurenko E V, Courtney HS, Maslow J, Siitonen A, Hasty DL. *Quantitative Differences in Adhesiveness of Type 1 Fimbriated Escherichia Coli Due to Structural Differences in FimH Genes*. Vol 177.; 1995. http://jb.asm.org/.
311. Sokurenko,' E V, Courtney HS, Ohman DE, Klemm P, Hastyl DL. *FimH Family of Type 1 Fimbrial Adhesins: Functional Heterogeneity Due to Minor Sequence Variations among FimH Genes*.; 1994. http://jb.asm.org/. Accessed April 9, 2019.
312. Hughes KT, Berg HC. The bacterium has landed. doi:10.1126/science.aaq0143
313. Schwan WR. Regulation of fim genes in uropathogenic Escherichia coli. 2011. doi:10.5495/wjcid.v1.i1.17
314. Brombacher E, Dorel C, B Zehnder AJ, Landini P, Landini landini P. The curli biosynthesis regulator CsgD co-ordinates the expression of both positive and negative determinants for biofilm formation in Escherichia coli. doi:10.1099/mic.0.26306-0
315. Haiko J, Westerlund-Wikström B. The role of the bacterial flagellum in adhesion and virulence. *Biology (Basel)*. 2013;2(4):1242-1267. doi:10.3390/biology2041242

316. Evans LDB, Hughes C, Fraser GM. Building a flagellum outside the bacterial cell. *Trends Microbiol*. 2014;22(10):566-572. doi:10.1016/j.tim.2014.05.009
317. Taylor PL, Sugiman-Marangos S, Zhang K, Valvano MA, Wright GD, Junop MS. Structural and Kinetic Characterization of the LPS Biosynthetic Enzyme D-R,β-D-Heptose-1,7-bisphosphate Phosphatase (GmhB) from Escherichia coli. *pubs.acs.org/Biochemistry*. 2010. doi:10.1021/bi901780j
318. Beloin C, Michaelis K, Lindner K, et al. The Transcriptional Antiterminator RfaH Represses Biofilm Formation in Escherichia coli. *J Bacteriol*. 2006;188(4):1316-1331. doi:10.1128/JB.188.4.1316-1331.2006
319. Anderson BN, Ding AM, Nilsson LM, et al. Weak Rolling Adhesion Enhances Bacterial Surface Colonization. *J Bacteriol*. 2007;189(5):1794-1802. doi:10.1128/JB.00899-06
320. O'Toole GA, Wong GC. Sensational biofilms: surface sensing in bacteria. *Curr Opin Microbiol*. 2016;30:139-146. doi:10.1016/j.mib.2016.02.004
321. Zajdel TJ, Teravest MA, Rad B, Ajo-Franklin CM, Maharbiz MM. *Probing the Dynamics of the Proton-Motive Force in E. coli*. https://libids1.uncg.edu/illiad/illiad.dll?Action=10&Form=75&Value=318238.
322. Hospenthal MK, Costa TRD, Waksman G. A comprehensive guide to pilus biogenesis in Gram-negative bacteria. *Nat Rev Microbiol*. 2017;15(6):365-379. doi:10.1038/nrmicro.2017.40
323. Manson MD, Tedesco P, Berg HC, Haroldt FM, Van Der Drift C. *A Protonmotive Force Drives Bacterial Flagella*. Vol 74.; 1977. https://www.ncbi.nlm.nih.gov/pmc/articles/PMC431412/pdf/pnas00029-0472.pdf.
324. Strahl H, Hamoen LW. Membrane potential is important for bacterial cell division. *PNAS*. 2010;107(27):12281-12286. doi:10.1073/pnas.1005485107
325. Krasnopeeva E, Lo C-J, Pilizota T. *Single-Cell Bacterial Electrophysiology Reveals Mechanisms of Stress Induced Damage*. https://arxiv.org/pdf/1809.05306.pdf.
326. Spindler EC, Hale JDF, Giddings TH, Hancock REW, Gill RT, Gill RT. Deciphering the mode of action of the synthetic antimicrobial peptide Bac8c. *Antimicrob Agents Chemother*. 2011;55(4):1706-1716. doi:10.1128/AAC.01053-10
327. Soto SM, Singh A, Pletzer D, Chang C-Y. Surface Sensing for Biofilm Formation in Pseudomonas aeruginosa. *Front Microbiol*. 2018;8:2671. doi:10.3389/fmicb.2017.02671
328. Persat A, Nadell CD, Kim MK, et al. The mechanical world of bacteria. *Cell*. 2015;161(5):988-997. doi:10.1016/j.cell.2015.05.005
329. Coursolle D, Baron DB, Bond DR, Gralnick JA. The Mtr Respiratory Pathway Is Essential for Reducing Flavins and Electrodes in Shewanella oneidensis †. *J Bacteriol*. 2010;192(2):467-474. doi:10.1128/JB.00925-09
330. Pirbadian S, Barchinger SE, Man Leung K, et al. Shewanella oneidensis MR-1 nanowires are outer membrane and periplasmic extensions of the extracellular electron transport components. doi:10.1073/pnas.1410551111

331. Teravest MA, Ajo-Franklin CM. Transforming exoelectrogens for biotechnology using synthetic biology. *Biotechnol Bioeng*. 2016;113:687-697. doi:10.1002/bit.25723/abstract
332. Jensen HM, Teravest MA, Kokish MG, Ajo-Franklin CM. CymA and Exogenous Flavins Improve Extracellular Electron Transfer and Couple It to Cell Growth in Mtr-Expressing Escherichia coli. 2016. doi:10.1021/acssynbio.5b00279
333. Bruni GN, Weekley RA, Dodd BJT, Kralj JM. Voltage-gated calcium flux mediates Escherichia coli mechanosensation. 2017. doi:10.1073/pnas.1703084114
334. Mizuno K, Furukawa S, Usui Y, Ishiba M, Ogihara H, Morinaga Y. Fimbriae and lipopolysaccharides are necessary for co-aggregation betIen Lactobacilli and Escherichia coli. *Biosci Biotechnol Biochem*. 2014;78. doi:10.1080/09168451.2014.921562
335. Heck DE, Shakarjian M, Kim HD, Laskin JD, Vetrano AM. Mechanisms of oxidant generation by catalase. *Ann N Y Acad Sci*. 2010;1203:120-125. doi:10.1111/j.1749-6632.2010.05603.x
336. Inaba S, Hashimoto M, Jyot J, Aizawa S-I. Exchangeability of the flagellin (FliC) and the cap protein (FliD) among different species in flagellar assembly. *Biopolymers*. 2013;99(1):63-72. doi:10.1002/bip.22141
337. Larsonneur F, Martin FA, Mallet A, et al. Functional analysis of Escherichia coli Yad fimbriae reveals their potential role in environmental persistence. *Environ Microbiol*. 2016;18(12):5228-5248. doi:10.1111/1462-2920.13559
338. Parreira P, Magalhães A, Gonçalves IC, et al. Effect of surface chemistry on bacterial adhesion, viability, and morphology. *J Biomed Mater Res Part A*. 2011;99A(3):344-353. doi:10.1002/jbm.a.33178
339. Kohnen W, Jansen B. Changing Material Surface Chemistry for Preventing Bacterial Adhesion. 2000:581-589. doi:10.1007/978-1-59259-224-1_36
340. Marine J, Myers CP, Picquet GA, Zaidel LA, Wu D, Uhrich KE. Reduction of bacterial attachment on hydroxyapatite surfaces: Using hydrophobicity and chemical functionality to enhance surface retention and prevent attachment. *Colloids Surfaces B Biointerfaces*. 2018;167:531-537. doi:10.1016/J.COLSURFB.2018.04.045
341. Li X. Bactericidal mechanism of nanopatterned surfaces. *Phys Chem Chem Phys*. 2016;18(2):1311-1316. doi:10.1039/C5CP05646B
342. Pavithra D, Doble M. Biofilm formation, bacterial adhesion and host response on polymeric implants—issues and prevention. *Biomed Mater*. 2008;3(3):034003. doi:10.1088/1748-6041/3/3/034003
343. Tse JR, Engler AJ. Preparation of hydrogel substrates with tunable mechanical properties. *Curr Protoc Cell Biol*. 2010;(SUPPL. 47):1-16. doi:10.1002/0471143030.cb1016s47
344. ASTM International. Standard Test Method for Tensile Properties of Plastics 1. *ASTM Int*. 2003;(January):1-16. doi:10.1520/D0638-10.1
345. Chua G, Chatfield-Reed K, Gugala N, Lemire J, Yan Y, Turner R. Using a Chemical Genetic Screen to Enhance Our Understanding of the Antibacterial Properties of Silver. *Genes (Basel)*. 2018;9(7):344. doi:10.3390/genes9070344

346. Zeiner SA, Dwyer BE, Clegg S. FimA, FimF, and FimH Are Necessary for Assembly of Type 1 Fimbriae on Salmonella enterica Serovar Typhimurium. *Infect Immun*. 2012;80(9):3289-3296. doi:10.1128/IAI.00331-12
347. Goyal P, Krasteva P V, Van Gerven N, et al. Structural and mechanistic insights into the bacterial amyloid secretion channel CsgG. doi:10.1038/nature13768
348. Chapman MR, Robinson LS, Pinkner JS, et al. Role of Escherichia coli curli operons in directing amyloid fiber formation. *Science*. 2002;295(5556):851-855. doi:10.1126/science.1067484
349. Chirwa NT, Herrington MB. CsgD, a regulator of curli and cellulose synthesis, also regulates serine hydroxymethyltransferase synthesis in Escherichia coli K-12. doi:10.1099/mic.0.25841-0
350. Minamino T, Imada K, Namba K. Molecular motors of the bacterial flagella. *Curr Opin Struct Biol*. 2008;18(6):693-701. doi:10.1016/j.sbi.2008.09.006